Development and characterization of hybrid constructs of porous polymer scaffold and cell sheet for vascular tissue engineering

アジザ インタン パンジェスティ

DEVELOPMENT AND CHARACTERIZATION OF HYBRID CONSTRUCTS OF POROUS PLCL SCAFFOLD AND CELL SHEET FOR CARDIOVASCULAR TISSUE ENGINEERING

PhD Thesis

Submitted as a partial fulfillment of the requirement for the degree of Doctor Philosophy

BY

AZIZAH INTAN PANGESTY

3ES15029M

Department of Molecular and Material Sciences

Interdisciplinary Graduate School of Engineering Sciences

Kyushu University

Japan

2018

ACKNOWLEDGMENTS

I am immensely grateful that finally this doctoral dissertation is completed after three years of hard work to a challenging topic. I would like to express my greatest gratitude to Associate Professor Dr. Mitsugu Todo for giving me an opportunity to work under his supervision for these past 5 years from master to doctoral study. I am really thanks to his intellectual input, continuous guidance, and support. I am also indebted to Assistant Professor Dr. Takaaki Arahira of Fukuoka Dental Collage for his assistance and contribution during my study.

I would like to thank to my seniors, Dr. Yos Phanny, Dr. Yusuke Nakamuta and other senior members at Todo laboratory, for their assistance and patience to teach me all about technical stuff during my early study. Not forgetting all current lab members, Mr. John Duckworth, Mr. Endo, Mr. Wu, Mr. Imamura, Ms. Kondo, Ms. Inoue, Ms. Ikeda, Mr. Kisaki and Mr. Kurita for their help and warm togetherness. Hang in there, guys!

I would also like to express my gratitude to the Advanced Graduate Program in Global Strategy for Green Asia for giving me such a huge opportunity to achieve my dream. Big thanks for their help and support during my stay in Japan to Ms. Hayashi, Ms. Fujikura (former staff), Ms. Kano and all staff members in Green Asia program that I could not mentioned one by one here. Without them I could not survive in Japan.

I would also like to acknowledge the Indonesia Endowment Fund for Education, Ministry of Finance Indonesia for the scholarship. My grateful also goes to my parents and brother for their endless support. Last but not least, special thanks to my husband, Dr. Sunarso, for his endless care and encouragement.

ABSTRACT

Cardiovascular tissue engineering offers a promising solution to repair the injured and damaged cardiac patches and blood vessels. Chapter 1 described cardiovascular diseases and the current treatments as the backgrounds of this study. Advances in cardiovascular tissue engineering are also discussed including the scaffold based-tissue engineering and the cell sheet engineering. The aim of this study is to develop hybrid graft by combining porous poly-(lactide-co-caprolactone) (PLCL) scaffold and cell sheet.

In Chapter 2, the novel hybrid patch was developed by layering Human Mesenchymal Stem Cells (HMSC) sheet on the porous PLCL sheet. Porous PLCL scaffold was fabricated by phase separation and freeze-drying method. The HMSC sheet, prepared by the temperature-responsive dish, was then layered on the top of the PLCL sheet and cultured for 2 weeks. During the *in vitro* study, cellular properties such as cell infiltration, spreading and proliferation were evaluated. Tensile test of the layered construct was performed periodically to characterize the tensile mechanical behavior. It was found that HMSC from the cell sheet were able to migrate into the PLCL sheet and actively proliferated into the porous structure then formed a new layer of HMSC on the opposite surface of the PLCL sheet. Mechanical evaluation revealed that the PLCL sheet with HMSC sheet showed enhancement of tensile strength and strain energy density at the first week of culture which is characterized as the effect of HMSC proliferation and its infiltration into the porous structure of the PLCL sheet. New technique was presented to develop tissue engineered patch by combining HMSC sheet and porous PLCL sheet, and it is expected that the layered patch may prolong biomechanical stability when implanted *in vivo*.

In Chapter 3, the vascular construct by layering cell sheet onto PLCL cylindrical scaffold was developed. The cell sheet prepared by co-culturing HMSC and Human Pulmonary Artery Endothelial Cells (HPAEC) were able to infiltrate through porous structure of the tubular PLCL scaffold and further proliferated on luminal wall within a week of culture. Moreover, the co-culture cell sheet within the tubular scaffold has demonstrated a faster proliferation rate than the monoculture cell sheet composed of HMSCs only. It was also found that the co-culture cell sheet expressed a strong angiogenic marker as compared with the monoculture cell sheet within 2 weeks of culture, indicating that the co-culture system could induce differentiation into endothelial cell lineage. The preformed-endothelial layer on the luminal surface of the tubular scaffold could prevent thrombus formation (blood clot) when implanted into the patients.

In Chapter 4, several approaches to improve the mechanical properties of the PLCL scaffold were presented. The first approach is by developing multiple layers of PLCL scaffold. It was found that developing the PLCL scaffold into double and triple layers improved the mechanical properties, approximately 400% and 600%, respectively, from the single layer scaffold. In the second approach, polymer blends PCL/PLCL scaffolds were developed. The elastic modulus increased as PLCL content increased. However, the tensile strength of the blends scaffolds at all ratio were tend to be lower than those of neat PCL and PLCL scaffolds due to phase separation. By increasing the temperature of the blends solution, the tensile strength of the blends scaffolds can be increased. In the third approach, melt spinning method successfully developed the microfibrous PLCL scaffold by utilizing cotton candy machine. This method significantly improved the mechanical strength, approximately 150% from the microporous scaffold fabricated by phase separation method. The initial cell study

using hMSCs also suggested that the microfibrous scaffold provided more favorable environment for cells growth than the microporous scaffold, evidenced from better cell morphology and higher proliferation. The simplicity of melt spinning method provides an opportunity for scale-up in a simple and cost-effective way.

TABLE OF CONTENT

LIST OF TABLES

LIST OF FIGURES

CHAPTER 1 : INTRODUCTION

1.1 Cardiovascular Heart Disease

Cardiovascular disease (CVD) remains the leading cause of death globally [1-4]. CVD is defined as a condition that affects the normal function of heart and/or blood vessel. This includes congenital heart disease (CHD) and coronary artery disease (CAD). CHD involves a defect in the structure of the heart that changes the normal flow of blood through the heart. CHD affects 8 out of 1000 newborns in the United States. Although many of CHD cases are simple since the defects will close by itself as the baby grows, others are often associated with a complex defect that need a surgical intervention to close the defects or maintain the blood flow [5, 6]. CAD is the most common form of cardiovascular diseases that affect adults over the age of 20. CAD is caused by a plaque (a combination of fat, cholesterol and calcium) that builds up inside the blood vessel [7, 8]. This plaque would eventually harden and clog the blood flow which can cause a heart attack if the medical treatment is not performed [9, 10].

The three major treatments for cardiovascular disease include angioplasty (balloon catheter), stent, and surgical intervention by graft implantation [1]. The treatment depends on the progressive states of the vascular disease, as illustrated in Figure 1.1. At the early stages of plaque development, angioplasty is usually performed. As plaque progress and develop angina, stent deployment is included in

balloon catheter. When plaque occlusion occur, surgical intervention is required by replacement of the diseased part of the artery with the cardiovascular patch or graft

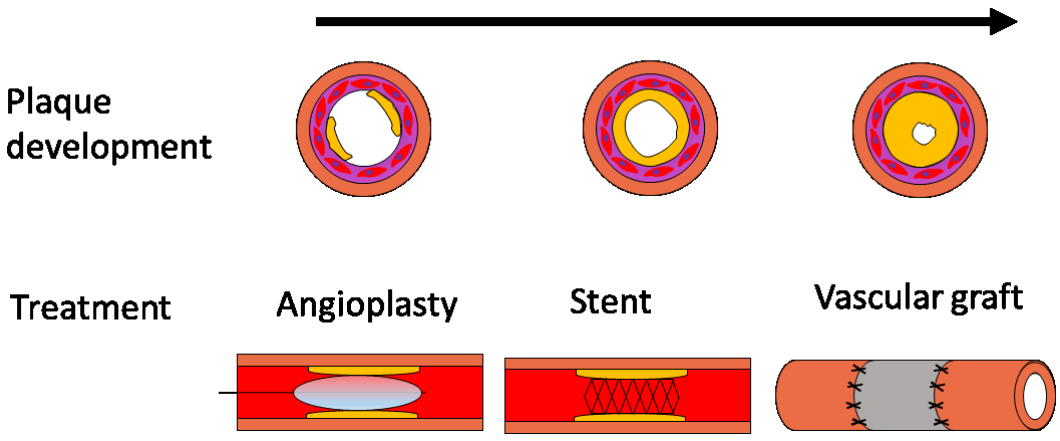

Figure 1.1 Stages of coronary heart disease and the corresponding treatment. (Plaque, yellow).

The first successful of blood vessel replacement was performed by Kunlin [2] in 1948 to treat patient with a rest pain of the lower leg. Despite undergone amputation as a major treatment at that time, Kunlin removed the diseased artery and established a bypass using saphenous vein [3]. Surprisingly, the patient's foot healed within 3 weeks after the surgery. Following this success, the use of saphenous vein become a major procedure to treat of the diseased artery. In the United States, autologous blood vessels is used in 400,000 of heart bypass surgeries every year [4]. Saphenous vein, harvested from the leg, has long feature and large diameter which make it technically easy to use for multiple grafts [5]. However, several studies reported that the performance of saphenous vein in a high-pressure artery site is limited due to mechanical mismatch, leading thrombosis and intimal hyperplasia [6,7]. Consequently, the durability is not ideal because a repeat surgery is needed after several years, but then it is also limited by the availability of saphenous vein [8].

Autograft such as saphenous vein is always preferred for the patient since the risk of immune response such as graft rejection, can be eliminated, but one of third patients experiences that this autograft is inadequate or unsuitable [9]. Alternatively, synthetic grafts are therefore needed. The use of synthetic grafts such as polyethylene terephthalate (PET, DACRON®) and poly-tetrafluoroethylene (PTFE, Gortex®) are quite common, especially in North America and Europe. The sales of synthetic grafts in those regions reached US$1.3 billion in 2005 [10]. However, it has been widely known that Dacron® and Gortex® work well only for the large diameter (>6mm) vascular graft while the results for the small diameter (<6 mm) vascular graft is disappointing. Studies have shown 20-25% of patency rate with 1 mm diameter PTFE grafts [11–13]. The low patency rate of the small-diameter vascular graft is caused by the material itself which activates thrombus formation on its lumen while the compliance mismatch between the graft and the native vascular contributes to the formation of intimal hyperplasia [14,15]. Consequently, patients with synthetic grafts often required prolonged anticoagulant medications [16].

1.2 Cardiovascular Tissue Engineering

To address the limitations of the current available grafts, tissue engineering [17] offers the most promising method that may alter the future treatment of CVD. Cardiovascular tissue engineering is an interdisciplinary approach between biology, medicine and engineering to develop a vascular graft that has ability to grow similar to the native vascular tissue. Using tissue engineering concept, the term of "replacement" in the conventional vascular surgery is shifted to "regeneration" of the vascular tissue. To mimic the native vascular tissue, an engineered-vascular graft

should has a burst pressure more than 1700mmHg [1] and an endothelium layer in the lumen area (similar with the intimal layer of native vascular) [18].

Cell is one of the important component to develop an engineered-vascular graft. To regenerate tissue, cells must be highly proliferative, non-immunogenic and easily harvested [19]. The use of autologous cells such as vascular cells is preferable to prevent the risk of immune-rejection and disease transmission. The first engineered-vascular graft was constructed by Weinberg and Bell [20] in 1986 made of collagen scaffold with seeded vascular cells. However, the harvesting procedure of vascular cells can be quite painful for the patients [21]. Moreover, long cultivation time of vascular cells limits the use in emergency situation [22]. The most-widely used cell in cardiovascular tissue engineering is mesenchymal stem cells (HMSC) [23]. HMSC can be isolated from bone marrow or can be harvested from other tissues such as adipose tissue and umbilical cord [24,25]. Due to its highly proliferative property and ability to differentiate into multi-type of cells, MSC is a promising candidate as a cell source for regeneration of engineered-vascular graft.

1.3 Approach in Cardiovascular Tissue Engineering

Regardless of the cell sources that have been explored and used, attempts to develop cardiovascular tissue engineering can be majorly classified into: scaffold tissue engineering and cell sheet engineering.

1.3.1 Scaffold Tissue Engineering

The concept of tissue engineering usually utilizes a scaffold biomaterial which act as a template for tissue regeneration. Figure 1.2 shows an illustrative procedure to develop engineered-tissue using a scaffold. Cells are seeded into a porous scaffold.

With the help of growth factor, cell growth was then guided by the scaffold to form a new tissue. The scaffold also provides the structural support and affects the cellular functions such as adhesion, proliferation, differentiation and secretion of extracellular matrix components. It is therefore important that scaffold must be biocompatible with an appropriate mechanical properties. To encourage the cell migration, scaffold should be porous and interconnected. An interconnected-porous structure also provides channels to deliver the nutrient and remove the waste during the tissue growth.

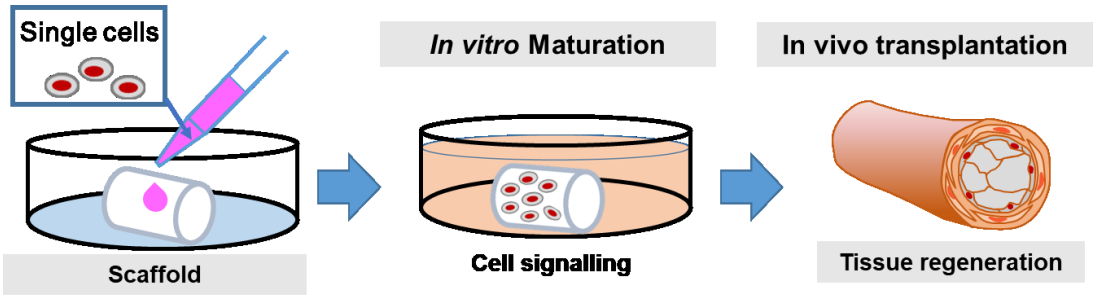

Figure 1.2 The Concept of Scaffold Tissue Engineering

Various methods to fabricate scaffold have widely been reported including particulate-leaching techniques, phase separation, textile technology, and electrospinning [26]. The resulted scaffold by particulate-leaching technique and phase separation is a porous scaffold. In particulate-leaching technique [27], small particle of salts are mixed with a polymer solution. After the solvent is evaporated, the salt crystals are leached away, resulting the pores of the scaffold. Phase separation [28] is another technique that has been widely used to fabricate scaffolds for tissue engineering applications. Phase separation is achieved by lowering the temperature to induce solvent crystallization from a polymer solution. Upon freeze-drying, the solvent is evaporated to form the pores and the polymer-rich phase solidified to form

the struts. Fibrous scaffold can be fabricated using textile technology and electrospinning. Poly glycolic acid (PGA) nonwoven scaffolds have been produced using textile technology for engineering of cartilage [29], blood vessels [30], heart valves [31] and other tissues. Recently, electrospinning [32] is getting much attention to fabricate fibrous scaffold with fibers bundles varying in micro/nano scale. Although the electrospinning have extensively been studied, its low production rate and complexity of control parameters may limit its clinical application [33]. Other alternative techniques must be developed to fabricate fibrous scaffolds without toxic solvents.

Materials for scaffold can be either bio-stable in a long-term period or biodegradable at a rate equal to the tissue regeneration. Both type of scaffolds can produced from decellularized tissue, natural materials and synthetic polymers. Synthetic materials have attracted a special interest to construct a prosthetic graft since they are commercially available and reproducible. However, in the field of cardiovascular tissue engineering, the work has been much focused on the use of synthetic polymer that can be hydrolyzed and degraded in the body without generating harmful products. Such biodegradable polymers that have received much attention in cardiovascular tissue engineering are poly glycolic acid (PGA), poly caprolactone (PCL), poly lactic acid (PLA), and copolymer of lactic acid and caprolactone (PLCL), as summarized Table 1.1.

Table 1.1 Biodegradable Polymers Used in Cardiovascular Tissue Engineering.

Biodegradable polymers	Result	Drawback	References
PGA	In vivo in pig: good patency and non thrombogenic.	Degrade too fast within 4 weeks	[30]
PCL	Mechanical properties that match with native soft tissue.	Too long degradation time	[34,35]
PLGA	Capable of resisting compressional forces in vitro.	Lack of structural stability in vivo	[36,37]
PLCL	Controllable mechanical properties and degradation time. Good biocompatibility to smooth muscle cells.	Depend on copolymer composition	[38]

PGA has been widely used in the application of medical devices such as bioresorbable surgical suture [39] which provides a high initial tensile strength. Tubular scaffold made of PGA with the seeded-vascular cells demonstrated a good patency and non-thrombogenic in a pig model [40] . Unfortunately, the application of this PGA made-scaffold is limited due to fast degradation property. It was reported that PGA loses its strength *in vivo* within 4 weeks and was completely degrade in 6 months[41]. With this fast degradation, a concern is raised whether the regenerated-tissue is mechanically strong enough to withstand the arterial pressure when the materials degrade. As a solution, PGA is frequently combined with other biodegradable polymer to tailor the degradation rate such as polyhydroxyoctanoate (PHO). This additional work showed a patency more than 5 months with an improved mechanical strength in a lamb model [42]. Despite its wide application, a recent study conducted by Higgins et.al. [43] revealed that the degradation product of PGA could

induce dedifferentiation and reduce the growth of SMCs during *in vitro* study, thus the use of PGA for vascular tissue engineering is not recommended.

Other biodegradable polymer candidate that has also been widely studied in development of cardiovascular tissue engineering is PCL. PCL has a low melting point with elastic and flexible characteristics [44], slow degradation time and is regarded as a soft tissue compatible material [45–47]. Yeong et.al. [35] fabricated porous PCL scaffold by using the selective laser sintering which allows for the fabrication of uniform pore size and patterns. His result demonstrated an ability of this technique in tailoring the mechanical properties of PCL scaffold to match with that of the native tissue.

In order to control the degradation time, PCL is usually copolymerized with lactic acid (LA) to form copolymer of PLCL. PLCL was first synthesized by Feng et.al. [34] through ring opening polymerization. In intend to seek materials that can replace the non-biodegradable silicon rubber, they combined the excellent permeability of PCL with the faster biodegradation of PLA. The resulted copolymer, PLCL, possessed a very similar properties with silicone rubber, but its degradation is faster than that of PCL or PLA homopolymers. This is due to the decreasing of crystallinity and an increase in water absorption which depend on the hydrophilicity of monomer.

1.3.2 Cell Sheet Engineering

Historically, tissue engineering has relied on the use of materials (synthetic or natural) to provide structural and mechanical support. This has been true since mechanical strength is a critical factor. However, the risk of autoimmune rejection is

always presence if synthetic materials is used. In 1998, L'heureux and his colleagues [48] reported a different approach to develop tissue-engineered blood vessel based on the human cells completely, without scaffold. The technique included culturing of smooth muscle cells and adult fibroblast cells in a medium enriched with ascorbic acid to induce production of collagen type 1. After 30 days of culture, cell sheets from both type of cells were formed. They were then manually peeled off from the culture flask and wrapped around a mandrel to produce a tubular structure composed of cell sheets, as shown in Figure 1.3.

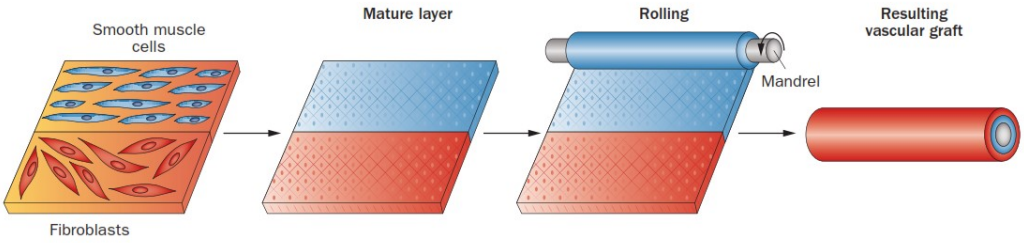

Figure 1.3. Tissue engineered-blood vessel production based on exclusively on the use of human cells, as described in [1].

After additional culture for maturation, the resulting construct was seeded with endothelial cells on the lumen side, so that the vascular graft had three layers, resembling the native blood vessel which consist of intima, media and adventitia layer. This graft performed quite well during *in vivo* test in dog which could withstand physiological flow conditions. The burst pressure of this graft is >2000 mmHg, comparable to saphenous vein. However, the construction time of this cell sheet based-graft is quite long [49]. Overall, the production of the graft needs 3 months: 3 weeks for sheet formation, 1 week for media maturation, 7 weeks for adventitia maturation

and 1 week for endothelial cell growth. Additional potential drawback of this production involves the peeling technique to harvest the cell sheet which could lead to tearing and create a potential defect for bursting during maturation.

This potential drawback is now possible to be alleviated by allowing cell sheets to detach themselves without an external force using temperature-responsive dish. This dish is covalently grafted by poly (N-isopropylacrylamide) on its surface which allows to change its hydrophobicity-hydrophilicity over specific range of temperature [50,51]. For example, at temperature of 37°C, the surface is hydrophobic so that cells can attach and grow on its surface. The surface properties will change to hydrophilic when the temperature is decreased to less than 32°C, so that the confluent cells could detach by themselves as an intact sheet, as described in Figure 1.4.

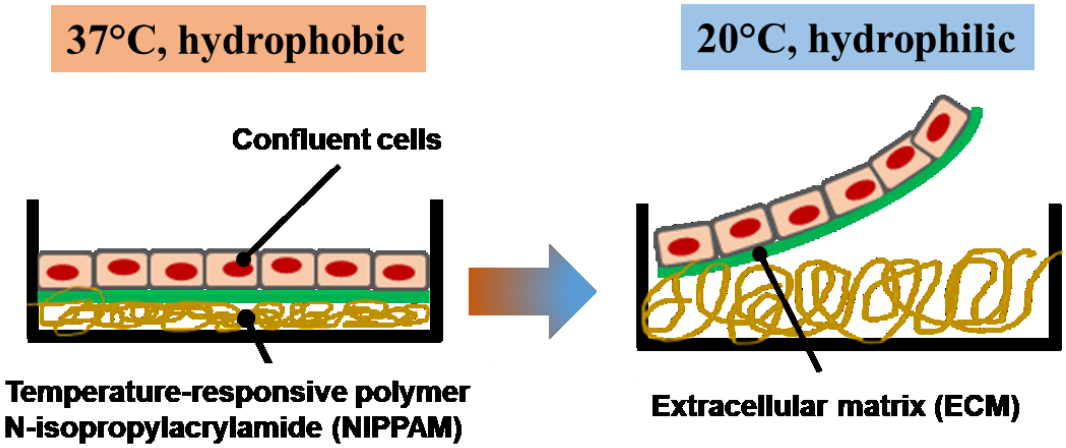

Figure 1.4 Cell sheet detachment cultured in temperature-responsive dish.

Transplantation of cell sheet onto the damaged tissue showed satisfactory result in various animal model [52–55]. For example, this technology has been used to prepare a cardiac patch from MSC sheet to repair myocardial infraction [56]. MSC

sheet allows for cell-to-cell connections and intact extracellular matrix on its basal surface which are essential factors for cell proliferation and differentiation. As a result, after transplantation in an infracted rat heart, MSC sheet was able to differentiate into endothelial cells and cardiomyocyte cells and improve cardiac function [56]. Temperature-responsive dish has also been reported to prepare a myocardial tube from cardiomyocyte cells [57]. Four weeks after transplantation into rat, the myocardial tube demonstrated spontaneous and synchronous pulsation independent of the host heartbeat. In clinical trial, cell sheets have been implemented into heart, esophagus and cornea [58,59]. This technology [60] also provides time-effectiveness in the cell sheet preparation. Using, temperature-responsive dish, cell sheet can be harvested in relatively short time; 3-4 days for HMSC, 4-5 days for cardiomyocyte cells [61,62], and 2 weeks for epithelial cells [58,63].

1.4 Problem Statements

In Japan, the first tissue engineered vascular graft was implanted into a human patient in 2001[64]. The grafts , made of PGA/PLCL with seeded-bone marrow cells (BMCs) [65], showed normal function without any evidence of graft failure in 20 out of 25 the clinical patients [66]. However, after long-term follow-up, graft stenosis and thrombosis were identified in 16% of patients [67]. As previously described, the native blood vessel has intima layer that consist of endothelial layer coating the lumen surface. This endothelium performs the function of preventing thrombosis and reducing the extent of intimal hyperplasia[68–70]. In order to improve the long patency of the vascular graft, many studies have attempted to optimize the endothelium formation by seeding endothelial cells (ECs) in the lumen surface of the vascular graft [69]. The result, reported by Schneider et.al. [69], showed that endothelial layer could prevent

the platelet deposition in PTFE graft. The initial clinical application of this endothelial-coated graft resulted an improvement in the graft patency, compared to that without ECs seeding.

Mature ECs sheet is currently possible to be created efficiently *in vitro* using temperature-responsive dish, as described in 1.3.2. The preformed-EC sheet is possible to be layered on the vascular graft directly, avoiding a prolonged *in vitro* maturation like when the dissociated cells are used. Cell sheet also has superior properties than the dissociated cells such as, greater survival rate (ten times at 4 weeks after transplantation *in vivo*) [71] and more effective therapeutic effects and tissue regeneration [72]. Okano et.al. [50] reported that the cells dissociated by trypsin have a reduced-substrate adhesivity due to the disruption of cell membrane proteins which is essential for cell attachment. Using this cell sheet technology, Shimizu et.al.[73] reported the fabrication of three-dimensional myocardial tissue by stacking the cardiomyocyte sheets. Although the tissue can beat synchronously like real heart, the number of sheet that can be stacked is limited up to three layers due to hypoxia, nutrient insufficiency, and waste accumulation[73,74]. This is a clear evidence that the creation of 3D and functional tissue from stacked-cell sheet is remained hardly to be realized if the tissue ischemic environment is not addressed.

In this study, a new approach to develop engineered-hybrid graft for cardiovascular tissue engineering by combining scaffold tissue engineering and cell sheet engineering was investigated. By combining the two techniques, the mutual benefits will be resulted. From the scaffold point of view, cell sheet could provide a more mature cellularization as compared with the conventional seeding method using the dissociated cells, thus a cellularized graft could be produced time-efficiently *in*

vitro. On the other hand, scaffold could provide the structural and mechanical support for cell sheet. This also could address the previous limitation of the engineered-cardiovascular graft based on cells exclusively [48] which lack of structural and mechanical stabilities.

1.5 Goal of Study

The goal of this study is to develop hybrid graft by combining PLCL scaffold and cell sheet for cardiovascular tissue engineering. In the first chapter, cardiovascular patch was developed by layering PLCL sheet scaffold with MSC sheet. Second chapter is aimed to develop hybrid vascular graft from PLCL tubular scaffold and co-culture sheet. The third chapter addressed the limitation of mechanical and structural properties of PLCL scaffold by developing the multiple layer scaffold, physically blending with PCL, and fibrous PLCL scaffold using the melt spinning method

CHAPTER 2 : DEVELOPMENT OF LAYERED HYBRID CONSTRUCT OF PLCL SCAFFOLD AND HMSC SHEETS

2.1 Overview

In this chapter, a novel hybrid structure by combining of cell sheet and porous PLCL sheet was developed. Cell sheet was prepared from MSC because of multipotent capacity to differentiate into various cells including vascular endothelial cells [75,76]. The use of porous PLCL sheet is aimed to provide channels for nutrient supply as well as to support mechanical properties. PLCL sheet was fabricated using solid-liquid phase separation method followed by freeze drying method. Then HMSC sheet, prepared by temperature-responsive dish, was layered on PLCL sheet to form hybrid graft. The variational behavior of mechanical strength was evaluated. The cell proliferation during two weeks of *in vitro* study were monitored and the cell spreading behavior was evaluated by histological staining and electron microscopic analysis.

2.2 Materials and Methods

2.2.1 Fabrication of PLCL Scaffold

Porous tubular scaffolds composed of (PLCL) at 75:25 ratio (Gunze Ltd., Kyoto, Japan) were fabricated by solid liquid phase separation method followed by freeze-drying under vacuum. The fabrication process was illustrated in Figure 2.1. The polymer granules were dissolved in 1.4-dioxane solvent with final concentration of

6% (w/v). A Teflon tube of 10 mm in diameter, taken from -80°C was vertically dipped into polymer solution and pulled out at a constant rate (100 mm/min). This sample was frozen again at -80° C for at least 1 hour before being freeze-dried at -50°C for 24 hours. Finally, the fabricated graft was pulled out from the Teflon tubes and cut to make into sheets**.** To evaluate the degradation process, PLCL sheet was incubated in a phosphate buffer saline (PBS) solution at 37°C/5% CO_2 for 1, 4, 7 and 14 days. The percentage of weight loss of PLCL sheet was calculated by comparing the weight before incubation with the weight after incubation.

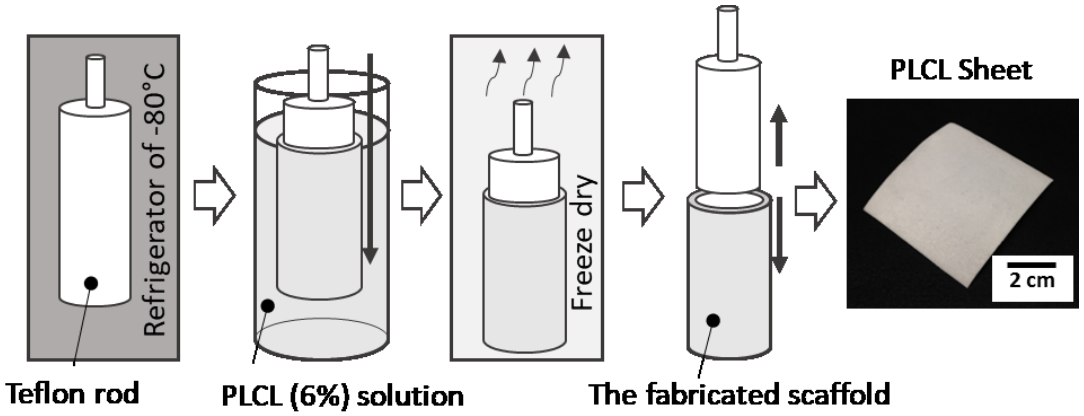

Figure 2.1 Schematic fabrication of PLCL scaffold.

2.2.2 Fabrication of Hybrid Construct

Human HMSC (UE6E7TE, Riken BRC, Tsukuba, Japan) of passage 4-5 were cultured on a 24-multi well temperature-responsive dish (CellSeed Inc., Tokyo, Japan) at a density of 5 x 10^4 cells/well. The cells were cultured in cell growth medium containing α-MEM (Wako Chem.,Tokyo, Japan), 10% FBS, and 1% penicillin streptomycin in a humidified atmosphere with 5% CO_2 at 37° C for 4 days. The cell sheets were obtained by detaching the confluent cells from the dishes at room temperature for 20 minutes. Cell shifter was utilized to transfer cell sheet onto PLCL

sheet. Each cell sheet was transferred onto a PLCL sheet (10 mm x 10 mm) which had been sterilized by ethanol 70% and ultraviolet. After removing media, the layered construct was incubated for 1 hour to promote adhesion between cell sheet and PLCL sheet. Finally, the layered construct was incubated in 2 mL of cell growth medium and cultured for 2 weeks. Fabrication of hybrid sheet was illustrated in Figure 2.2.

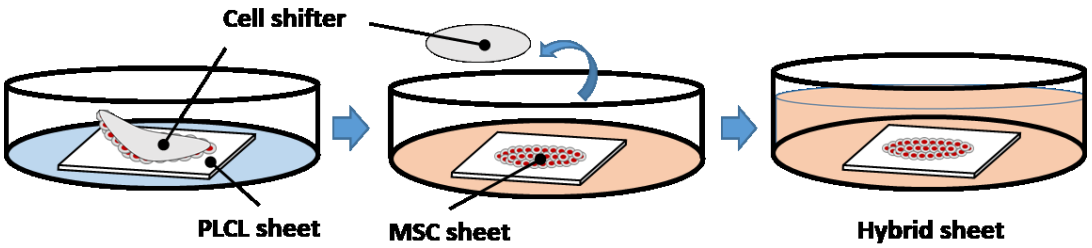

Figure 2.2 Fabrication of hybrid sheet.

2.2.3 SEM Imaging

The microstructure of each sample was observed using field-emission scanning electron microscope (FE – SEM) (Hitachi Ltd., S-4100). For the layered construct, the sample was washed with phosphate buffer saline, dehydrated in ascending concentration of ethanol (40%, 50%, 70% and 100%) and soaked in t-butyl alcohols. Then the sample was freeze-dried in freeze drying machine (ES-2040, Hitachi,Ltd., Tokyo, Japan) and sputter-coated with Pt–Pd using an anion sputter coater (E-1040, Hitachi, Ltd., Tokyo, Japan). Both the cross section and surface area were observed.

2.2.4 Cell Proliferation Analysis

The cell viability of each layered construct was evaluated by using a Cell Counting Kit (Dojindo Laboratories, Kumamoto, Japan). The layered construct was soaked in PBS and the cell counting kit, and incubated in a CO_2 incubator for 2 hours.

The absorbance was measured by spectrophotometric plate reader (2040 ARVO^{TM} X2, Perkin Elmer Co., Yokohama, Japan) at a wavelength of 450 nm.

2.2.5 Hematoxylin and Myosin (H&E) Staining

After incubating for 1, 4, 7, and 14 days, the layered construct was recovered from the dish, washed with PBS, and dehydrated with ascending ethanol solution (40%, 50%, and 70%). The layered construct was embedded in paraffin, sectioned and stained with Hematoxylin and Eosin (H&E). The image was observed using a microscope digital camera (Olympus DP12, Olympus Optical Co. Ltd., Japan).

2.2.6 Mechanical Characterization

Tensile mechanical tests were performed after 1, 4, 7, and 14 days of cell cultures by using a Shimadzu Compact Tabletop Testing Machine with a 10 N load cell and a crosshead speed of 1 mm/min. The region under measurement was rectangular in shape (10 mm in length, 10 mm in width, 0.5 mm in thickness). Based on the load-displacement relation that was monitored during the test, the stress (σ) and strain (ε) were evaluated using the following formulas.

$$\sigma = F/A \qquad \text{Equation 2-1}$$

$$\varepsilon = \Delta L/L \qquad \text{Equation 2-2}$$

where F is the force under tensile test, A is the area of cross sectional sample, L is the length of sample under measurement and ΔL is the displacement after loading at each time. The elastic modulus was calculated by identifying the linear region in the resulting stress-strain curve.

2.2.7 Statistical Analysis

All data were expressed as mean ± SD. Statistical analysis were performed by Fischer's LCD comparison test in which P values of less than 0.05 were considered statistically significant.

2.3 Results

2.3.1 Morphology and Microstructure of PLCL and MSC Sheet

The thickness of PLCL sheet was around 0.5 mm. SEM images (Figure 2.3a) showed that the PLCL sheet consists of porous structure with an average pore size of 21 µm ± 4.5 µm. The cross section image (Figure 2.3b) showed elongated pores connected to each other, indicated that PLCL sheet was very interconnecting.

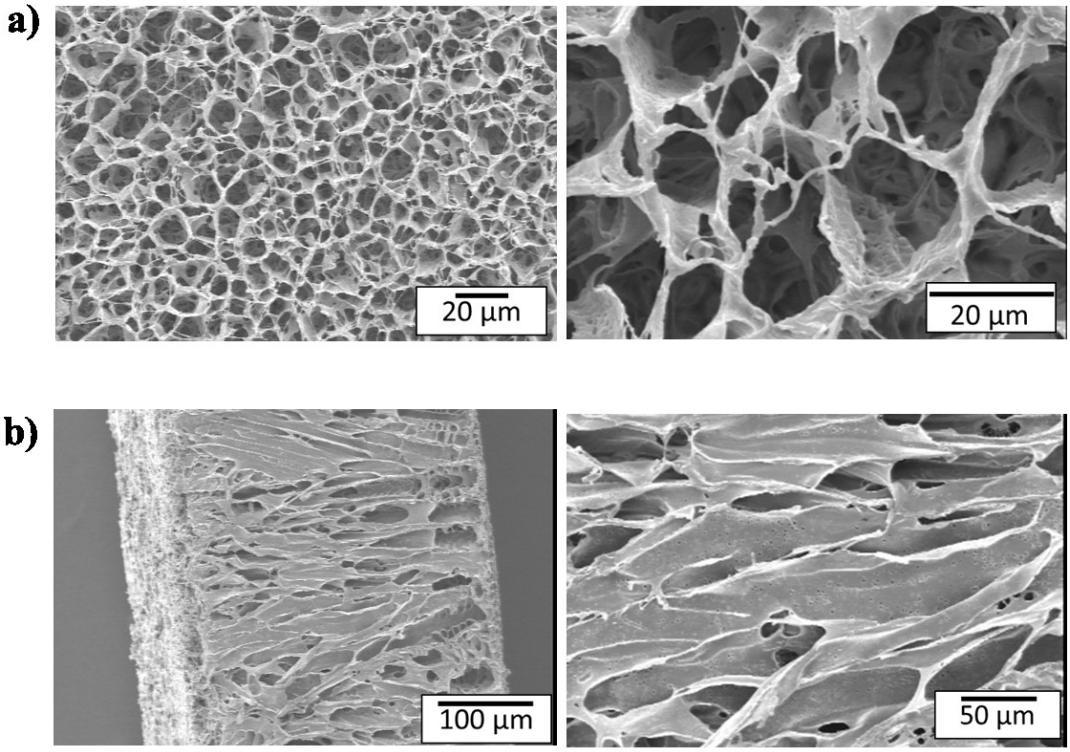

Figure 2.3. SEM images of porous PLCL scaffold. a) outer-layer and b) cross section.

Upon transferred to room temperature, HMSC sheet was spontaneously detached within 20 minutes and shrank to approximately 25% of its original diameter. SEM observation of HMSC sheet (Figure 2.4) revealed an intact cell sheet with abundance of extracellular matrix. However, it was impossible to observe of each cells distinctly due to high cell density. Numerous mound texture were indicated as a result of cells sheet contraction after detachment.

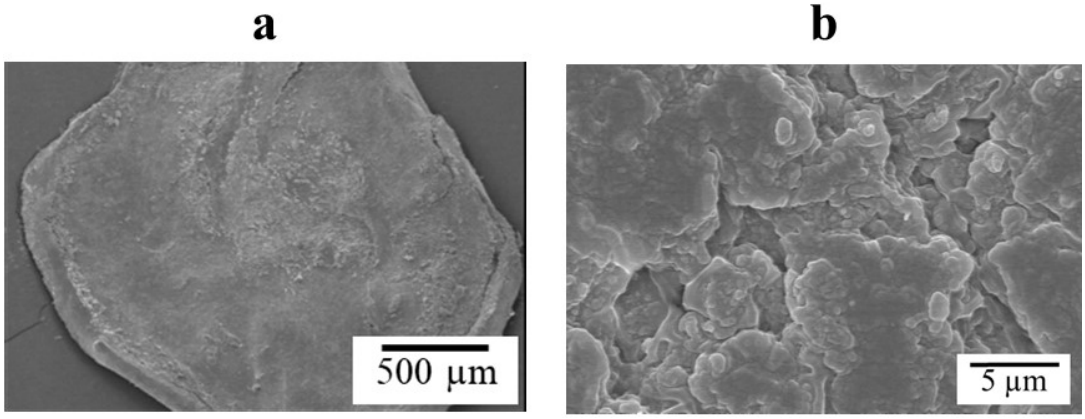

Figure 2.4. SEM images of MSC sheet. Low magnification (Left), High magnification (Right).

For fabrication of hybrid construct, one layer of HMSC sheet was layered on PLCL sheet (10 x 10 mm in size) using pipet. Figure 2.5 showed gross appearance a hybrid layered construct with HMSC sheet remained attached (as indicated in yellow) at 7 days of culture.

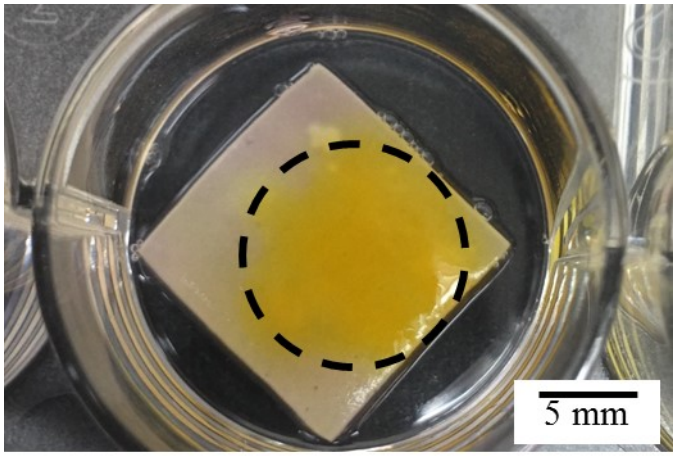

Figure 2.5. Hybrid sheet of PLCL sheet and cell sheet. MSC sheet (*yellow*).

2.3.2 Cell Spreading and Infiltration

To observe the behavior of cell sheet spreading on the PLCL sheet, SEM imaging was performed. SEM images of surface region at 14 days of culture were shown in Figure 2.6 . The cell sheet (indicated in red head arrows) covered half surface of PLCL sheet (Figure 2.6a), making the pore structure of PLCL sheet completely unobservable (Figure 2.6b). The cell sheet was able to proliferate actively across the entire surface of the polymer sheet by creating a network structure of extracellular matrix (Figure 2.6c).

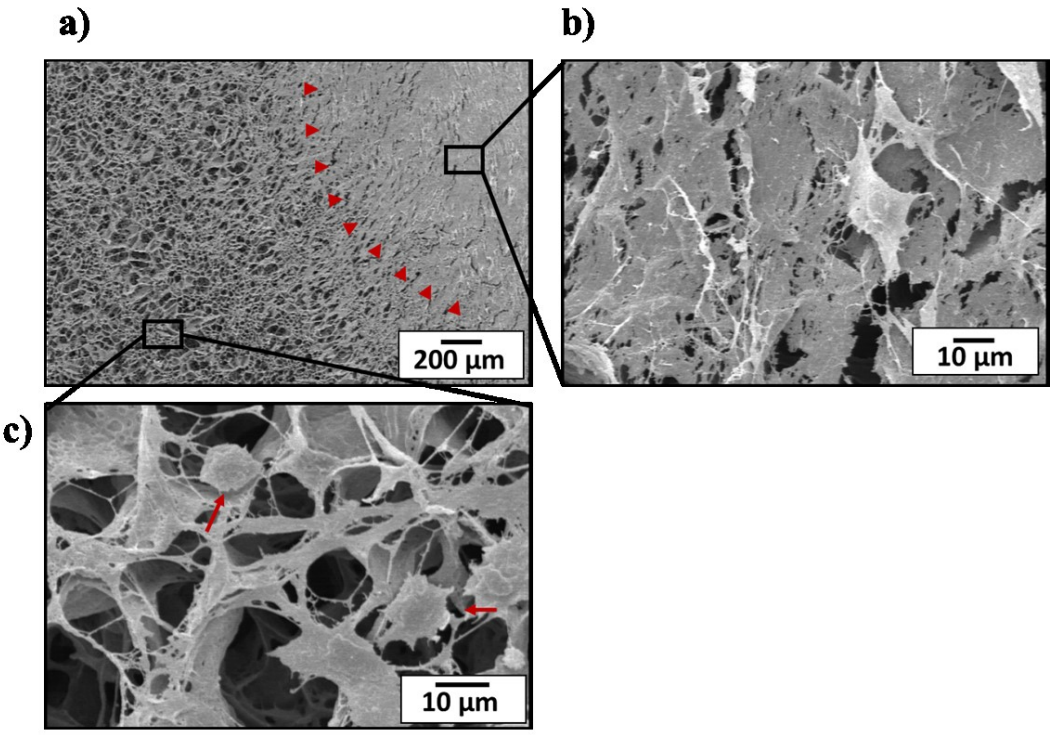

Figure 2.6. SEM images of cell spreading behavior on PLCL sheet at 14 days of culture. A) HMSC sheet (head arrows) on porous PLCL sheet and b) covered the porous structure. C) HMSC sheet spread horizontally by creating a network structure (red arrows).

Histological analysis was performed to examine the cell infiltration into PLCL sheet. The cross section images at 1 day culture showed that HMSC sheet well attached on PLCL sheets (Figure 2.7a). It is clearly seen that cells from HMSC sheet migrate inside the PLCL sheet through connecting porous (Figure 2.7b). After 4 days of culture, the cells had continued to proliferate deeper through the connecting pores as shown in Figure 2.7c and d. After 7 days of culture, a new layer-like cell sheet had formed on the bottom side of the polymer sheet, resulting in a unique, sandwich-like structure (Figure 2.7e and f).

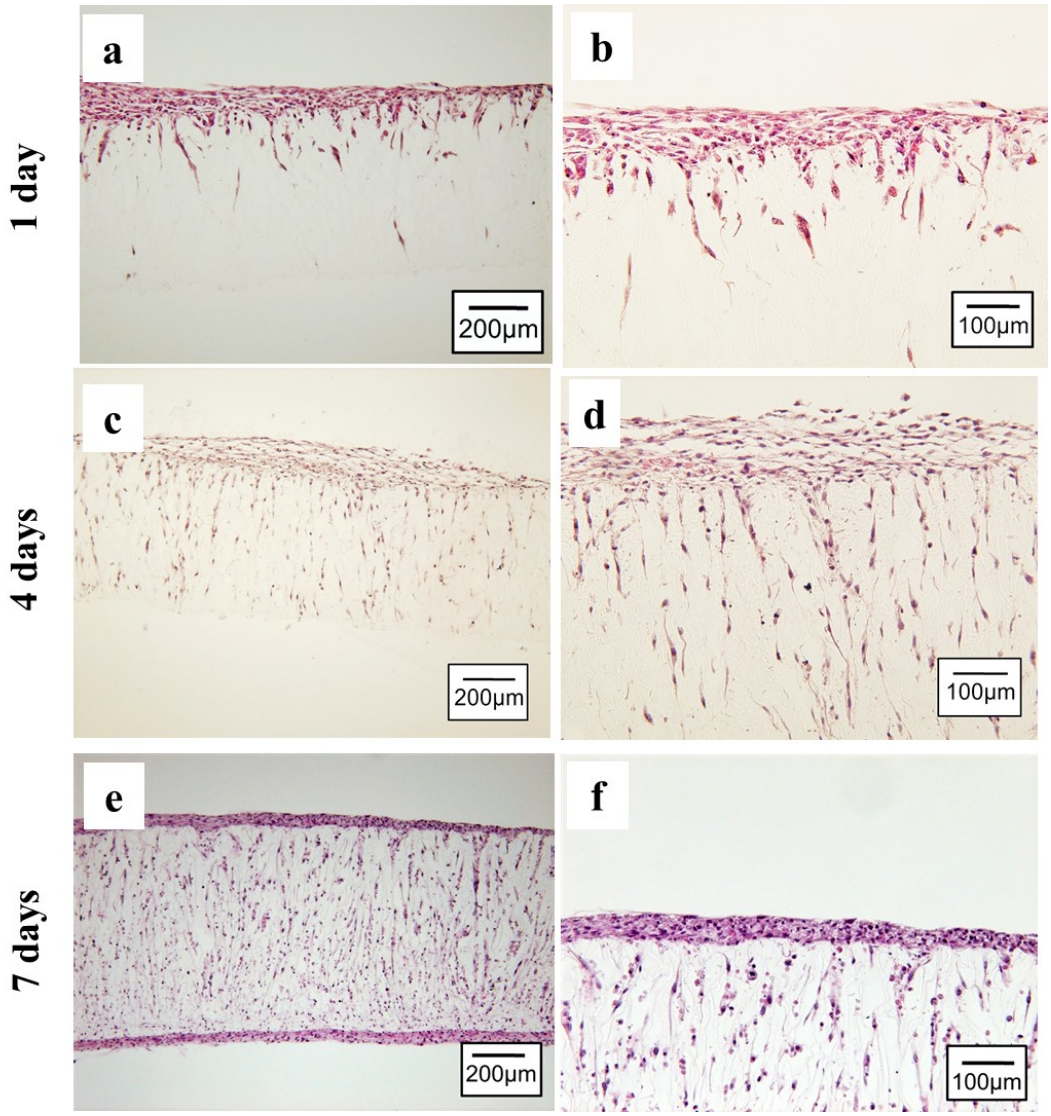

Figure 2.7. H&E staining of PLCL sheet with MSC sheet in cross section at 1 day (a,b), 4 days (c,d) and 7 days (e,f) of culture. (Cells, red-pink). Low magnification (left), high magnification (right).

2.3.3 Cell Proliferation

Cell proliferation is a critical part for a complete cellularization of patch graft and a good indication for tissue regeneration. Cell proliferation on PLCL sheet was examined quantitatively at 1, 4, 7, 14 and 30 days of culture using cell counting kit which contains water soluble tetrazolium salt, generating a yellow color from only viable cells. As shown in Figure 2.8, HMSC actively proliferated in significant amount from day 1 to day 14. At day 30, the number of live cells was increased more than 2 folds from day 14. This experiment therefore gives strong evidence that PLCL sheets are compatible for cells growing.

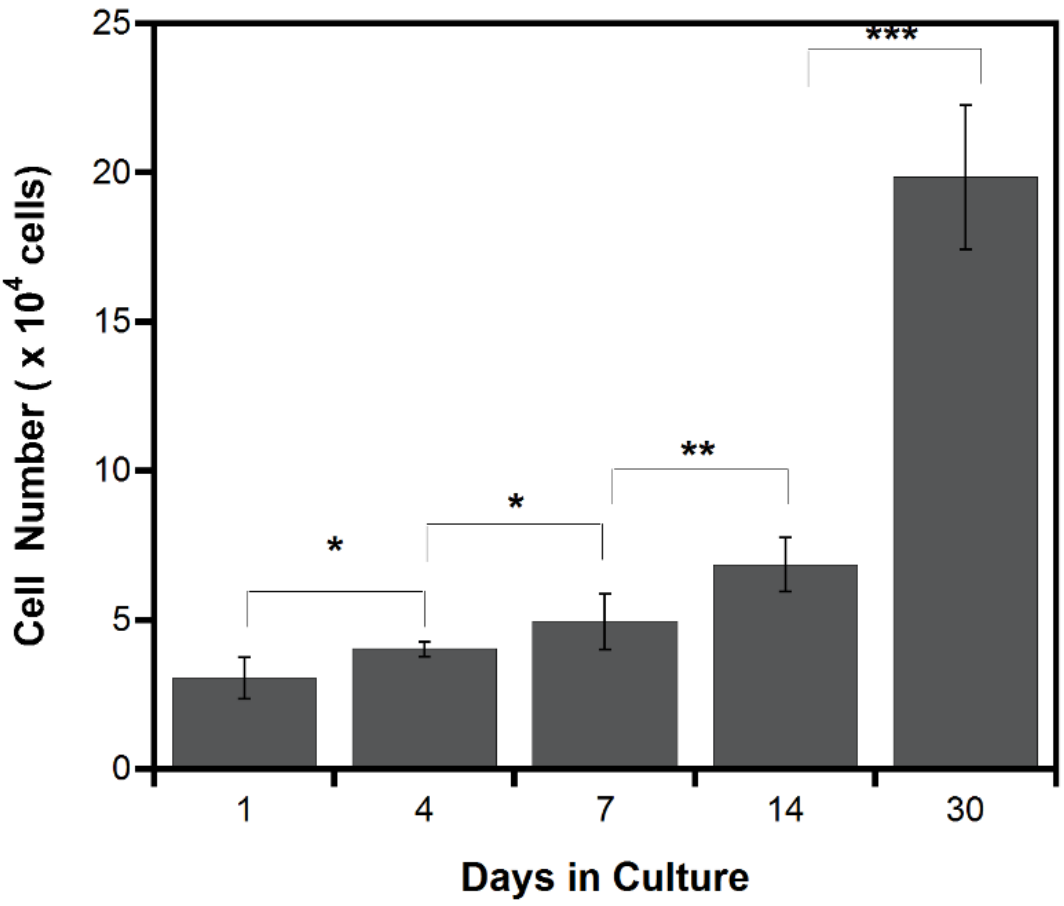

Figure 2.8. Number of viable cells in hybrid graft. Each data represented as mean ± SD, n=4, *P<0.05, **P< 0.001, ***P<0.0001.

2.3.4 Tensile Mechanical Evaluation

To evaluate mechanical properties of both the PLCL sheet with and without HMSC sheet, tensile tests were performed. The PLCL sheet with HMSC sheet exhibited steeper stress-strain curves compared to PLCL sheet only as shown in Figure 2.9a. In Figure 2.9b, PLCL sheet with cell sheet showed an increasing of elastic modulus significantly at day 1 culture. However, the elastic moduli of PLCL sheet with HMSC sheet from 4 days to 14 days can be maintained insignificantly different with that of PLCL sheet only. Figure 2.9c showed averaged ultimate tensile strength during culture. At 1 day culture, the effect of HMSC sheet on the increasing of tensile strength of PLCL sheet was less apparent, however, PLCL sheet with HMSC sheet showed improvement of tensile strength in significant amount at 4 and 7 days of culture. The differences of failure strain between PLCL sheets with and without HMSC sheet were not clearly obvious during cell culture period (Figure 2.9d). It was also found that the strain energy density of PLCL sheet with HMSC sheet showed a significant enhancement compared with PLCL sheet at 4 and 7 days culture (Figure 2.9e). In general, it can be recognized that there were tendency of decreasing the mechanical properties at 14 days of culture. The scaffold mass evaluation revealed that the PLCL sheet lost its weight around 4% after 14 days incubation, as shown in Figure 2.9f.

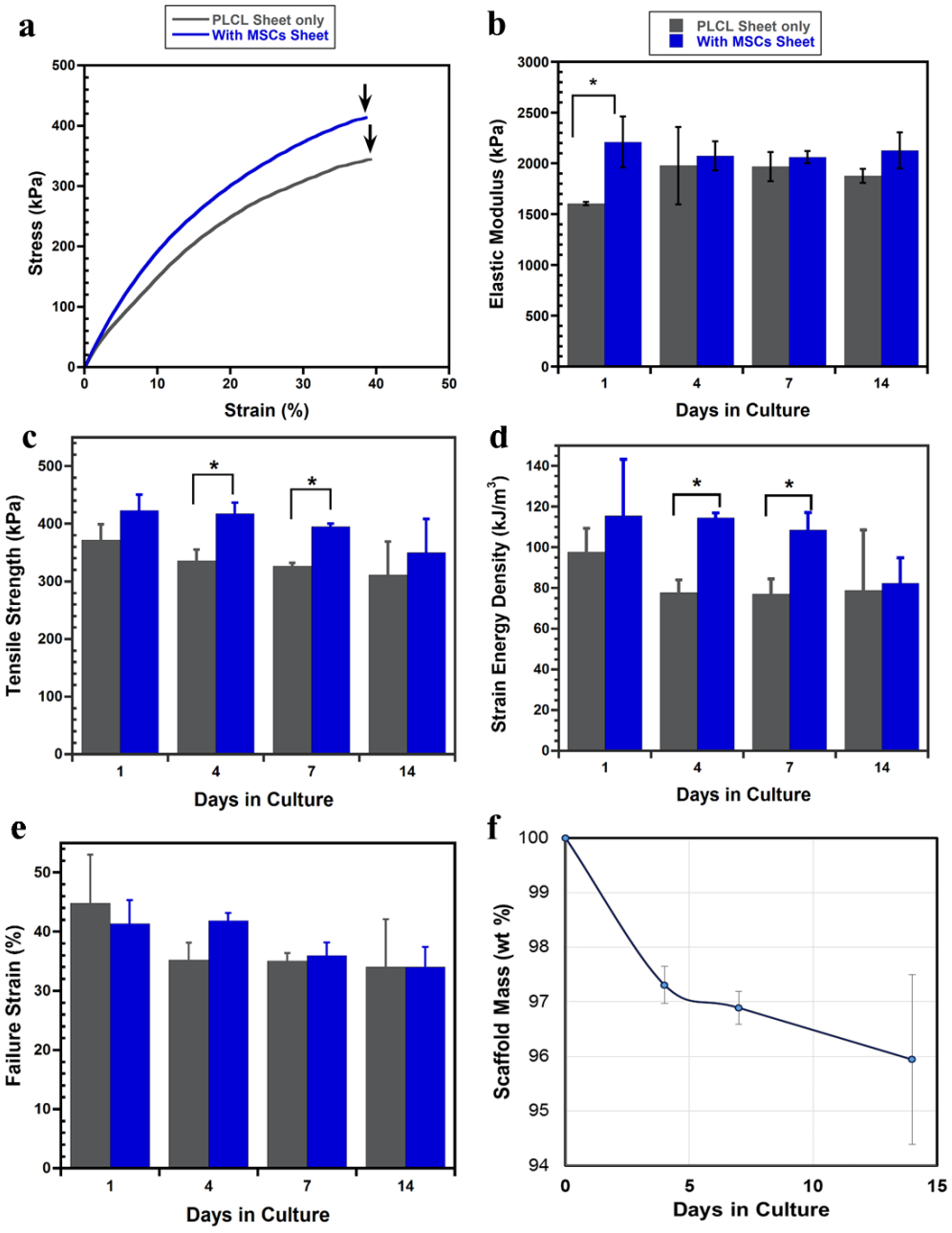

Figure 2.9. Tensile Mechanical behavior during *in vitro* course. (a) Typical stress-strain curve at 1 day culture. Black arrow indicates point of breaking. (b) Elastic modulus. (c) Tensile strength. (d) Strain energy density. (e) Strain at failure. (f) Scaffold mass of PLCL sheet during 14 days incubation. Data represent as mean ± SD, n=3, * $P < 0.05$.

SEM images of typical microstructural deformation at break point are shown in Figure 2.10. Both of PLCL sheet and PLCL sheet with HMSC sheet exhibited a ductile deformation. However, the deformation region of PLCL sheet with HMSC sheet is wider than that of PLCL sheet only, as indicated in Figure 2.10a and d (blue head arrow). The cross section images showed tearing failure (Figure 2.10. SEM images of deformed structure of 7 days of culture after tensile test. (a, d) The appearance of pore deformation at break point. (b, c, e and f) Fracture appearance in cross section. e and f show greater magnification.. It is surprising that the cells can be found inside the elongated pore which formed a connecting network around strut walls (Figure 2.10f).

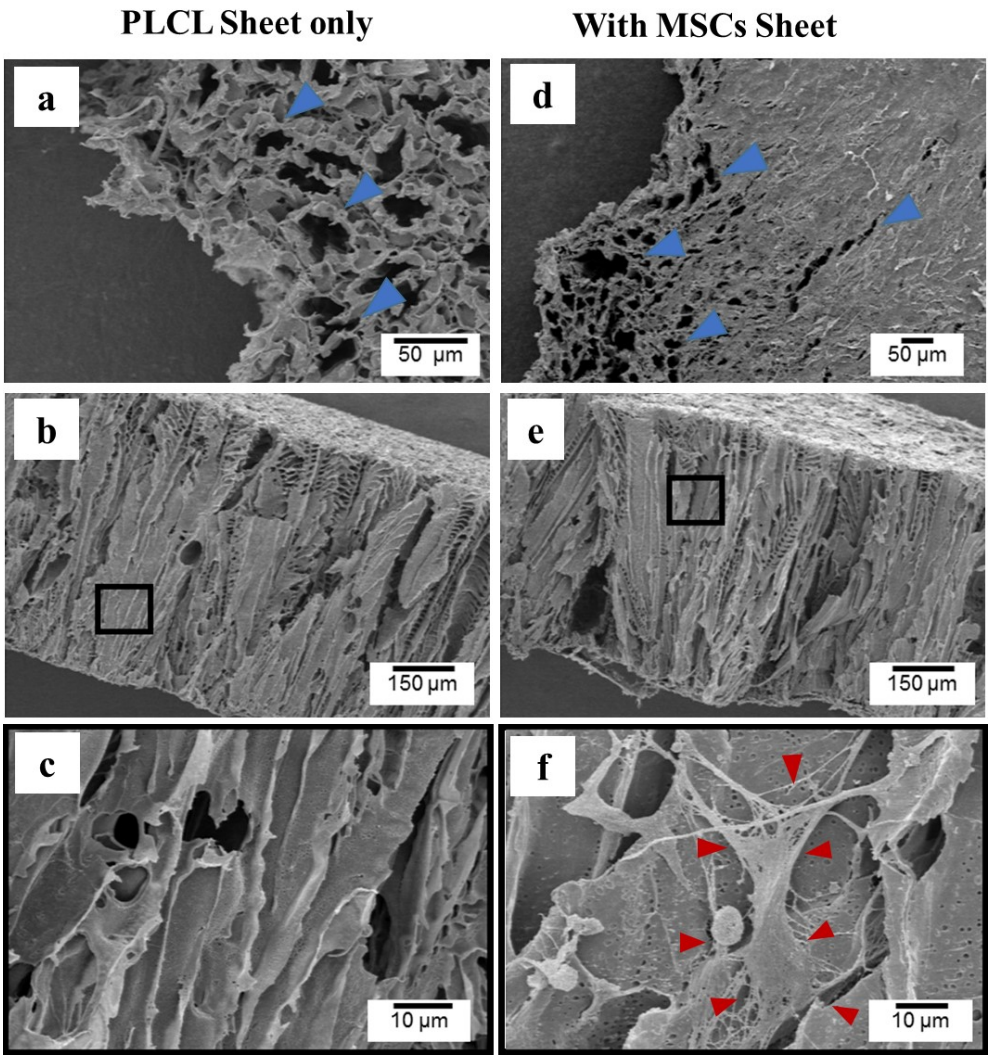

Figure 2.10. SEM images of deformed structure of 7 days of culture after tensile test. (a, d) The appearance of pore deformation at break point. (b, c, e and f) Fracture appearance in cross section. e and f show greater magnification. (cells, red head arrow).

2.4 Discussion

One of key success in tissue engineered vascular patch is the capability of cellularized patch scaffold to regenerate into new tissue and able to integrate with native vascular tissue. To encourage cellularization of patch graft, the scaffold should

promote cell migration and cell growing in three dimensional. Therefore, it is necessary to design scaffold with highly porous structure and interconnected. Solid-liquid phase separation subsequent with freeze drying method is a facile technique to construct scaffold with suitable porous structure and has been practiced to prepare tissue engineered patch for clinical trial [66]. In the present study, PLCL sheet fabricated by these methods had a porous structure with average pore diameter of 21 μm ± 4.5 (Figure 2.3a, b and c) which provides an adequate size to support cell infiltration (Figure 2.7) and proliferation (Figure 2.8).

Furthermore, to be able to integrate with native vascular tissue, it is important that tissue-engineered patch are anti-thrombogenic and resistant to immune response thus improving its durability. As such, it has been reported that matured endothelial layer on lumen area of vascular graft could maintain good long-term patency [77,78] . The scaffold is seeded with endothelial cells then cultured *in vitro* to allow the formation of endothelial layer on luminal surface of scaffold prior implantation. Therefore, this approach is potentially applicable in developing antithrombogenic tissue engineered patch. The technique, however, is mainly limited by two factors. First, cell seeding efficiency is low as not all cells attach on the scaffold. Second, the extended time to form a mature endothelial cell layer reduce its cost efficiency. In the present study, we addressed the mentioned limitations by employing cell sheet technology with biodegradable scaffold. Since the confluent HMSC can be harvested as an intact layer of HMSC, the seeding efficiency is higher compared to manual seeding using dissociated cells[79]. Moreover, HMSC sheet has been reported to repair myocardial infraction [56] and has capacity to differentiate into endothelial cells[75,76]. In this study, HMSC sheet was layered on porous PLCL sheet and remained attached and intact at 1 day of culture (Figure 3a and d). This combination technique enables the

preparation of mature cell sheet in parallel with scaffold fabrication, thus may allow construction process more efficiently in which usually take additional 1-4 weeks to create an endothelium on scaffold [80].

Apart from that, combination of cell sheet and porous scaffold could be an alternative way to overcome the cell sheet limitation. Previous study reported a difficulty to construct a thicker cell sheet because such high cell density environment showed necrosis and apoptosis due to lack of nutrient and oxygen supply [73,74,81]. We hypothesized that when cell sheet is combined with scaffold, the porous structure can provide channels for nutrient delivery and metabolic waste removal, thus enabling cell sheet to survive even in high cell density. In the present study, cells from HMSC sheet could migrate into PLCL sheet through connected porous and formed a new layer of HMSC sheet on the opposite side of PLCL sheet. The cross section image of histological staining (Figure 2.7c) revealed that cell sheet could reach thickness approximately 54 μm, without giving any indication of decreasing cell number during cell culture study, as supported with proliferation assays result (Figure 2.8).

This study focused on the influence of HMSC sheet on the mechanical behavior of PLCL sheet. It has been shown that PLCL sheet with HMSC sheet showed higher elastic modulus at 1 day of culture, however, from 4 to 14 days of culture, the elastic moduli of PLCL sheet with and without HMSC sheet could be maintained insignificantly different (Figure 5). It means that HMSC sheet is able to maintain the elasticity of graft. This influence on elasticity was also agreed with the previous study that reported cell sheet of smooth muscle cells improved the elasticity of electrospinned PLCL tubular graft[79]. In contrast, HMSC sheet gave a variational tensile strength behavior during *in vitro* which is characterized by the influence of cellular proliferation and infiltration, as summarized in Figure 2.11. On the initial day

of culture, the cells that migrated from HMSC sheet did not affect strongly in the increasing of tensile strength change. However, over the next 4 days of culture, cells were actively proliferating in the inner region and penetrated entirely into the pores, thus increase tensile strength around 26%. This kind of improvement is thought to be the effect of increasing of cell number which support on the collagen production, leading to increasing of tensile strength [82,83]. At 7 days of culture, a unique, layered, sandwich-like structure was observed, with cell sheets on both the surface and the bottom and polymer scaffold in the center. This layered construct had a tensile strength significantly greater than the PLCL sheet only although percentage of increase was decreased. At 14 days of culture, although cells continued to proliferate and formed a more mature layered construct, the degradation of PLCL sheet affected greater to the decreasing of tensile strength than strengthening effect by cellular infiltration. This degradation was supported by weight loss data of the PLCL sheet during incubation (Figure 2.9f). In 2 weeks, PLCL sheet had lost approximately 4% of its weight. This result suggested that hydrolytic degradation might have caused a significant structure erosion and strut thinning, thus affects greatly to the decreasing of tensile strength.

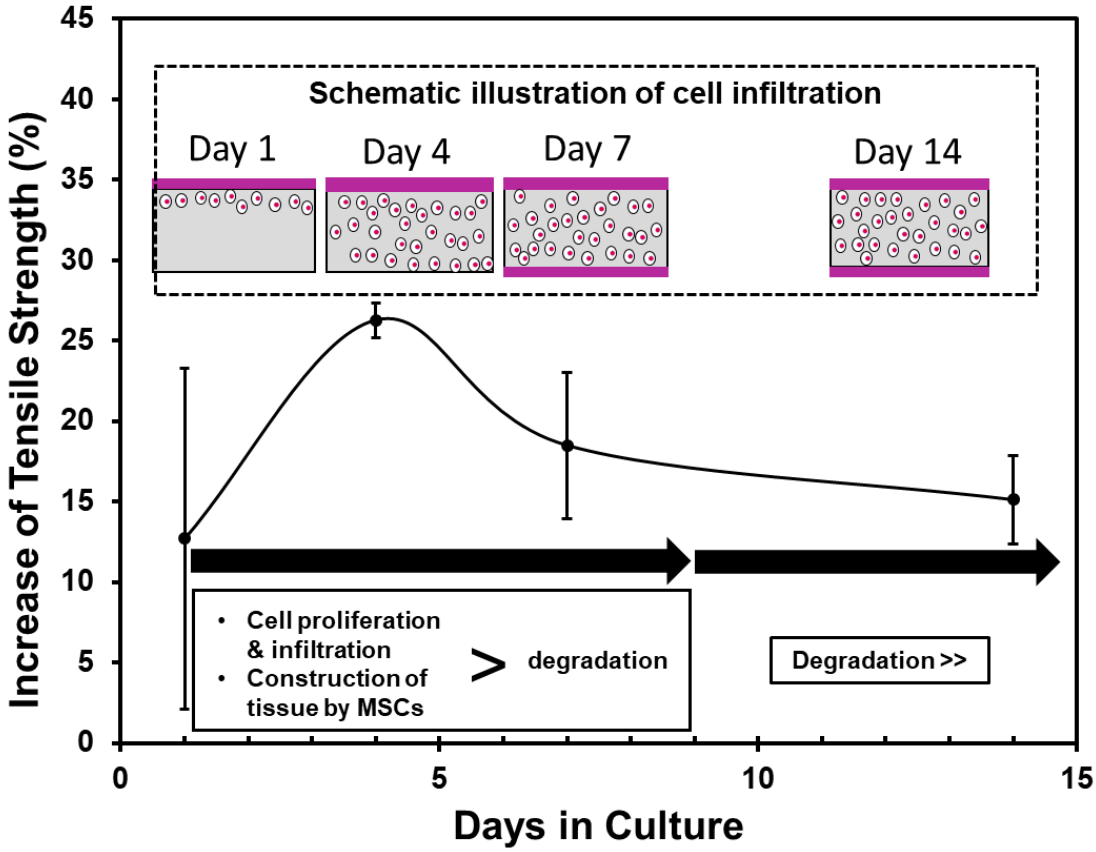

Figure 2.11. Variation of increase in tensile strength and its relation with cell infiltration.

The increasing material density due to cell penetration into the pores is considered to effect on the increasing of strain energy density greatly particularly at day 4 and 7 of culture (Figure 2.9e). The deformation mechanism of both PLCL sheet with and without cell sheet were characterized by ductile tearing failure of strut under tensile test. Both of them showed elongated pores at critical stress, however, the deformation region of PLCL sheet with cell sheet is wider than PLCL sheet only which is characterized to be the influenced of strain energy density increasing (Figure 2.10).

Finally, the described results demonstrates two important point. First, combining cell sheet with porous scaffold could be one of promising way to preserve

the critical properties of cells as well as provide better environment for tissue growth. Second, the results suggested that cell sheet could enhance the tensile strength and strain energy density of PLCL sheet thus may prolong biomechanical stability when implanted *in vivo*.

2.5 Conclusions

In this study we have developed new technique to construct tissue engineered patch by layering HMSC sheet on porous PLCL sheet. The conclusions were obtained as follows:

1. HMSC sheet was able to survive (even in a thicker density) and actively proliferated on porous PLCL sheet, suggesting that a porous structure is important in transporting nutrient and oxygen supply while removing metabolic waste.
2. Variations in the tensile strength of layered constructs were affected by two factors, cell proliferation and infiltration and the degradation of the PLCL sheet. Once the cell sheet had proliferated entirely into the pores of the polymer and formed a new layer on the opposite surface, the layered construct exhibited significantly higher tensile strength than that without the cells. However, after 14 days of culture the effect of the degradation of the polymer sheet overtook that of cell proliferation, resulting a decreasing of tensile strength.

CHAPTER 3 : DEVELOPMENT OF CYLINDRICAL HYBRID CONSTRUCT OF PLCL TUBULAR SCAFFOLD AND HMSC/HPAEC CO-CULTURE SHEET

3.1 Overview

In Chapter 2, we have developed an engineered-patch by layering HMSC sheet on porous PLCL sheet [84]. Using temperature-responsive dish, HMSC could be prepared within 4 days only. Simultaneously, PLCL sheet could also be prepared, therefore, with additional 1 weeks for maturation, the engineered construct could be ready within 2 weeks. Therefore, this combined techniques can be used to engineer the graft in emergency situations. Moreover, MSC sheet was able to penetrate into porous structure and form a new layer. We hypothesized if cell sheet can be combined with porous tubular scaffold, it can form a sheet on the lumen of the tubular scaffold, mimicking intima layer of the native blood vessel. As mentioned in Chapter 1, intima layer which contains of endothelial layer is a critical part to prevent platelet deposition and thrombus formation in vascular graft.

Therefore, in this chapter, a vascular construct by layering cell sheet onto PLCL cylindrical scaffold was developed. The cells sheet was prepared by co-culturing of HMSC and ECs because co-culture system was reported to promote higher proliferation rate[85]. Moreover, the angiogenic potential of co-culture HMSC and ECs is superior to that of monoculture containing either HMSC or ECs only

[75,86,87]. In addition, we expected that co-culture sheet could form a new layer on lumen of tubular scaffold and differentiate into endothelial cells resembling an intima layer.

The cylindrical PLCL scaffold was fabricated through solid-liquid phase separation method followed by freeze drying. The fabricated scaffold was then wrapped with co-cultured cell sheet. We monitored cell spreading behavior of cell sheet and whether cell sheet could penetrate into scaffold. We also investigated the effect of co-culture system to the proliferation and differentiation of cells on cylindrical scaffold. We also characterized the variational behavior of the tensile mechanical properties of the hybrid structure during the cell culture period.

3.2 Materials and Methods

3.2.1 Fabrication of Cylindrical Scaffold

Cylindrical scaffold was fabricated from PLCL (75:25) (Gunze ltd., Kyoto, Japan) by solid-liquid phase separation method followed by freeze drying, as previously described in Chapter 2. The resulted tubular graft was shown in Figure 3.1.

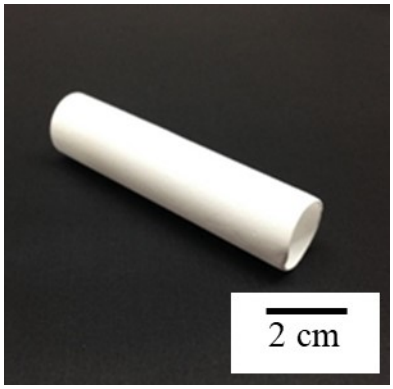

Figure 3.1 Overview of PLCL tubular scaffold

3.2.2 Preparation of Cell Sheet

The schematic procedure of the cell sheet preparation is illustrated in Figure 3.2. The co-culture cell sheets were prepared by seeding 5 × 10 cells composed of HHMSC (UE6E7TE, Riken RBC, Japan) and human pulmonary artery endothelial cells (HPAECs) (KA-4109, Kurabo, Japan) at cell ratio of 1:1 into 24 multi-wells of the temperature-responsive dishes (CellSeed Inc., Tokyo, Japan). The seeded cells were cultured in the cell growth medium (CGM) containing MEM-a (Wako, Osaka, Japan), 10% FBS, and 1% Penicillin-Streptomycin and EGM 2 (supplemented with 0.02 ml/ml FCS and 0.5 ng/ml VEGF) (Promo Cell, Heidelberg, Germany) at ratio of 50:50. For comparison, monoculture cell sheets were also prepared from only HMSC (5 × 10 cells) in the similar medium. After 4 days of culture, the confluent cells were detached spontaneously at room temperature for 20 min. The detached cell sheet was easily shrunk from original size, as shown in Fig. 2b. Therefore, after the medium was removed, the thin layer of membrane was layered on the top of confluent cells immediately. This membrane was used to prevent the confluent cells from shrinking and ease the transfer process on the cylindrical scaffold. The diameter of the cell sheet was approximately 10 mm.

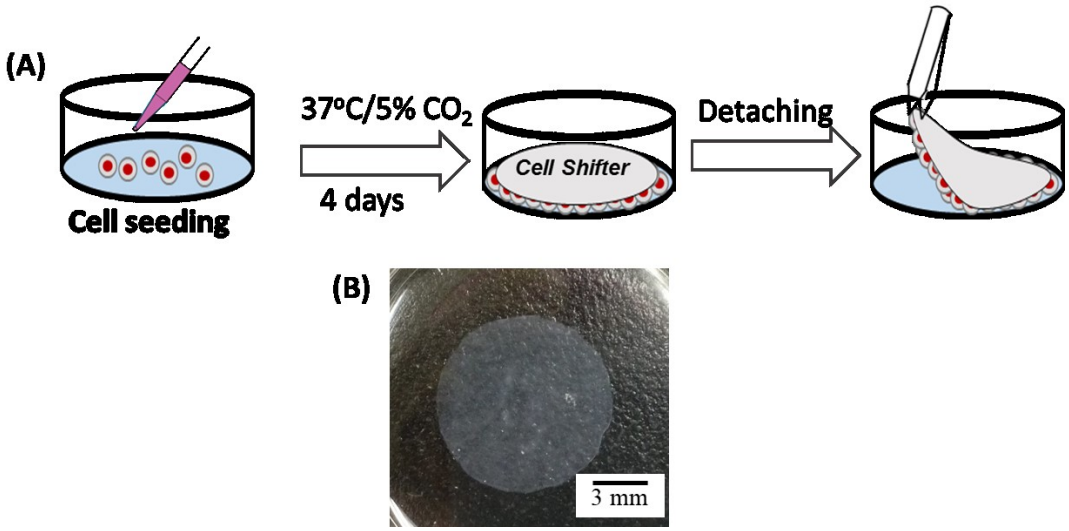

Figure 3.2 Schematic preparation of cell sheet.

3.2.3 Fabrication Hybrid Structure

Two pieces of HMSC/ECs or HMSC cell sheets were layered on the surface of a cylindrical PLCL scaffold as shown in Figure 3.3. These tubular structures were then cultured for 11 days in a mixed medium of CGM and EGM (50:50) for both type of cell sheets.

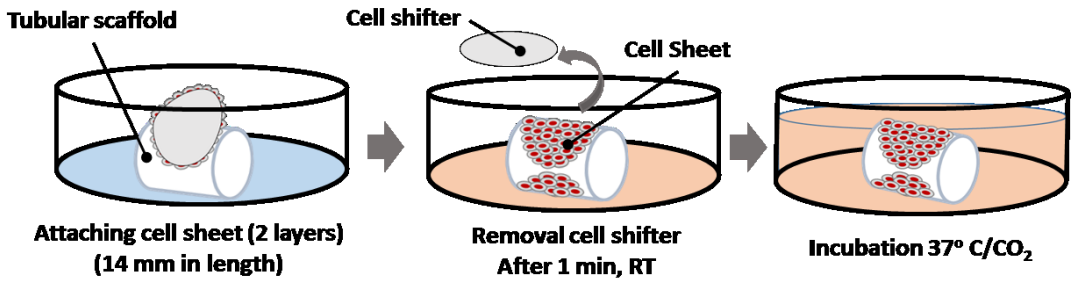

Figure 3.3 Schematic preparation of tubular scaffold layered with cell sheet.

3.2.4 Observation of Cell Growth Behavior

Cell spreading and infiltration were observed by a field emission scanning electron microscope (FE-SEM) (S-4100, Hitachi, Japan).. The samples were washed

with phosphate buffer saline (PBS), dehydrated in ascending concentration of ethanol (40%, 50%, 70% and 100%) and soaked in t-butyl alcohols. Then they were freeze-dried in a freeze drying machine (Hitachi, Tokyo, Japan), sputter-coated with Pt–Pd with an anion sputter coater (Hitachi, Tokyo, Japan) and analyzed by FE-SEM

3.2.5 Cell Proliferation Analysis

Cell proliferation was monitored by the colorimetric assay using cell counting kit (Dojindo, Kumamoto, Japan). The samples were washed with PBS, then soaked in a reagent containing tetrazolium salt that generate yellow when in contact with viable cells.The more intense the generated color, the more live cells contained within the graft. After incubating for 2 hours in 5% CO_2/37°C, the absorbance was measured at 450 nm with a microplate reader (Perkin Elmer, Yokohama, Japan).

3.2.6 RT-PCR

The expression of angiogenic gene was characterized using real-time Polymerase Chain reaction (RT-PCR). The samples were frozen in liquid nitrogen followed by grinding in a mortar to make into powder. The RNAs were isolated using RNA isolation kit (Nucleospin RNA, Germany) according to manufacturer's instruction. The RNA templates were then reverse-transcribed into cDNA with primescript (Takara Bio, Otsu, Japan) at ratio of 4:1, respectively. The RT-PCR was carried out using Thermal Cycler System (Takara Bio, Shiga, Japan). Each reaction contained: PCR forward primer (1µL), PCR reverse primer (1µL), cDNA (2µL), RNAse-free H_2O (8.5µL) and SYBR green (Takara Bio, Otsu, Japan). The list of primers was provided in Table 3.1. β-actin was used as housekeeping gene and the expression of angiogenic marker (VEGF and VEGFR) was calculated using the $\Delta\Delta C_t$ relative quantification method.

Table 3.1 List of primers sequence.

Gene	Primers	Size
β-actin	F TCCACCTTCCAGCAGATGTG	20
	R GCATTTGCGGTGGACGAT	18
VEGF (Vascular Endothelial Growth Factor)	F GTGGACATCTTCCAGGAGTACC	22
	R GAAACTCATCTCCCCTATGTGC	22
VEGFR (Vascular Endothelial Growth Factor-Receptor)	F CCAGCAAAAGCAGGGAGTCTGT	22
	R TGTCTGTGTCATCGGAGTGATATCC	25

3.2.7 Mechanical Characterization

Tensile mechanical testing was performed by a universal testing machine (Shimadzu, Kyoto, Japan) using the ring tensile method, as shown in Fig. 4.

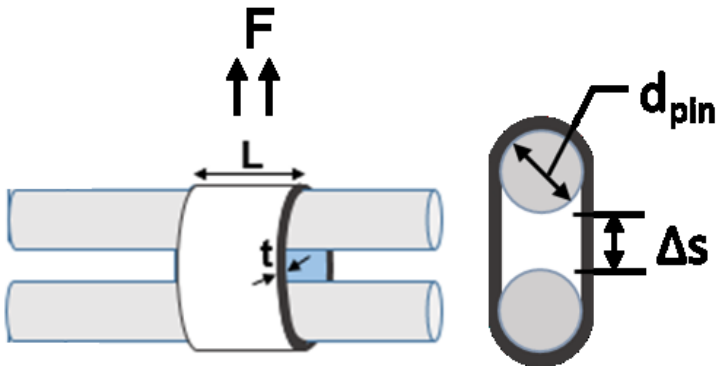

Figure 3.4 Illustration of ring tensile test.

It consisted of two small metal rods inserted into the lumen of the tubular specimen. One metal rod was then moved at a constant crosshead speed of 1 mm/min until the sample failed. The displacement and the load were recorded through a PC system. Using the displacement, Δs, the internal circumference, C, during deformation was calculated using the following formula [88],

$$C = d_{pin}\,(\pi + 2) + 2\Delta s, \qquad \text{Equation 3-1}$$

where d_{pin} is the diameter of metal rod. The strain was then evaluated as the ratio of C with the initial internal circumference, C_{init}, using the following formula:

$$\varepsilon = \frac{C - C_{init}}{C_{init}} \qquad \text{Equation 3-2}$$

The circumferential stress, s, was also calculated using the following formula:

$$\sigma = \frac{F}{2Lt} \qquad \text{Equation 3-3}$$

where F is the applied load during testing and, L and t are the length and thickness of tubular specimen, respectively. The elastic modulus was calculated from the slope of linier region of a stress–strain curve obtained from a ring tensile test.

The burst pressure, P, was also be able to estimate from the ring tensile tests by assuming that P is a critical value corresponding to the maximum load, F_{max} , at the failure of the tubular specimen [88]. The relationship between P and the stress σ is expressed on the basis of the Laplace's law equation:

$$\sigma t = PR_i \qquad \text{Equation 3-4}$$

where R_i is the internal radius of the tubular specimen. Then, substituting Equation 3-3 in Equation 3-4 with use of $D = 2R_i$ where D is the internal diameter one can obtain:

$$P = \frac{F}{LD} \qquad \text{Equation 3-5}$$

3.2.8 Statistical Analysis

Statistical significance was carried out using ANOVA with $P < 0.05$ considered as statistically significant and Fischer's LSD for mean comparison (KaleidaGraph® 4.0).

3.3 Results

3.3.1 Porous microstructure of cylindrical scaffold

FE-SEM micrographs of PLCL cylindrical scaffold is shown in Figure 3.5. The micrographs revealed that the size of pores on the external wall ranged between 22 and 600 µm with the average of 178.5 µm (Figure 3.5A and a). The cross-sectional images showed the extension of the pore channels connecting each other, creating continuous porous structures (Figure 3.5B and b). The internal wall also exhibited a porous structure in which the pore size ranged between 10 and 100 µm with the average size of 28.8 µm (Figure 3.5C and c).

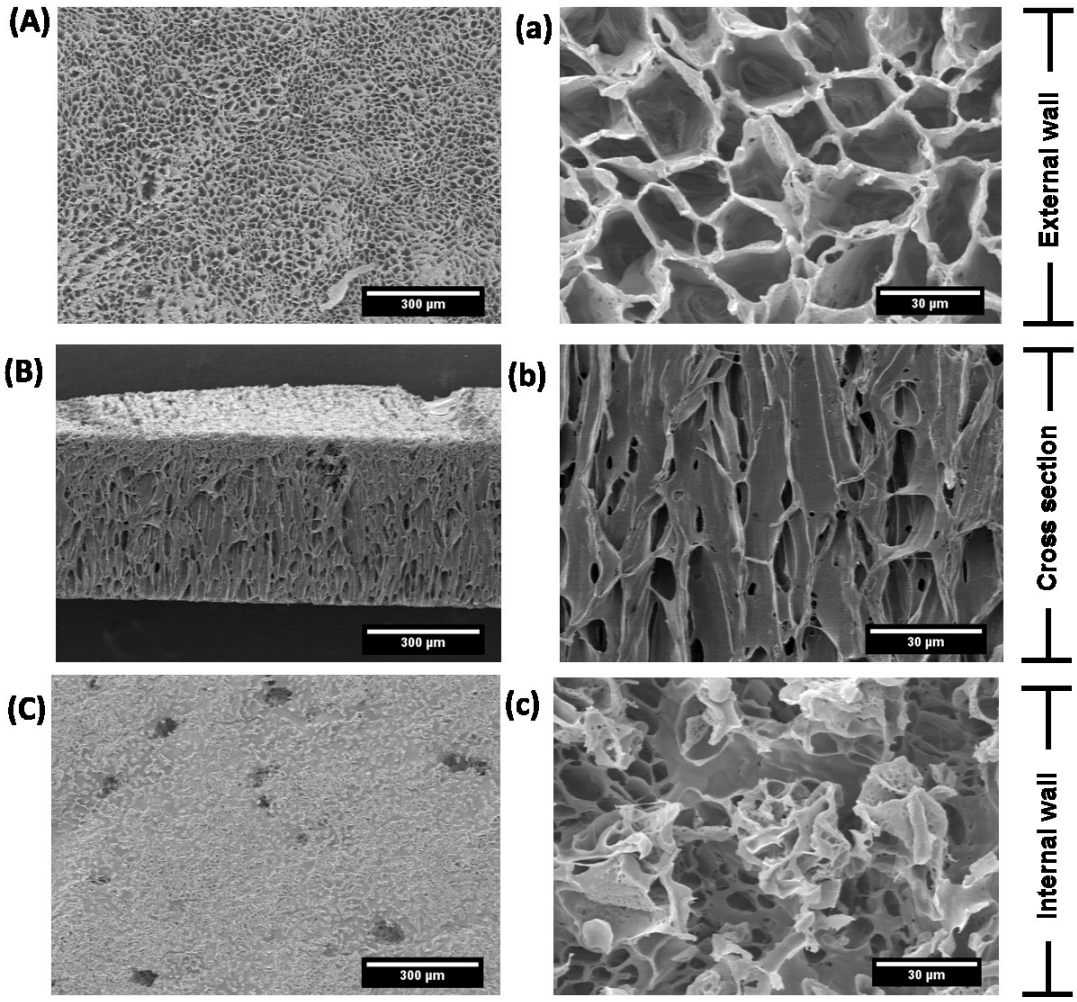

Figure 3.5 FE-SEM micrographs of PLCL cylindrical scaffold. A,B,C and a,b,c showed low magnification and high magnification images, respectively..

3.3.2 Morphology of Cell Spreading and Penetration

FE-SEM micrographs of a PLCL cylindrical scaffold with layered monoculture cell sheets are shown in Figure 3.6. It was observed that the proliferated cells and collagen fibrils creating a network structure covered the external wall of the scaffold (Figure 3.6 A and a). Collagen fibrils and bundles with spherical cells were also found in the elongated pore channels in the cross section images (Figure 3.6B and b). Moreover, collagen networks were created actively on the internal wall of the scaffold as shown in Figure 3.6 C and c.

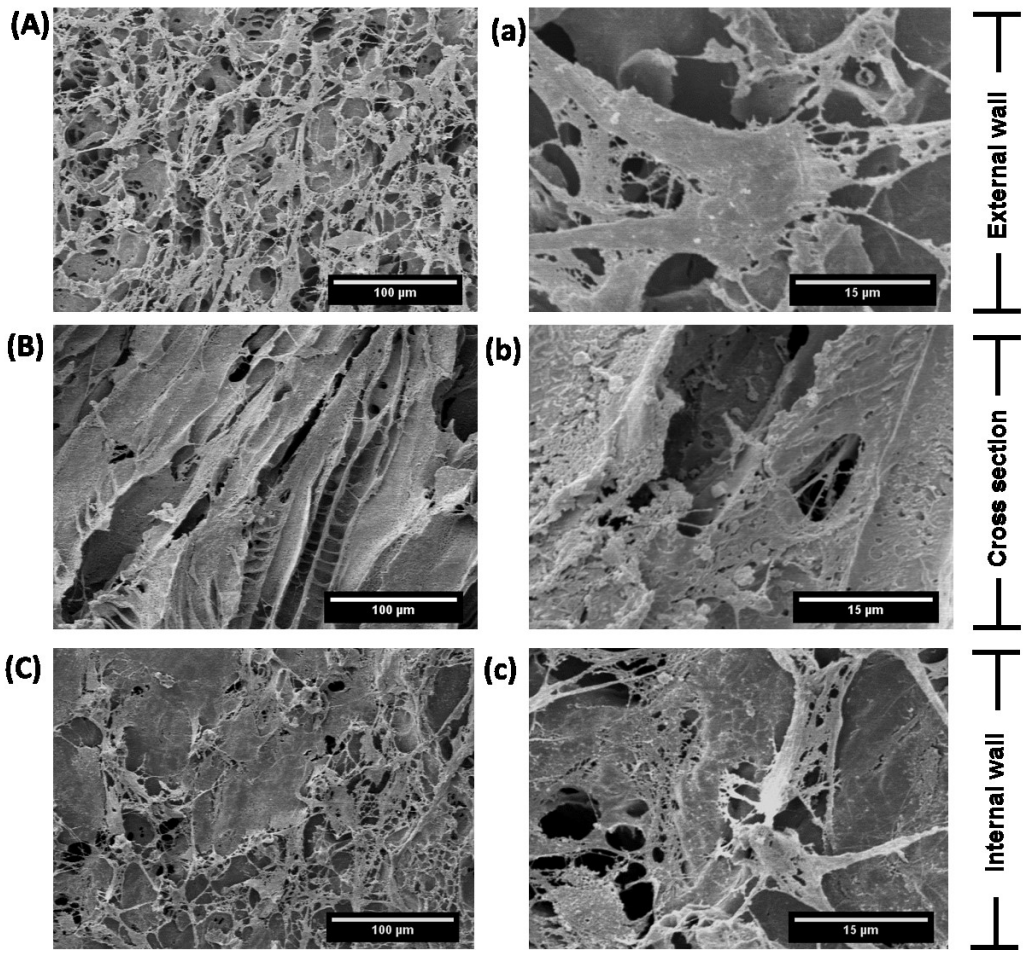

Figure 3.6 FE-SEM micrographs of PLCL tubular scaffold with monoculture cell sheet at 7 days of culture. A,B,C and a,b,c showed low magnification and high magnification images, respectively.

.

FE-SEM micrographs of the scaffold with the co-culture cell sheet at 7 days of culture are shown in Figure 3.7. On the external wall, a thick fascicle formation was found to completely cover the surface, resulting unobservable pores as shown in Figure 3.7A and a. Similar to the scaffold with the monoculture cell sheet, the collagen bundles were also observed in the elongated pore channels along with the spherical cells (Figure 3.7B and b). It was also seen in Figure 3.7C and (c) that cells actively spread on the internal wall. This suggested that cells were able to penetrate into the pores and further form a new layer on the luminal surface of the scaffold. Significant difference on the cell morphology between the monoculture and the co-culture cell sheets was not found from these FE-SEM micrographs.

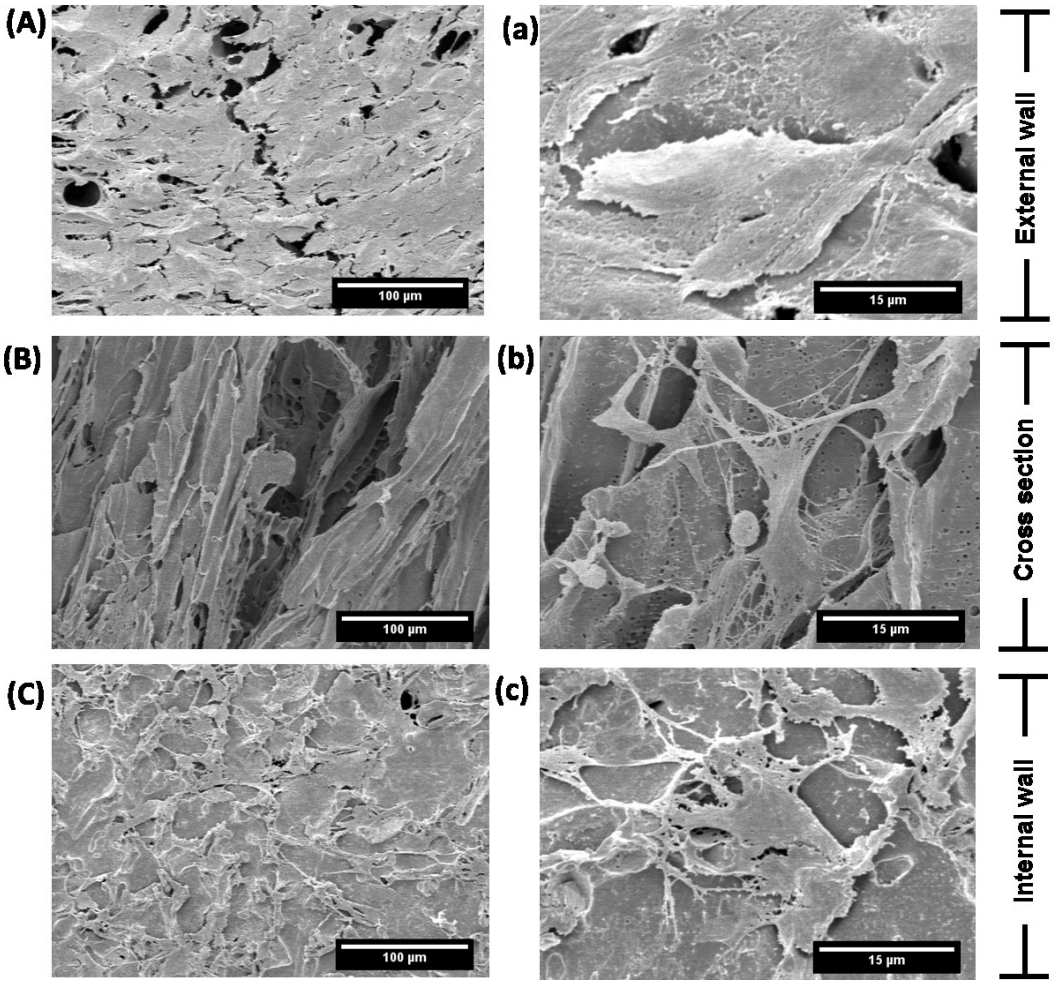

Figure 3.7. FE-SEM micrographs of PLCL tubular scaffold with co-culture cell sheet at 7 days of culture. A,B,C and a,b,c showed low magnification and high magnification images, respectively.

3.3.3 Cell Proliferation

Figure 3.8 show the scaffold with the monoculture cell sheets (Figure 3.8a, b) and with the co-culture cell sheets (Figure 3.8c, d), respectively. The intensity of yellow color in the co-culture system was much higher than that of the monoculture system, suggesting that the co-culture system contained more cells. At 7 days of culture, the co-culture system was colored entirely in yellow, indicating that the co-culture cell sheets completely covered the surface of the scaffold. Meanwhile, non-uniform color was observed in the monoculture system, suggesting that it might take more than 7 days to cover the entire surface.

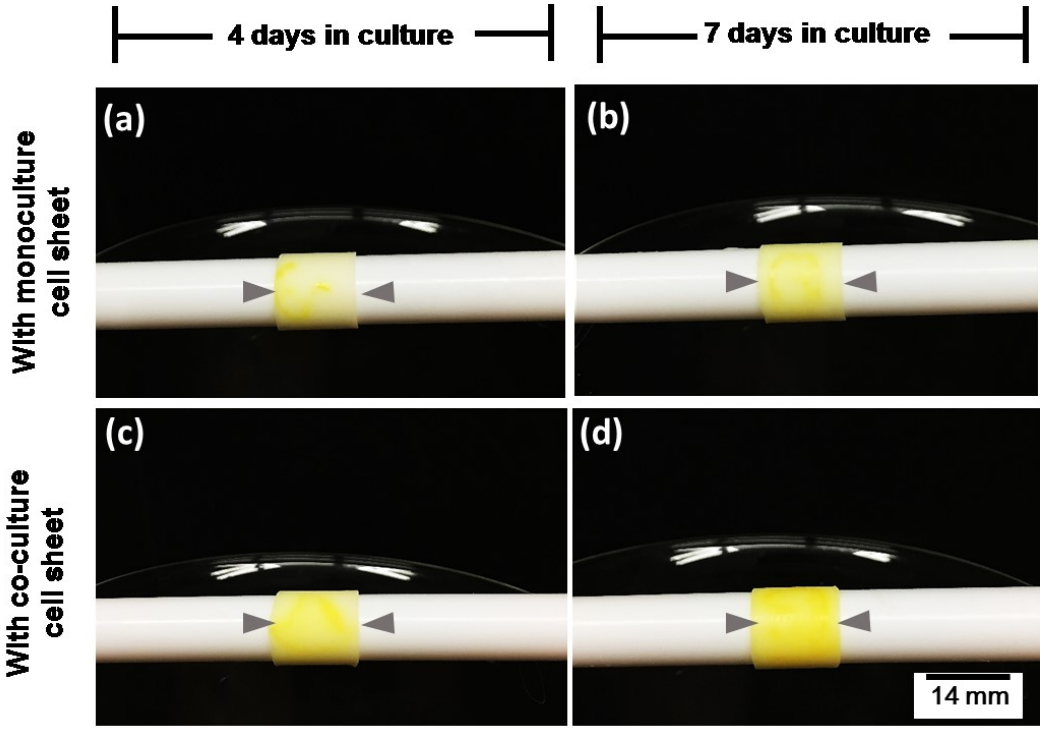

Figure 3.8 Colorimetric assay of the tubular scaffold with monoculture cell sheet and co-culture cell sheet. Light micrograph of tubular scaffold with monoculture cell sheet (a,b) and with co-culture cell sheet (c,d) at 4 days (left panel) and 7 days (right panel) in culture. Head arrows indicated the tubular scaffold.

The cell proliferation behavior in the both systems are shown in

Figure 3.9. It was obviously seen that cells in the co-culture system proliferated higher than that in the monoculture system, clearly suggesting that such co-culture environment enhanced proliferation of cells. Though cells proliferated aggressively in the first week of culture, the number of cells after 7 days maintained constant in both the systems. This behavior might be related to either over confluence or cell differentiation.

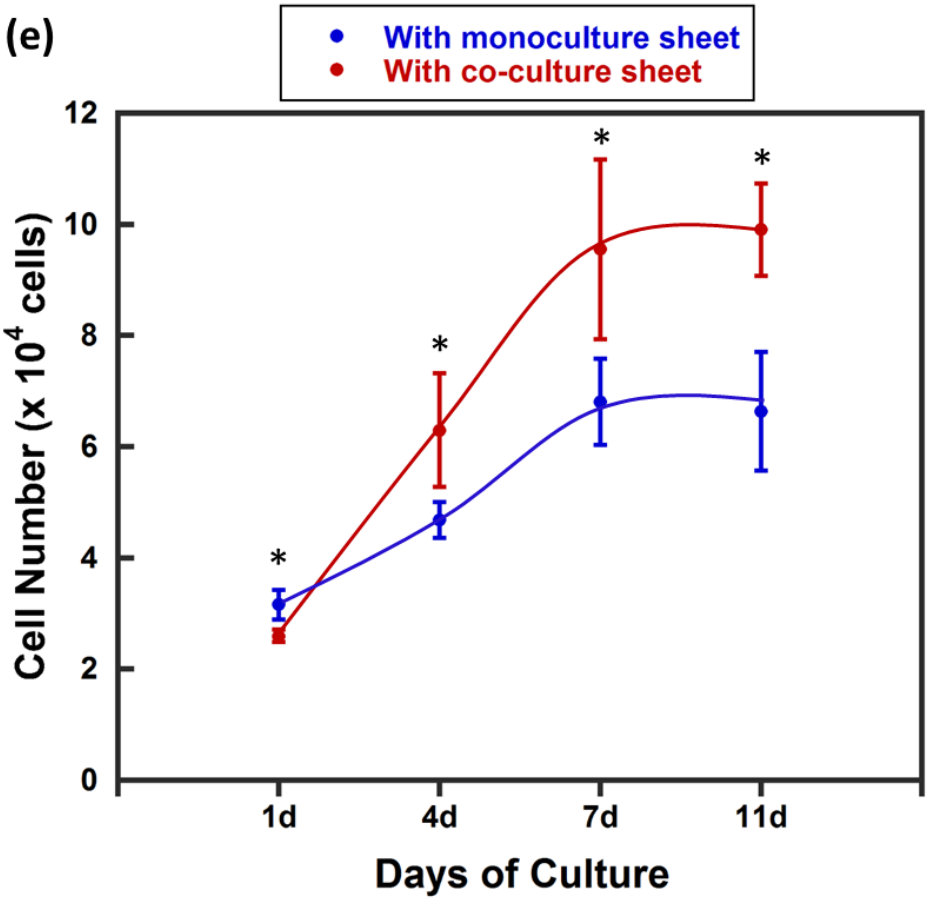

Figure 3.9 Cell proliferation within the tubular scaffold during *in vitro* course. Each data was presented as mean ± SD (n=3), * indicate $p<0.05$ versus the cell number at respective day.

3.3.4 Gene Expression

Figure 3.10 showed the gene expressions of some angiogenic markers, including VEGF and VEGFR, in both the culture systems. The expression of VEGF in the coculture system was higher than that in the monoculture system, particularly at days 11 (Figure 3.10a).VEGFR expression, the receptor of VEGF, was significantly enhanced in the co-culture system more than that in the monoculture (Figure 3.10b).

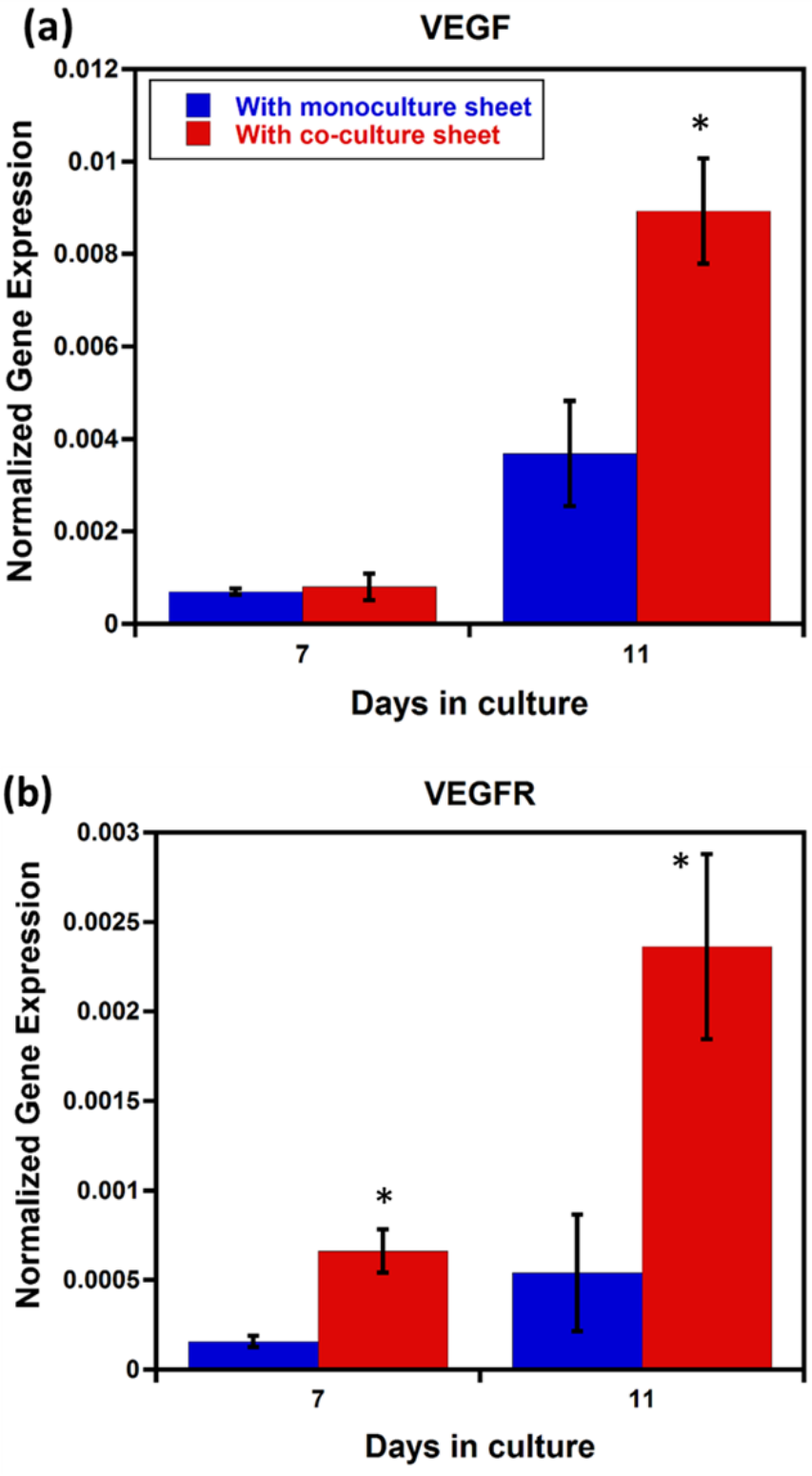

Figure 3.10 Gene expression of vascular endothelial growth factor (a) and its receptor (b) within the tubular scaffold. Each data was presented as mean ± SD (n=3), * indicate $p<0.05$ versus the cell number at the respective day.

3.3.5 Mechanical Characterization

The results of the ring tensile tests are shown in Figure 3.11a–c. The estimated burst pressure values are also shown in Figure 3.11d. All the stress–strain curves exhibited nonlinear deformation behavior mainly caused by the micro-porous structure of the scaffold. It was apparent that the modulus and strength of the scaffold only tended to decrease with days of culture, while those properties of the culture systems tended to be recovered at 11 days of culture as an effect of cell proliferation. The burst pressure also exhibited the same tendency with the modulus and strength. All of the estimated burst pressure values were greater than 120 mmHg that is almost equivalent to the normal blood pressure of human being.

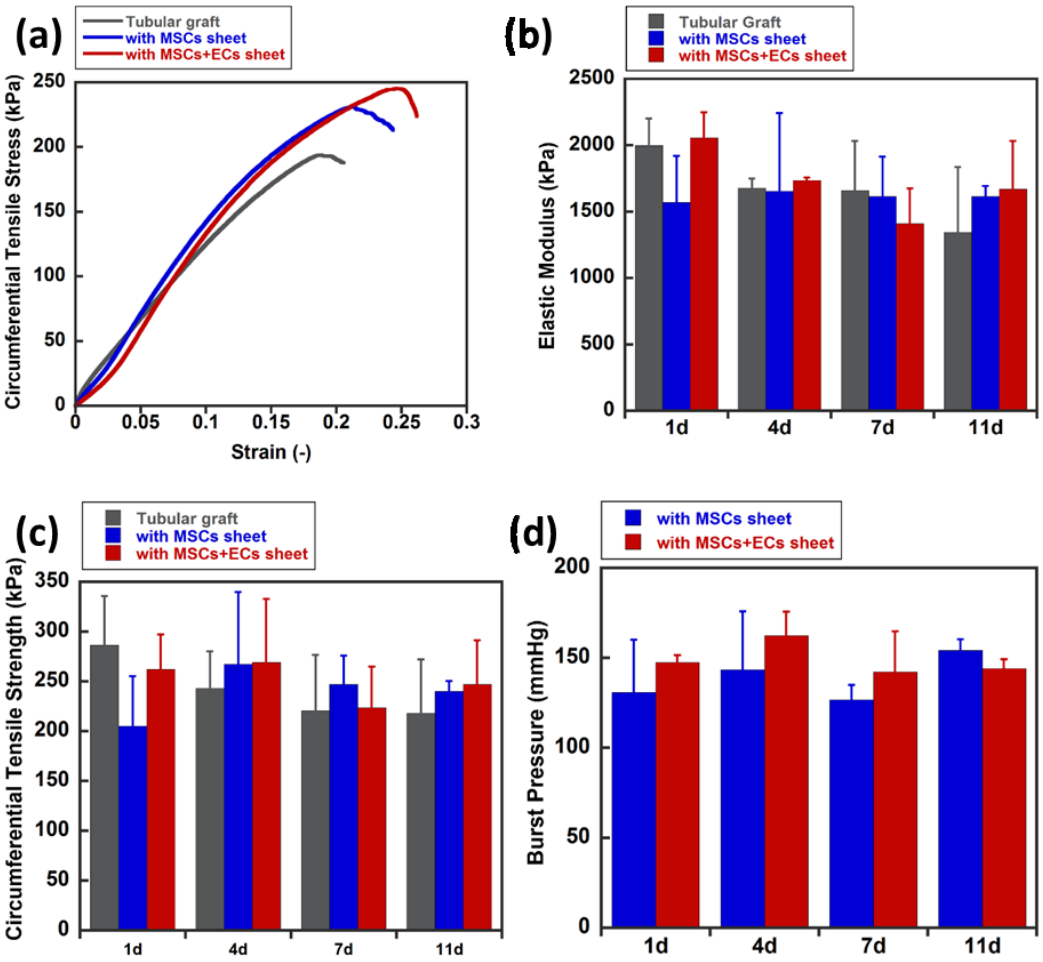

Figure 3.11 (a) Stress-strain curve at 11 day culture, (b) Comparison of average elastic modulus, (c) Comparison of average circumferential tensile strength, and (d) Comparison of estimated burst pressure. Each data was presented as mean ± SD (n=3).

3.4 Discussions

In the present study, we developed a tubular hybrid polymer-cell structure by combining the cell sheet and cylindrical scaffold technologies. To encourage cell migration and growth, the scaffold should be porous and interconnected with appropriate pore diameter greater than 10 μm [89,90]. The inability of cells to infiltrate into scaffolds due to limited pore size has been a major drawback in most of

vascular scaffolds [91–93]. The pore diameter of the porous scaffold developed in this study had an average pore diameter of 21 μm which was enough size for cell migration. Furthermore, it should be worth noted that the cells proliferated from the cell sheets could migrate into the pores and further formed a new layer on the luminal area of the scaffold as shown in Figure 3.6 and Figure 3.7 within a week after the cell sheet layering. Thus, this combining technique in which cell sheets placed on the surface of interconnected porous scaffold enabled the cells to grow and form a three dimensional biological structure. A large number of cells are required for creating engineered vascular tissues. An enhanced proliferation rate may shorten in vitro maturation period and further will accelerate new tissue regeneration after implantation. The present study exhibited that the cell number in the co-culture system increased higher than the monoculture system as shown in

Figure 3.9. Bidarra et al. [85] demonstrated that ECs stimulated the proliferation of HMSC via direct contact between the two cell types. They cultured HMSC and ECs in a well dish and monitored the number of each cell type using a flow cytometry after separating through magnetic separation. It was found that the number of HMSC in the co-culture increased rapidly throughout 21 days while the number of HMSC in the monoculture increased only in first 2 weeks of culture. Meanwhile, it was reported that HMSC proliferation was also enhanced via indirect co-culture with ECs [94]. The experiment was performed by cultivating ECs in a cell culture insert with pore size 1 μm to prevent direct heterotypic cell contact. These findings suggest that such stimulative effect of ECs on HMSC proliferation is not only contributed by heterotypic cell contact but also mediated by soluble-paracrine factors secreted by ECs. Moreover, Steiner et al. [94] revealed an anti-apoptotic effect on HMSC when co-cultivated with ECs. They performed BAD phosphorylation ELISAs to investigate if

ECs exerted their effect on HMSC apoptosis by modulating phosphorylation of BAD. It showed that ECs induced a significantly different amount of BAD phosphorylation in direct co-culture, suggesting that ECs was able to reduce apoptosis of HMSC.

It is well known that ECs stimulate the osteogenic differentiation of HMSC [75,95,96]. The present study also revealed that ECs had ability to induce angiogenic differentiation of HMSC via direct co-culture. Angiogenesis is a vital process in the development of new blood vessels. The expression was induced by growth factor such as VEGF [56,75]. At the first week of culture, cells in both of the culture systems experienced highly proliferation rate but the expressions of VEGF and VEGFR were relatively low as shown in Figure 3.10. At 11 days of culture, the cell number in both the culture systems remained almost same with that of 7 days. As we hypothesized that cells may started to differentiate after the first week passed, significant increases of both VEGF and VEGFR expressions were found in both the systems, suggesting that angiogenesis occurred. It should be underlined that both the culture systems used EGM-2 which contained VEGF. This factor might stimulate the angiogenesis in the monoculture system and further double the effect in the co-culture system since ECs also secret VEGF. Our finding was in accordance with Li and Wang [75] which showed that co-cultured cells expressed more angiogenic marker than mono-cultured cells.

Taking together, this study demonstrated that the layering co-cultured cell sheets on the cylindrical scaffold had benefits not only to promote high proliferation rate but also provide favorable environment for angiogenesis. This hybrid system might be crucial in development of engineered cardiovascular tissues since absent of endothelium on the luminal of prosthetic grafts could result in thrombosis and intimal

hyperplasia leading to graft failure. It is worth noting that real cardiovascular tissues have more complicated layered structures with higher mechanical properties than the simple dual layered system developed in this study; for example, a fibrous polymeric layer can be added to the outer surface as a reinforcement to improve its mechanical properties. Further studies are needed to apply this concept of hybrid system to the development of engineered cardiovascular tissues that can be clinically applicable.

3.5 Conclusions

In this study, a hybrid tubular structure was developed by layering HMSC/ECs cell sheets on a porous cylindrical PLCL scaffold. Cells from the cell sheets were able to infiltrate through the porous structure of the cylindrical scaffold and further proliferate on the luminal wall within a week of culture. Moreover, the co-culture cell sheet within the scaffold demonstrated a faster proliferation rate than the monoculture cell sheet. The gene expression of angiogenic differentiation in the hybrid system with the co-culture cell sheet was expressed in relatively large amount as compared to that with the monoculture cell sheet. This technique would activate the cellularization of engineered vascular tissues in a relatively short period with exhibiting a large amount of angiogenic properties.

CHAPTER 4 : IMPROVEMENT OF MECHANICAL CHARACTERISTIC OF PLCL SCAFFOLD

4.1 Overview

In Chapter 2 and 3, the development of hybrid grafts by combining PLCL scaffold and cell sheet prepared from either MSCs or MSCs/ECs have been demonstrated. It should be noted that the tensile strength of the fabricated scaffold is in the range of 200 kPa to 400 kPa with the estimated burst pressure of around 150 mmHg. In fact, the ultimate tensile strength of the human arterial tissue is in the range of 780 kPa to 1370 kPa [97] and burst pressure of ≥1700 mmHg (equal of saphenous vein) [1]. Thus, the fabricated scaffolds may be not sufficient to withstand the physiological pressure of blood flow when implanted into human body.

To improve the mechanical properties of PLCL scaffold, the three approaches were employed in this study. The first approach is by developing multiple layers of PLCL scaffold in order to reinforce the mechanical strength. Single layer of PLCL scaffold was further subjected to the phase separation and freeze drying method to create the double and the triple layer scaffolds. The mechanical tensile test were conducted to study the effect of reinforcement of the double and triple layers scaffolds. In the second approach, porous PCL/PLCL polymer blends were developed. By blending these two polymers, the mechanical properties can be controlled. Phase-separation and freeze-drying method were still utilized in this approach. The

mechanical properties as well the microstructure behavior were characterized. The third approach employed the melt spinning method [98] to fabricate PLCL tubular scaffold. One of the main advantages of this technique is that commercially available cotton-candy machines may be directly used to fabricate scaffolds for medical applications. In the cotton-candy machines, melted polymer is centrifugally forced through a small hole to make fibers. The aim of using cotton candy machine is to produce fibrous PLCL cylindrical scaffolds in a simple cost-effective way and free from toxic solvent. To the best of our knowledge, few attempts have been made to fabricate fibrous cylindrical scaffolds using the melt-spinning method. As the fundamental properties, tensile mechanical properties and cellular activities were examined. Furthermore, the fabricated microfibrous cylindrical scaffold was compared with the microporous cylindrical scaffold previously developed using the phase-separation and freeze-drying method.

4.2 Materials and Methods

4.2.1 Scaffold Fabrication

4.2.1.a Multiple Layers of PLCL Scaffold

The cylindrical scaffold was fabricated using solid-liquid phase separation with freeze drying method, as described previously in Chapter 2. In brief, a Teflon rod prepared at -80°C, was immersed quickly in PLCL (75/25) (Gunze Ltd., Japan) solution 6 % (w/v in dioxane). Then, the specimen was dried under freeze-drying vacuum for 24 hours. The above procedure was repeated to get double and triple layers of cylindrical scaffold. The fabricated scaffold was stored in a dehumidifier chamber before further use.

4.2.1.b PLCL/PCL Blends Scaffold

PCL and PLCL granule with various weight ratio (100:0, 75:25, 50:50, 25:75, 0:100) were dissolved in dioxane (Kishida Chemical, Osaka, Japan) with final concentration of 6% (w/v). A Teflon rod of 10 mm in diameter prepared at -80ºC was vertically dipped into the blending solution and pulled out at a constant rate of 100 mm/min. The blends solution was varied in temperature before the dipping process from 20 °C, 30 °C, 40 °C, 50 °C to 60°C. After frozen again into -80º C for 2 hours, it was dried into a freeze drying machine (Tokyo Rikakikai, Tokyo, Japan) at -50ºC for 24 hours. Finally, the fabricated graft was pulled out from the Teflon rod and stored in a dehumidifier chamber before further use.

4.2.1.c Melt Spinning of PLCL Scaffold

The microfibrous cylindrical scaffold was fabricated from PLCL (75/25) (Gunze ltd., Kyoto) using a cotton candy machine (EA-WA2805, EAST). Two gram of PLCL granules were put into the spinning head of cotton candy machine. The spinning speed is 1800 rpm. After 3 minutes and the temperature reached 180 °C, the PLCL fibers (Tm 163°C) started to form. The fibers were immediately collected on Teflon rod (ϕ 5 mm) and dried for one night. The fabrication illustration was shown in Figure 4.1a.

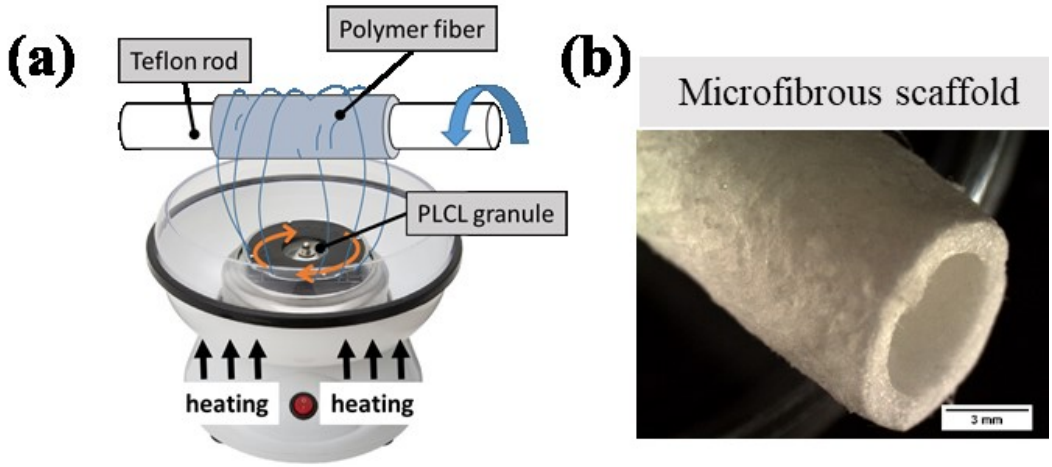

Figure 4.1 (a) Fabrication process of microfibrous scaffold using cotton candy machine. (b) Photograph of the fabricated scaffold.

4.2.2 Infrared Spectroscopy (IR)

Infrared spectroscopy (FTIR) (JASCO 4200, Japan) was performed to confirm chemical structure of blending polymer using FTIR.

4.2.3 Differential Scanning Calorimeter (DSC)

Thermal analysis including melting point (T_m) and glass transition temperature (T_g) were measured by a DSC (Shimadzu, Japan). 2.5 mg sample was used and put into an aluminum sample pan. The sample was heated from room temperature to 230°C at a rate of 10°C/min. The temperature and DSC curve was recorded.

4.2.4 Morphology

4.2.4.a Thickness and Microstructure Characterization

The thickness of scaffold was measured by Image J software [99] using representative images from SEM observation. The sample was sputter-coated with Pt-Pd by anion sputter coater (Hitachi, Japan). The microstructure was observed using Field Emission-Scaning Electron Microscopy (FE-SEM) (Hitachi, Japan). The

resulted SEM images were also used to measure pore size of sample using Image J (NIH).

4.2.4.b Porosity

The porosity was calculated using a direct method described by [100]. The scaffold samples were cut into 100 mm^2 and the weight at dry condition was measured accurately (W1). Then, the samples was impregnated in ethanol for 1 hour. The impregnated samples were removed from ethanol and the excess liquid was wiped with tissues, then weighed again (W2). Pore volume (Vp) was calculated using the following formula:

$$V_p = \frac{W_2 - W_1}{\rho_{ethanol}} \qquad \text{Equation 4-1}$$

$\rho_{ethanol}$ is 0.97 g/ml. The porosity was calculated using the following formula:

$$Porosity\ (\%) = (1 - \frac{V_m}{V_t})x100 \qquad \text{Equation 4-2}$$

where Vm is the scaffold volume and calculated by Vm = Vt-Vp.

4.2.5 Mechanical Characterization

The mechanical characterization was performed by universal testing machine (Shimadzu, Japan) using a ring tensile technique, as described in 3.2.7.

4.2.6 Cell Study

Human mesenchymal stem cells (hMSCs) (Riken BRC, Japan) were seeded into the microfibrous and microporous scaffolds, respectively, with cell density of 12000 cells/cm^2. They were then cultured for 7 days with cell growth medium

containing MEM-α, 10% Fetal bovine serum and 1% penicillin streptomycin at 37 °C / 5% CO_2. The number of viable cells was monitored using a cell counting kit (Dojindo, Japan). The cell morphology was observed using FE-SEM and analyzed using Image-J. Statistical analysis was performed using ANOVA with Fischer's LSD post hoc test. Each data represented as mean ± SD and $P < 0.05$.

4.3 Results

4.3.1 Properties of Multiple layers of PLCL Scaffold

4.3.1.a Morphology

Figure 4.2 showed microstructural behavior of outer wall of each scaffold. A typical pores structure was evidently observed on the three layered-scaffolds. These pores was created due to phase separation between polymer-rich phase and solvent. During freeze-drying, the polymer-rich phase solidified to form strut and the solvent evaporated creating pores structure. On the single layer scaffold, the average pore area was 219 μm^2. Larger pore area was observed on the double and triple layer scaffolds, 744 μm^2 and 684 μm^2, respectively. It was obvious that pores morphology on the double and triple layers were less often, compared to that on the single layer scaffold. On the inner wall (Figure 4.3), smaller pore size was observed compared to that on the outer wall. However, a less often pores were also observed on the double and triple layer scaffold, compared to that on single layer scaffold. SEM images of cross section wall were showed in Figure 4.4. The thickness of the single layer scaffold is around 583 μm. It was expected that the thickness increased as the number of layer increased. However, the double and triple layers did not exhibit an increased thickness significantly from the single layer scaffold. In fact, as the number of layer increased, the density also increased, while the porosity decreased. The single layer scaffold

showed oriented microtubular architecture that connecting each other, but it was then compacted as the next layers was introduced, observed on the double and triple layers scaffolds. The inter-layer boundary was clearly visible on the double and triple layer scaffold.

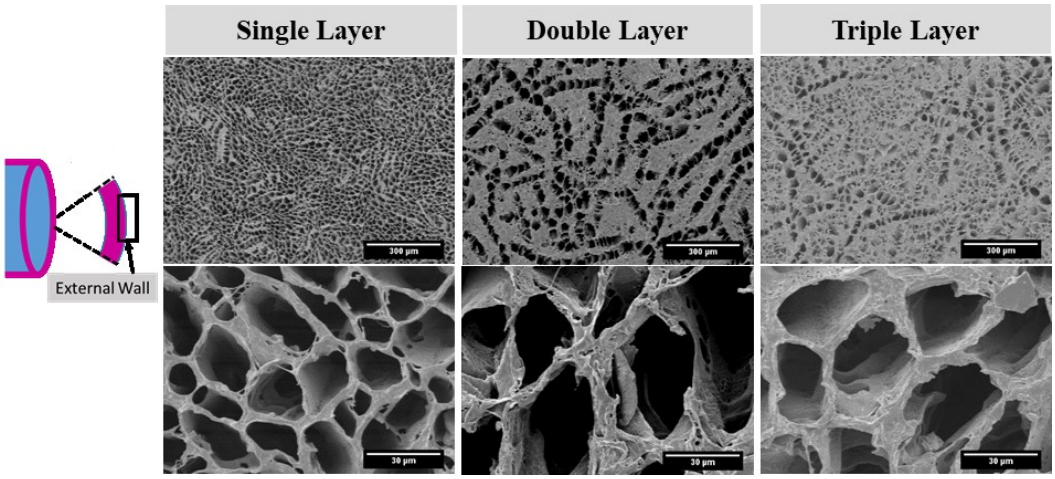

Figure 4.2 SEM images of the outer wall of single, double and triple layer scaffold.

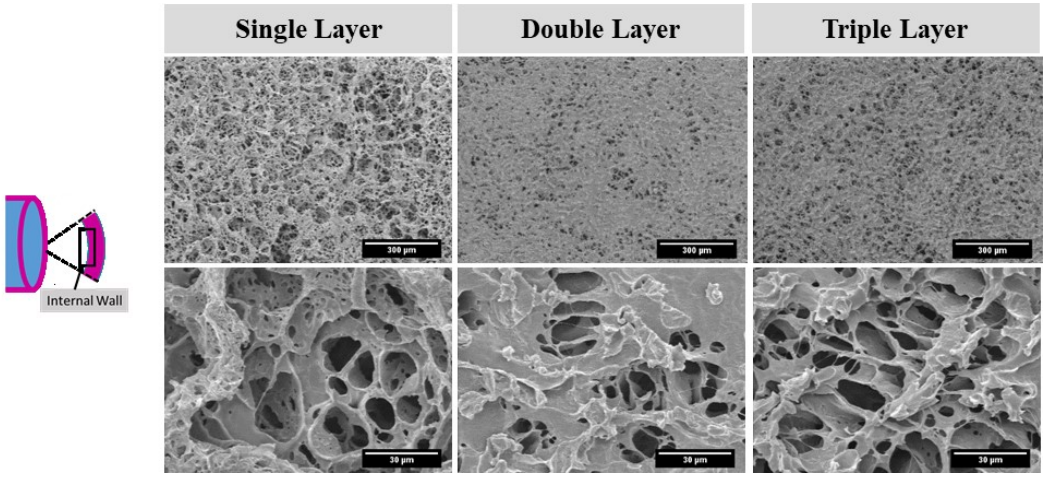

Figure 4.3 SEM images of the inner wall of single, double and triple layer scaffold.

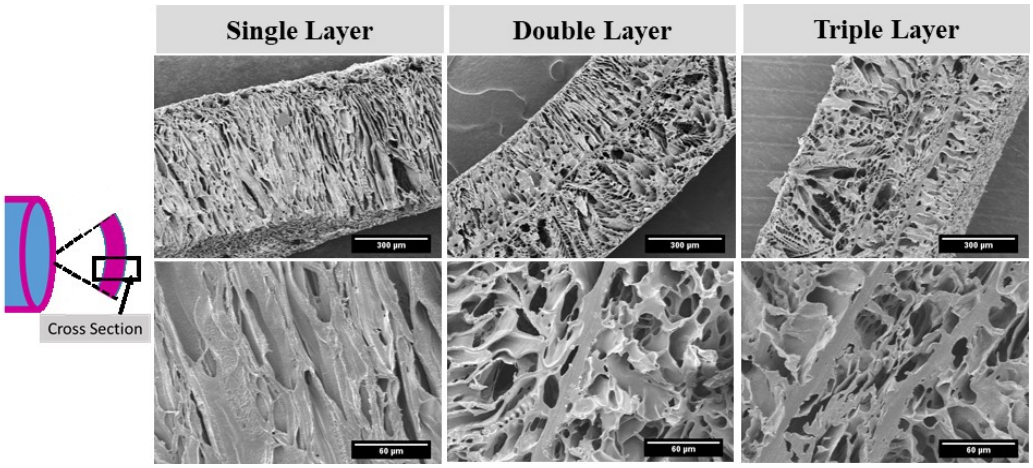

Figure 4.4 SEM images of the cross section of single, double and triple layer scaffold.

Table 4.1 Physical and Pore Morphology of the Layered Cylindrical Scaffold

Scaffold Type	Mean pore area (μm^2)	Thickness (μm)	Density (g/ml)	Porosity (%)
Single layer	219	583	0.201 ± 0.008	92.8 ± 3.79
Double layer	744	635	0.228 ± 0.011	68.9 ± 3.32
Triple layer	684	675	0.305 ± 0.012	64.9 ± 1.66

4.3.1.b Mechanical Properties

The typical stress-strain curve was shown in Figure 4.5a. It was found that the cylindrical scaffold exhibited steeper stress-strain curve as the number of layer increased. Figure 4.5b showed the elastic moduli of the multiple layers of cylindrical scaffolds. The elastic moduli were measured from the slope of linier region of stress-strain curve. The elastic moduli ranged between 0.93 MPa to 16.7 MPa. The single layer scaffold exhibited the lowest elastic modulus and the value significantly increased with increasing number of layer. The circumferential tensile strength was

shown in Figure 4.5c. The tensile strength was in the range between 0.2 MPa to 1.4 MPa and increased with the increased number of layer. However, the failure strain only increased from single to double layer and did not differ from the double to triple layers of scaffolds.

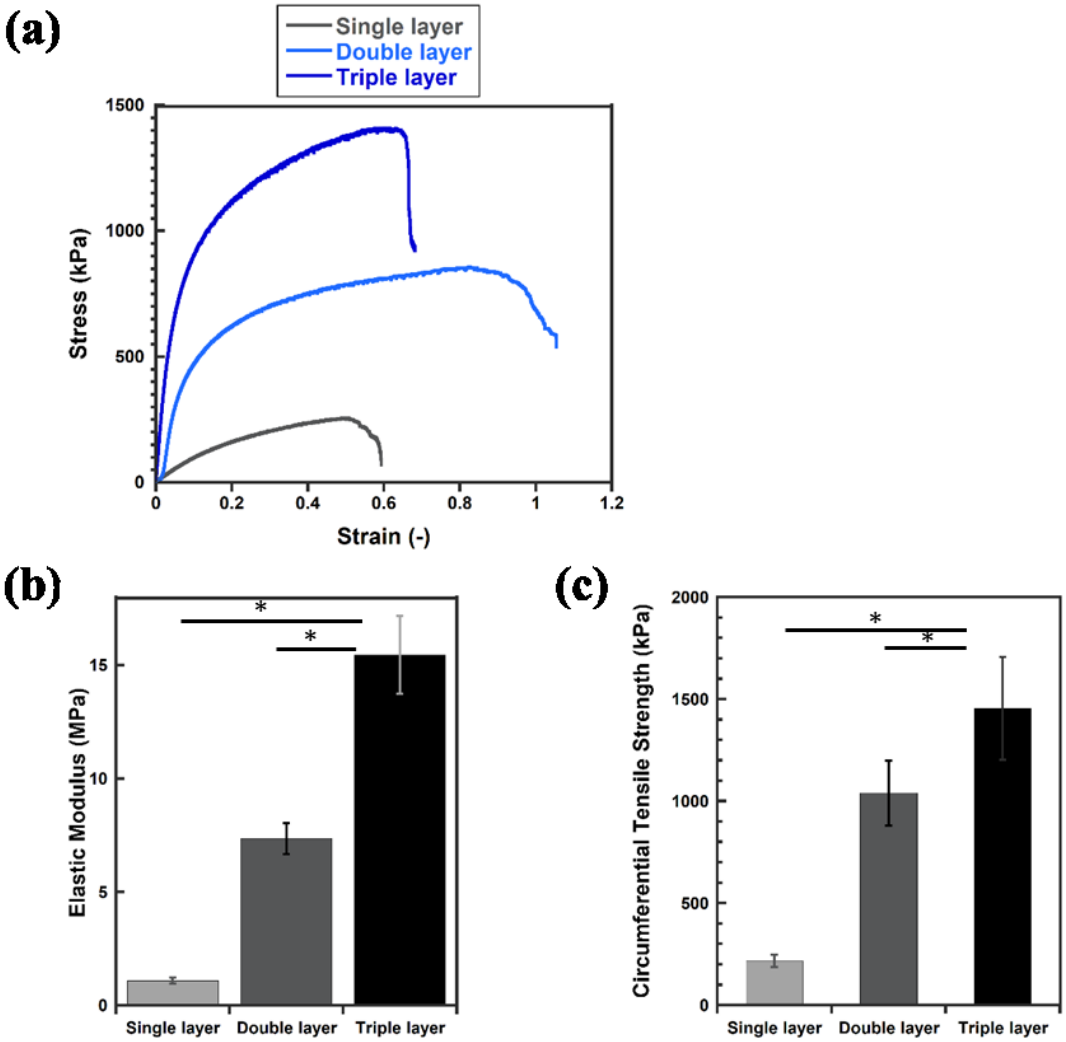

Figure 4.5 Mechanical properties of the multiple layers cylindrical scaffolds. A) Representative of stress-strain curve. B) Elastic moduli. C) Circumferential tensile strength.

The estimated burst pressure is shown in Figure 4.6. The estimated burst pressure ranged between 106 mmHg to 600 mmHg and increased as number of layer increased. It is important to design vascular graft that can withstand blood pressure more than 120 mmHg. In this work, the double and triple layer with burst pressure of 350 and 600, respectively. Thus, they were more appropriate to be used as vascular scaffold than the single layer scaffold.

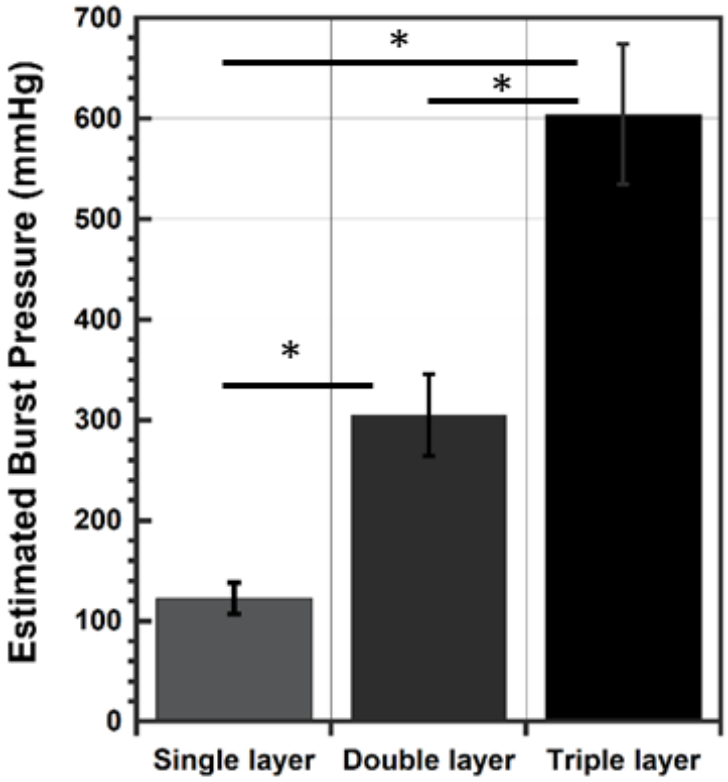

Figure 4.6 Estimated burst pressure of layered cylindrical scaffold.

4.3.2 Properties of PLCL/PCL Blends Scaffold

4.3.2.a Characterization

The infrared spectra of scaffold from PCL/PLCL blends with various weight ratio were shown in Figure 4.8. Pure PCL (PCL/PLCL 100:0) has peak absorptions at 1722 cm^{-1} corresponding to the C=O stretching vibration and at 2994 cm^{-1} due to stretching vibration of C-H bond (Figure 4.7a). As the addition of PLCL (PLCL25), the peak intensity at 2994 cm^{-1} absorption decreased because PLCL has less C-H bond compared to PCL whose longer methylene (CH_2) chain. Moreover, new peak at 1756 cm^{-1} was appeared PLCL25 due to stretching vibration of C=O from PLCL (Figure 4.7b). As the concentration of PLCL increased, the intensity of this peak became stronger, on the contrary, the peak intensity at 1722 cm^{-1} decreased. Pure PLCL did not show an absorption at 1722 cm^{-1}. The infrared spectra confirmed that PCL and PLCL were homogenously blended.

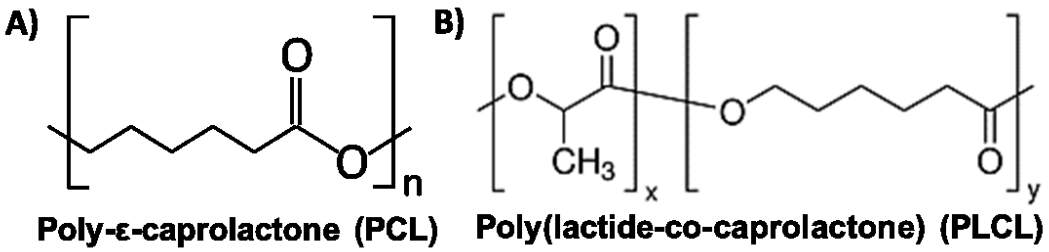

Figure 4.7 Chemical Structure of a) PCL and b) PLCL.

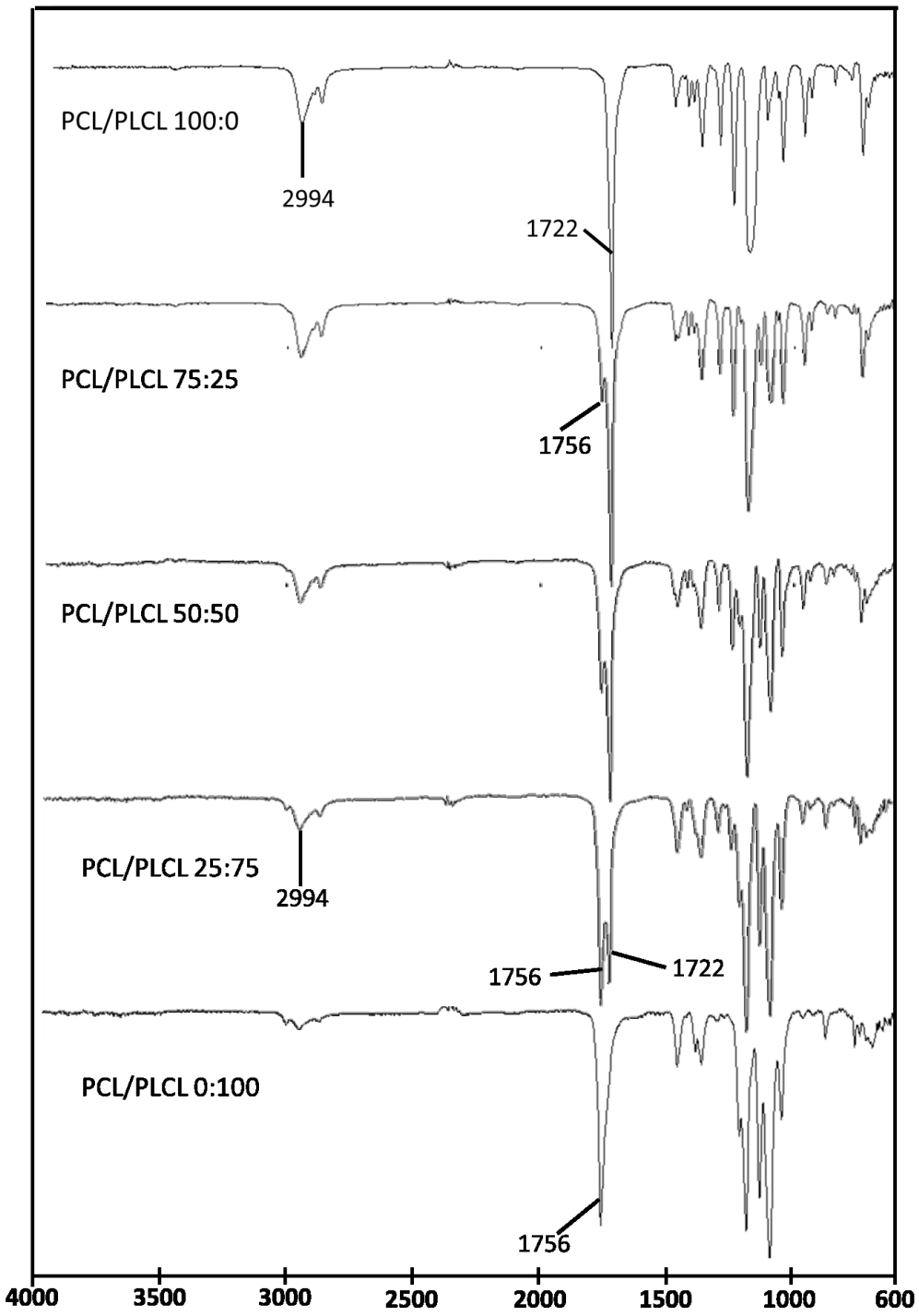

Figure 4.8 Infrared spectra of PCL/PLCL blends scaffolds with various ratio.

Figure 4.9 showed DSC thermograms of PCL/PLCL blends scaffolds at various ratio. DSC spectrum of neat PLCL characterized by endothermic melting peak of caprolactone at 53° C, followed by glass transition temperature of lactic acid at

around 65°C, an exothermic crystalline peak of lactic acid at 80°C which is appeared as a shoulder, and endothermic melting peak of lactic acid at 162°C. PLCL/PCL blends exhibited sharper endothermic peak at 59-60°C as the content of PCL increased, which indicated as a melting point of PCL. Also, peak at 162.34° C decreased steadily as the content of PLCL decreased. Neat PCL exhibited only one endothermic melting peak at 60°C.

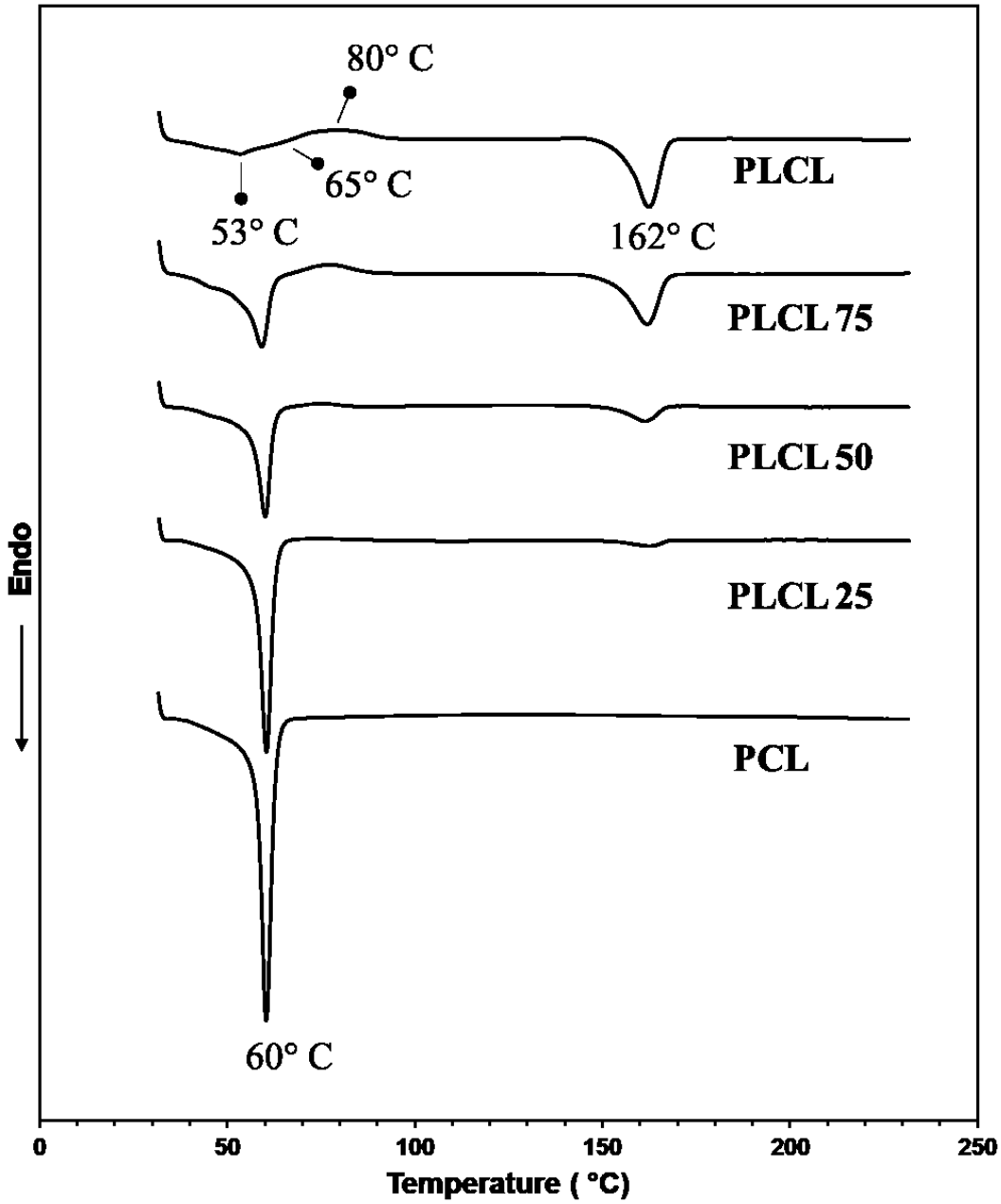

Figure 4.9 DSC thermograms of PCL/PLCL blends scaffolds.

4.3.2.b Microstructural Behaviour

Figure 4.10 showed the microstructural behaviour of PCL/PLCL scaffolds at various ratio. All the scaffold exhibited porous structures which oriented perpendicular to the surface. Pure PCL (Figure 4.10a) showed more fibrous struts compared to the pure PLCL. This is because of the rubbery properties of PCL. The fibrous struts were gradually disappeared as the PLCL content increased (Figure 4.10b, c, d and e). The pore diameters were tend to increase as the PLCL content increased, although there is no statistical difference of pore area with one another (Figure 4.10f). In contrast, the wall thickness of the tubular scaffolds decreased as the PLCL content increased (Figure 4.10g).

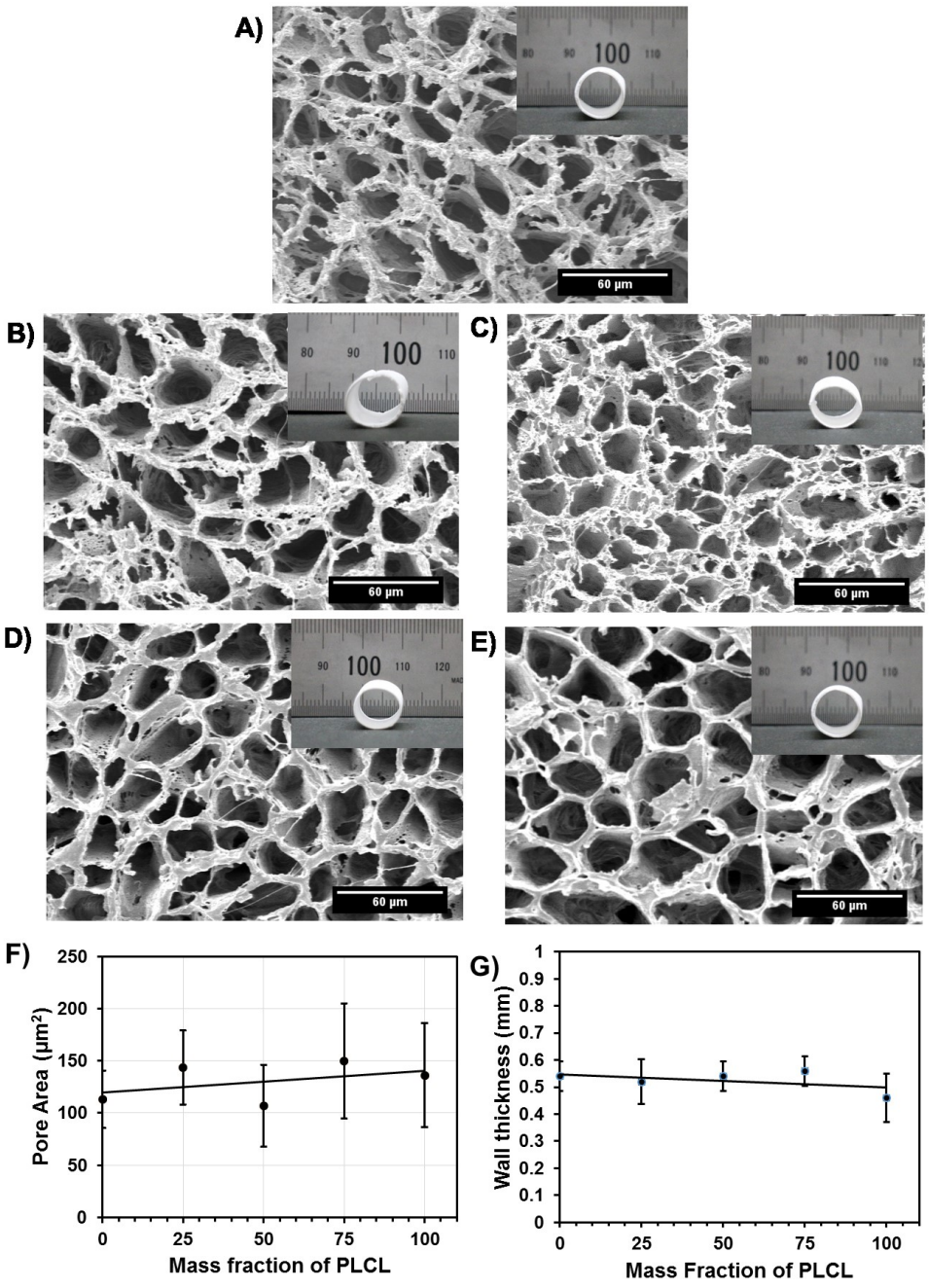

Figure 4.10 Macro- and microstructure of the tubular scaffolds from PCL/PLCL blends with various weight ratio. a) PCL, b) PLCL25, c) PLCL50, d)PLCL75, e) PLCL. f) Plot of pore area and g) the wall thickness of the tubular scaffolds as function of PLCL weight ratio.

Figure 4.11 showed surface morphology of PCL, PCL/PLCL blends and PLCL. Rough surfaces were found on PLCL 75, PLCL 50 and PLCL 25, indicated a phase separation between the two polymers. Meanwhile, neat PLCL and neat PCL exhibited smoother surface than the PCL/PLCL blends scaffolds.

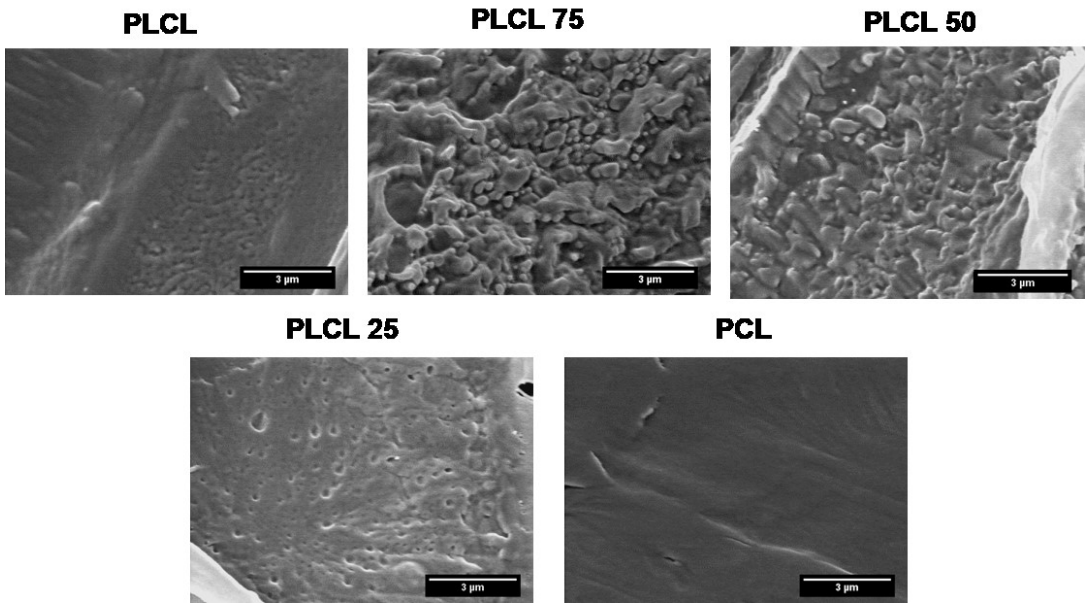

Figure 4.11 Surface morphology of neat PCL, PCL/PLCL blends and neat PLCL.

4.3.2.c Mechanical Properties

To evaluate the effect of blending to the mechanical properties, tensile tests were performed. Figure 4.12a showed a typical stress-strain curve of the blends scaffolds at various ratio. As shown in Figure 4.12 b, c, and d, PLCL has the highest tensile strength, failure strain and elastic modulus. PCL has an average tensile strength of 171.8 kPa. The tensile strength was suddenly decreased to 88.1 kPa when the PLCL content was added to 25% (PLCL25). This may be due to a phase separation between polymer coils of PCL and PLCL when the blends polymer were frozen suddenly to -80°C, as observed in Figure 4.11. This phase separation affected not only to the

mechanical properties but also to the physical properties. The resulted PLCL 25 scaffold had a cracked site on it and was easily to be torn.

However, the tensile strength was recovered as the PLCL content increased. The same behaviour was found at the failure strain. The elastic modulus increased as the PLCL content increased. Pure PCL has the lowest elastic modulus as predicted while the PLCL has the highest elastic modulus as the result of crystallisable hard and brittle properties from lactic acid monomer.

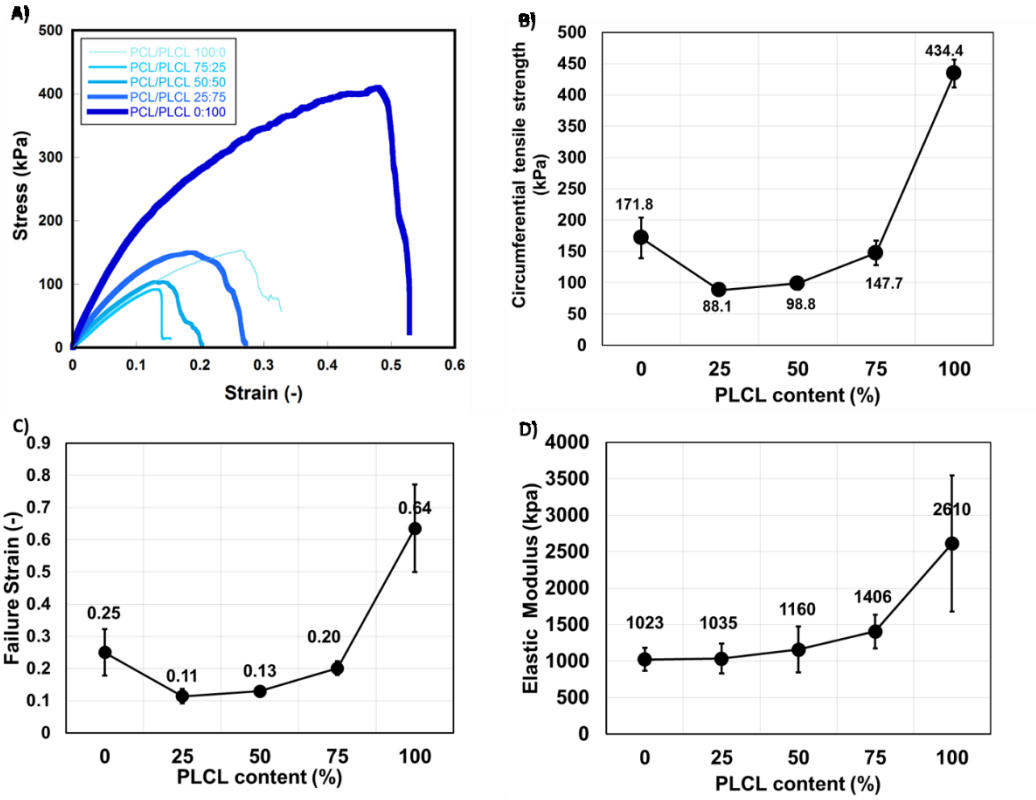

Figure 4.12 Mechanical properties of PCL/PLCL blends. a) Stress-strain curve. b) Circumferential Tensile Strength. c) Failure Strain. d) Elastic Modulus. Each data represented as mean ± SD (n=4).

It is important that the designated blood vessel has a rebound elasticity. To determine the optimum blending ratio, the rebound elasticity of the scaffolds were

performed. As shown in Figure 4.13, PCL/PLCL (25:75) was squeezed but it was able to rebound to its original shape. While pure PLCL failed to rebound to its luminal shape.

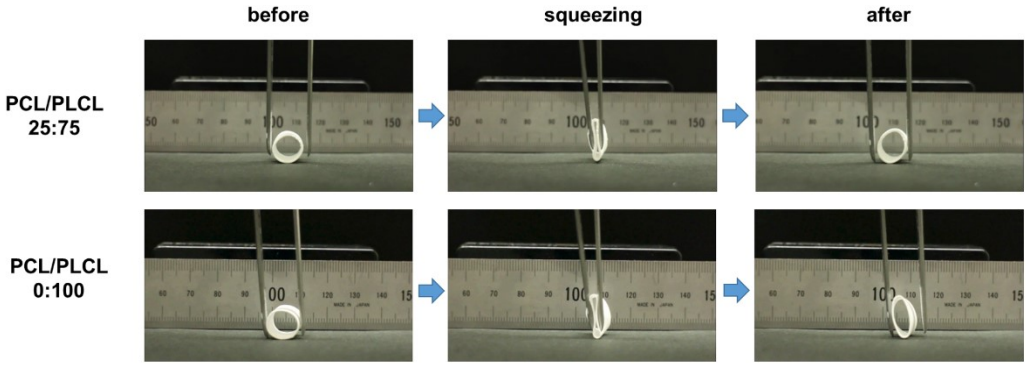

Figure 4.13 Photos of the rebound properties of scaffolds with PCL/PLCL ratio of 25:75 and 0:100 before and after deformed with tweezer.

4.3.2.d Effect of Blending Solution's temperature before dipping

The tubular scaffold with blending ratio of PCL/PLCL 25:75 was found to be the optimum blending ratio in term of elastic modulus and rebound properties. However, the tensile strength was only 147.7 kPa, which is lower than that of PCL tubular scaffold (171.8 kPa). To increase the tensile strength, the polymer solution of PCL/PLCL (25:75) was varied from 20° C to 60°C before the dipping process. Heating the blending solution was meant to improve the solubility of PCL and PLCL in the solution. Figure 4.14 showed that the increase of temperature decreased the thickness of the resulted tubular scaffold.

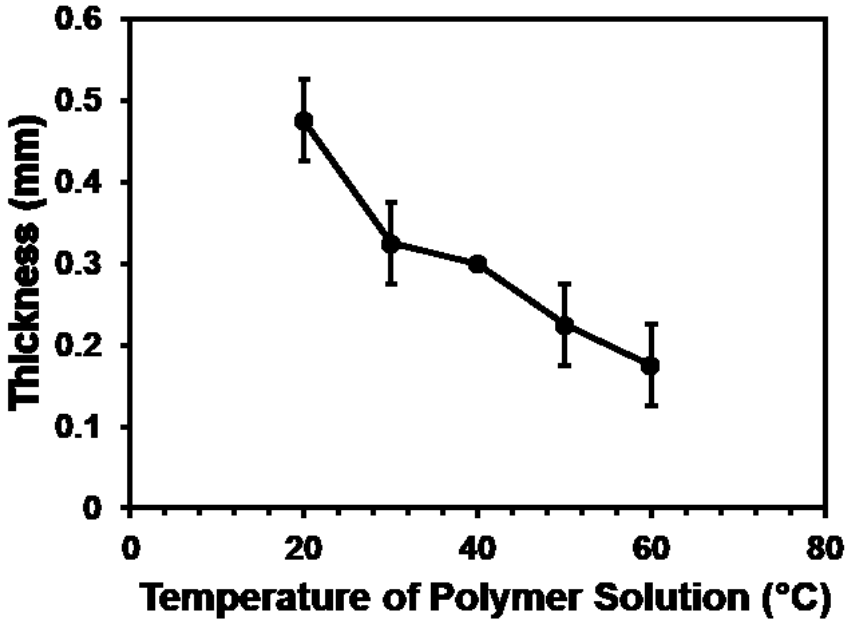

Figure 4.14 Thickness of PLCL 75 blends scaffolds depending on temperature of blending solution from 20°C to 60°C.

In contrast, the mechanical properties including tensile strengths and elastic moduli improved as the temperature increased, as shown in Figure 4.15 . Meanwhile, the strain reached optimum value at temperature of 50°C, and decreased at 60°C due to thickness limitation.

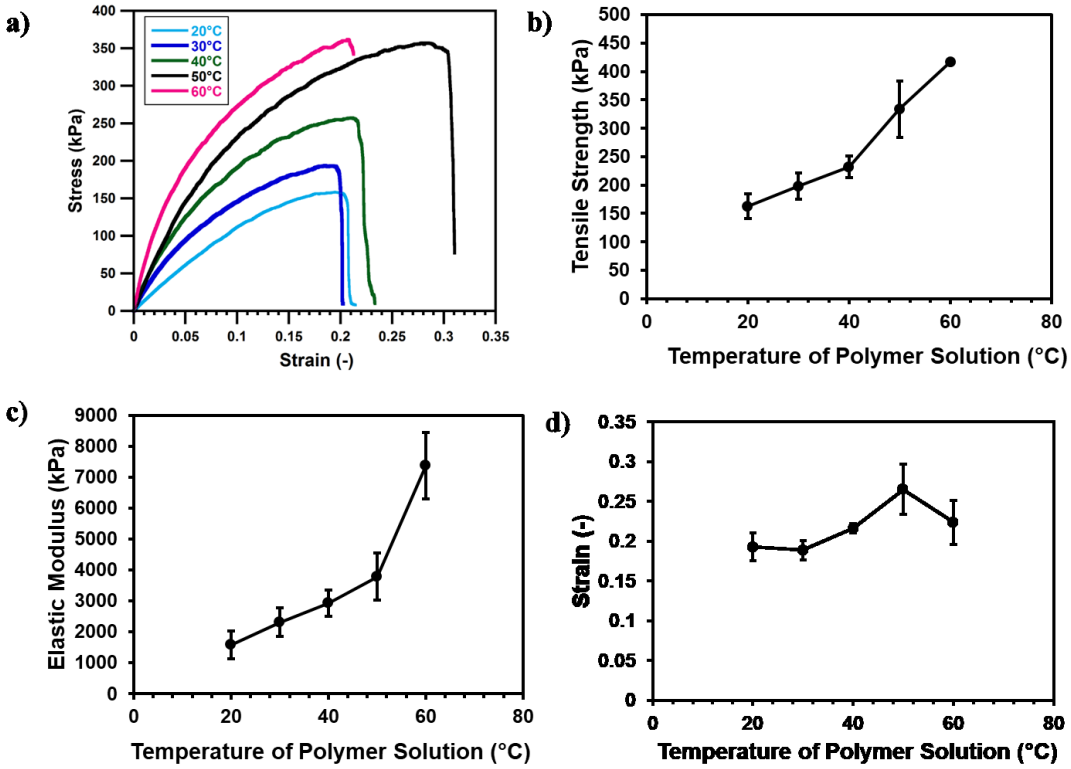

Figure 4.15 Mechanical properties of PCL/PLCL blends scaffolds. A) Representatives of stress-strain curve. B) Tensile strengths. C) Elastic moduli. D) Strain. All data represented as mean ± SD, n=3.

Figure 4.16 showed the morphology of the phase separation between PCL and PLCL made by solvent casting. At 20°C, PCL created small islands with diameter ranged between 116 µm to 368 µm in the main domain of PLCL. As the temperature increased to 50°C, the diameter of PCL phase became smaller ranged between 12 µm to 35 µm. Larger PCL phase may induce the more severe stress concentration in wider region than the smaller phase. Therefore it may reduce the mechanical strength of the cylindrical scaffold prepared from a lower temperature of the polymer blends solution.

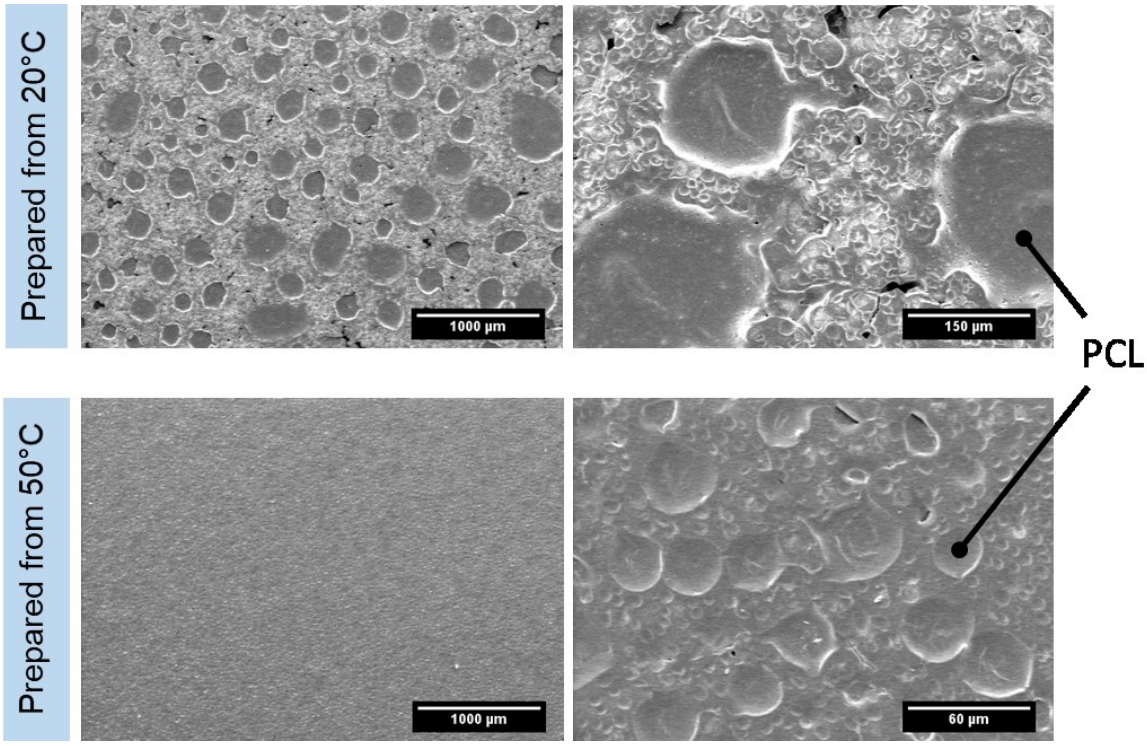

Figure 4.16 Morphology of phase separation of PCL/PLCL (25:75) at 20°C and 50°C made by solution casting.

4.3.2.e Cell Study

To evaluate the biocompatibility of PLCL scaffold, the endothelial cells (ECs) were seeded on PCL/PLCL blend scaffolds. Cells increasingly proliferated in all type scaffolds during 4 and 7 days of culture (Figure 4.17). However, it was evident that cells on neat PCL scaffold proliferated less significant than those on the blending and neat PLCL scaffolds. No significant different was found among PLCL 25, PLCL 50, PLCL 75 and neat PLCL at 4 and 7 days of proliferation. These results indicated that PCL/PLCL blends scaffold is more favorable for cell growing than neat PCL.

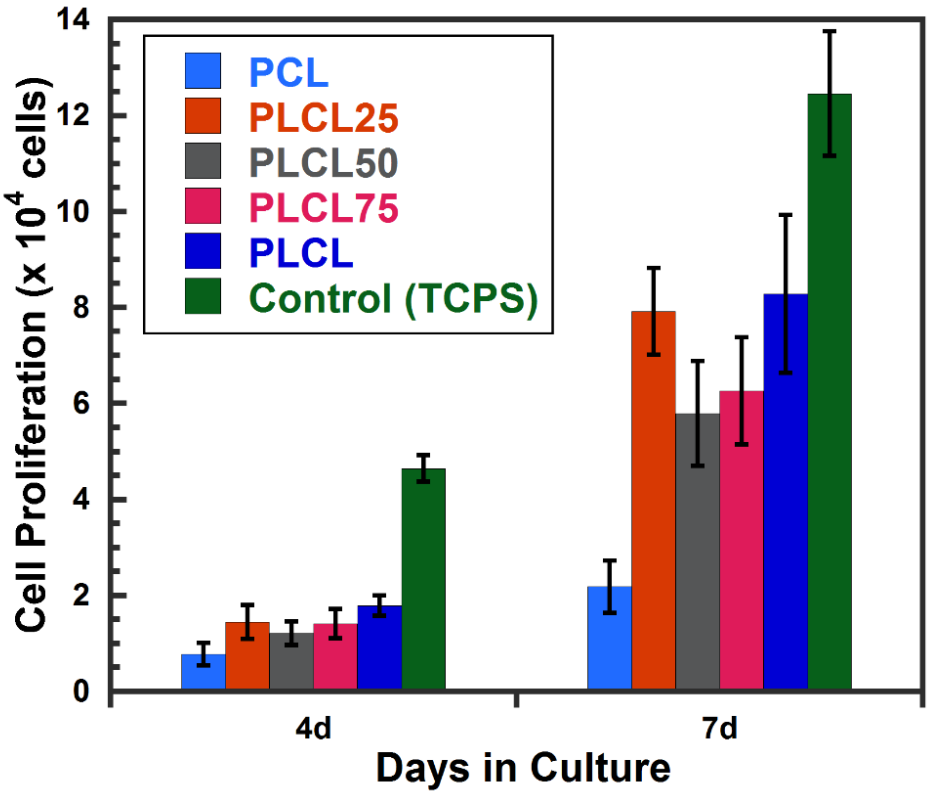

Figure 4.17 Cell proliferation of PCL/PLCL blends scaffold at 4 and 7 days of culture. (TCPS, Tissue Culture Poly Styrene dish).

4.3.3 Properties of melt-spun PLCL Scaffold

4.3.3.a Microstructural behavior

A cylindrical scaffold with thickness of 0.5 mm and the density of 0.37 g/cm^3 could be fabricated from two gram of PLCL (Figure 4.1b). The fibers were randomly oriented and overlapped each other three-dimensionally to form a fiber mesh with high porosity and large surface area, suitable for cell binding and spreading, as shown in Figure 4.18. In the internal wall, the diameter of fibers ranged from 2.0 µm to 17.0 µm (Figure 4.19). On the other hand, the fiber diameter ranged from 1.0 µm to 5.0 µm in the external wall. Viscosity of the melted polymer is considered to be one of the key factors that affect the fiber diameter and in general, the lower viscosity results in the

higher diameter. The increased temperature likely caused less viscosity of the melted polymer, therefore, the diameter decreased during fabrication process.

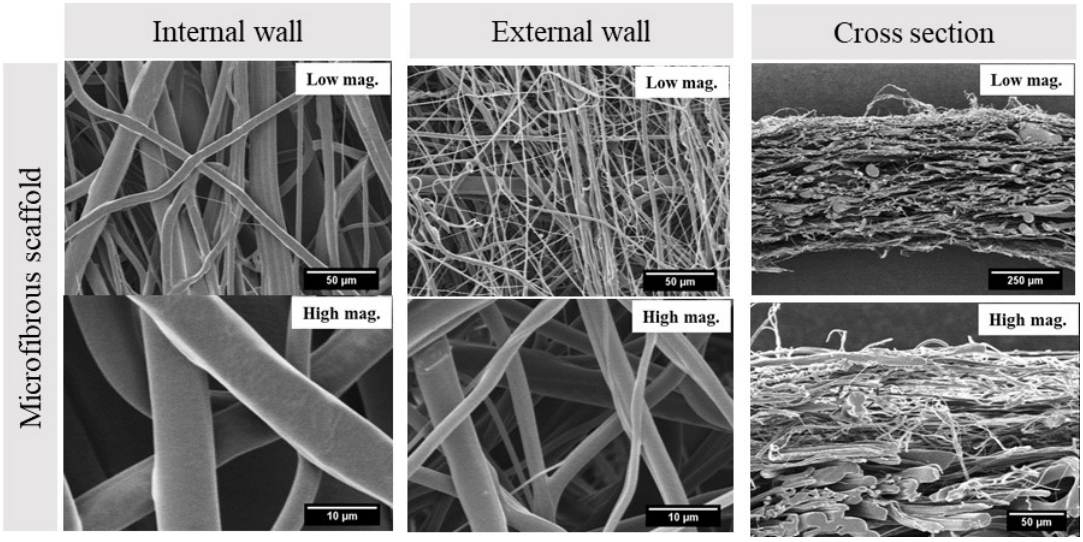

Figure 4.18 SEM images of the microstructure of the microfibrous cylindrical scaffold.

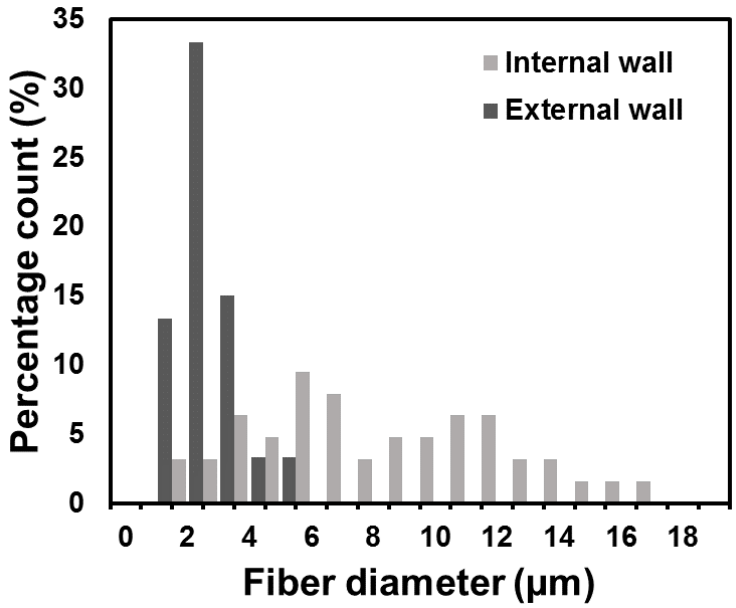

Figure 4.19 Distribution of fibers diameter of the microfibrous cylindrical scaffold.

4.3.3.b Mechanical Properties

The mechanical properties of the microfibrous cylindrical scaffold was evaluated in comparison with the microporous cylindrical scaffold that was previously fabricated in Chapter 2. The results of the mechanical tests are shown in Figure 4.20. The microfibrous scaffold demonstrated steeper stress-strain curve with higher stress and larger strain compared to the microporous scaffold (Figure 4.20a). The elastic modulus (Figure 4.20b) and the circumferential tensile strength (Figure 4.20c) of the microfibrous scaffold were approximately 1.5 times higher than those of the microporous scaffold. These results clearly demonstrated that the microfibrous structure resulted in the greater tensile mechanical properties than the microporous structure constructed with strut structures.

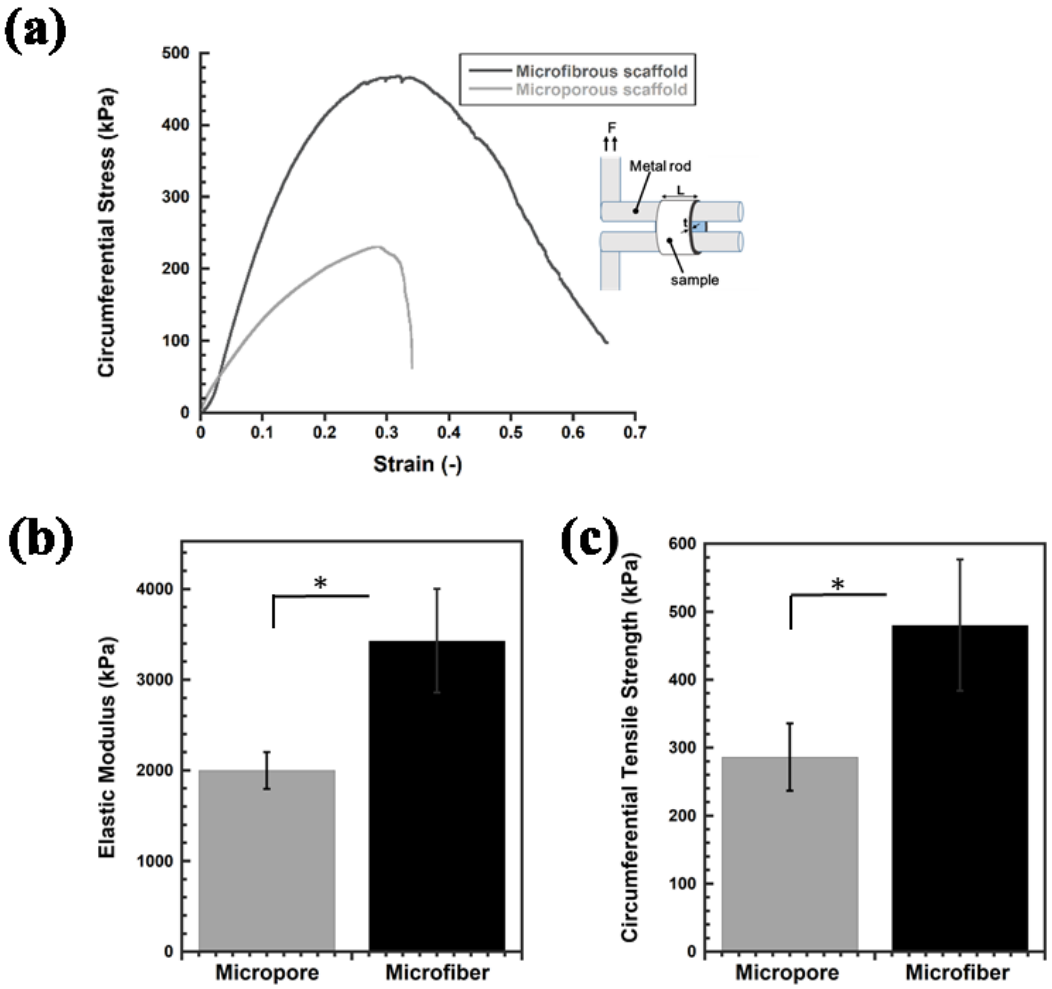

Figure 4.20 (a) Typical stress-strain curve measured using ring tensile test, (b) Elastic moduli, and (c) circumferential tensile strength. Each data represent as mean ± SD (n=3), * indicates $P < 0.05$.

4.3.3.c Cell Study

Cell study was conducted to evaluate the effects of surface topography of the scaffold to the cell response. Cell adhesion and proliferation on both of the microfibrous scaffold and the microporous scaffold were evaluated. The initial cellular responses to the microfibrous and microporous scaffolds at 3 hours of culture are shown in Figure 4.21. Cells on the microfibrous scaffold were flattened, stretched and

intimately adhered to the fibers. Meanwhile, cells tended to become round shape and less flattened on the microporous scaffold. Furthermore, unlike on the microporous scaffold, cells on the microfibrous scaffold have developed filopodia.

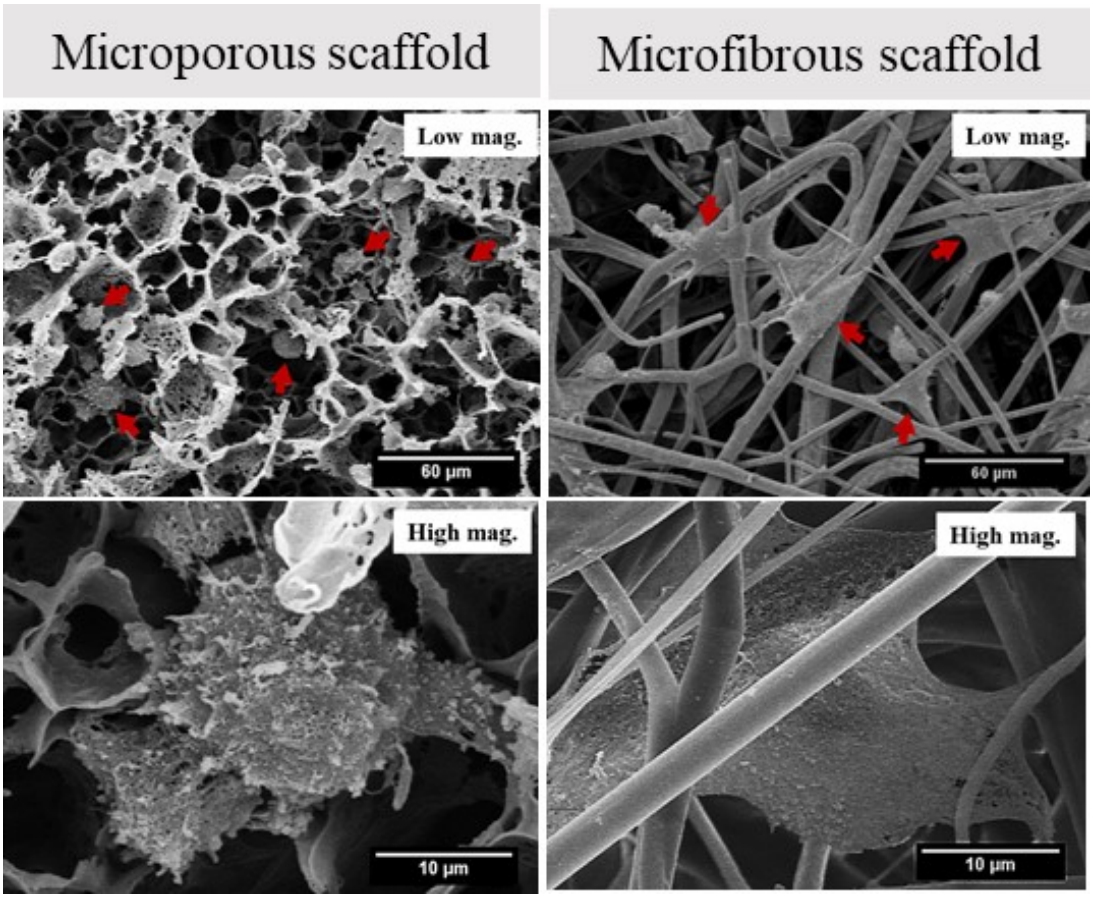

Figure 4.21 SEM images of cell attachment on microfibrous and microporous scaffold at 3 hours culture (cell, red arrow).

Cells further grew on both the scaffolds, after 24 hours cell culture. At this time, no distinctive cell features were observed on both the scaffolds (Figure 4.22). Cell morphology including cell area and aspect ratio was then evaluated quantitatively. Cells on the microfibrous scaffold had significantly larger cell area and aspect ratio than those on the microporous scaffold (Figure 4.23). Cells proliferation on the

microfibrous scaffold was significantly higher than that on the microporous scaffold, at 4 and 7 days cell culture (Figure 4.24).

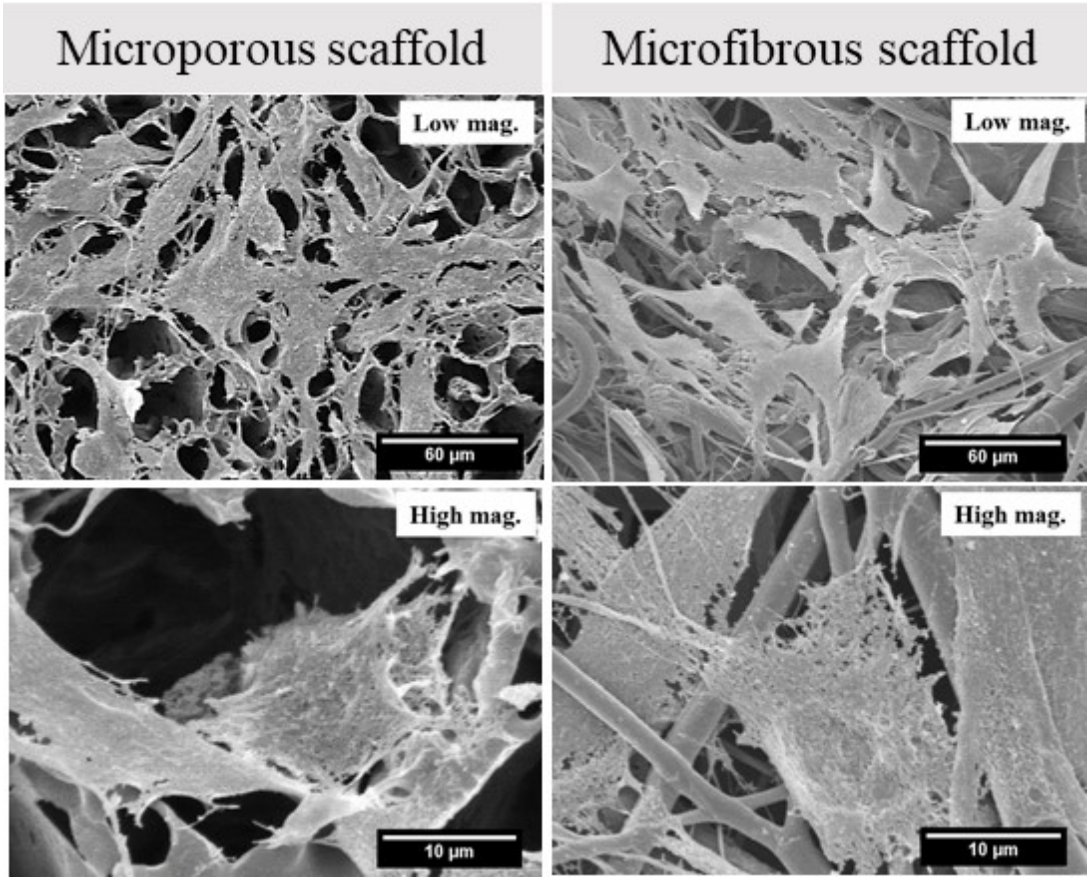

Figure 4.22 SEM images of cell attachment on the microfibrous and microporous scaffolds 24 hours culture.

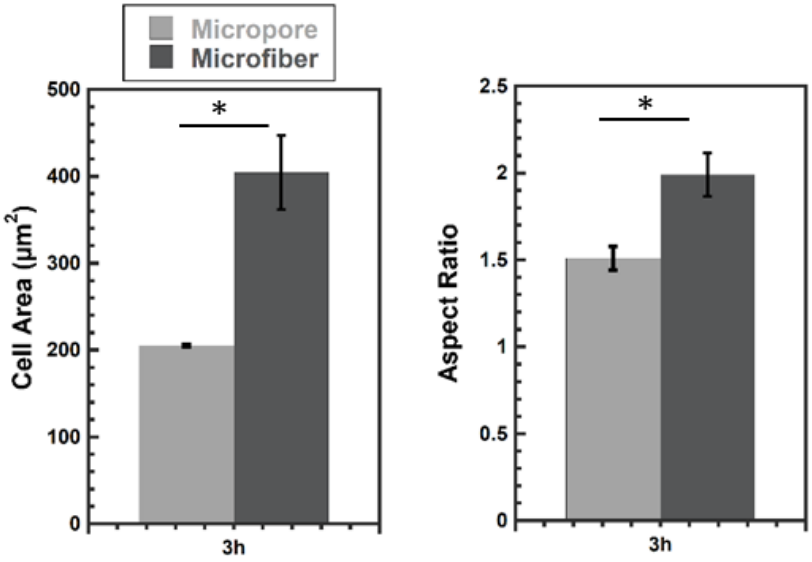

Figure 4.23 Quantification of cell area (*left*) and aspect ratio (*right*) at 3 hours of culture. Cell area and aspect ratio at 3 hours culture were quantified by Image-J ($n \geq 159$), * indicates $P < 0.05$.

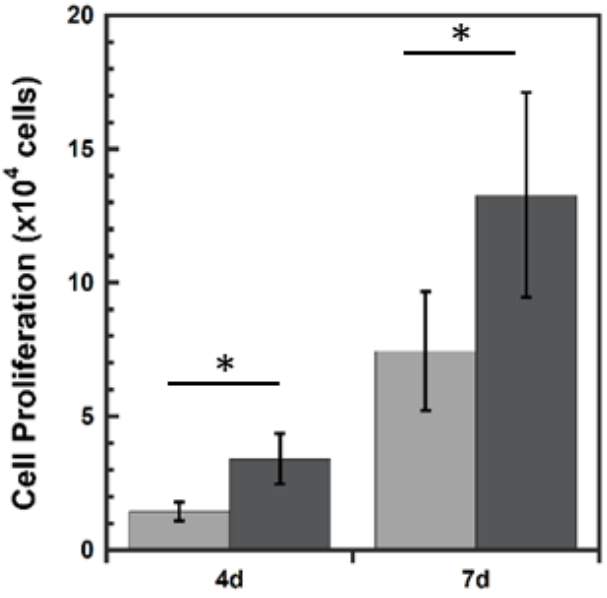

Figure 4.24 Cell proliferation on the microfibrous and the microsporous scaffolds. Data are represented as mean ± SD, n=6, * indicates $P < 0.05$.

4.4 Discussion

In this study, several attempts have been studied in order to improve the mechanical properties and controlling the porous structure of the PLCL cylindrical scaffold. In the first approach, multiple layers of cylindrical scaffold has been developed. At the double layer scaffold, the tensile strength increased 5 folds higher from the single layer scaffold, as shown in Figure 4.25. The highest tensile strength was achieved at 1400 kPa at the triple layers scaffold. The double and the triple layers scaffolds may seem as promising candidates for vascular tissue engineering because their tensile strength is in the range of the human arterial tissue. However, the porosity of the double and triple layers scaffolds decreased to 64-68% due to the increase in the material density (Table 4.1). Lack of porosity will seriously limit cells to grow into a three-dimensional scaffold [26].

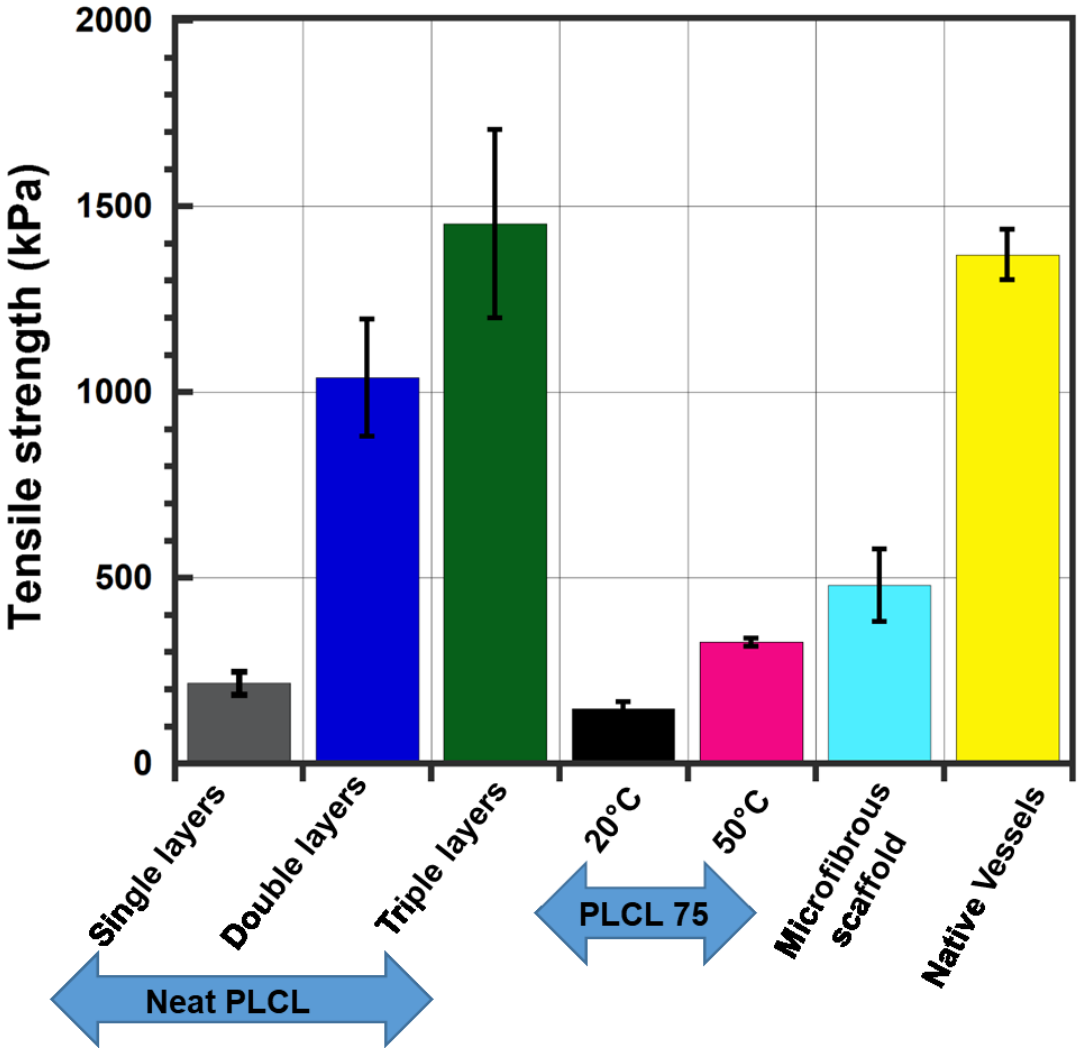

Figure 4.25 Comparison of tensile strength resulted in this study.

In the second approach, the cylindrical scaffolds from blending polymer of PLCL and PCL were prepared. It was found that PLCL75 is the optimum blending ratio due to good rebound property. However, the blending slightly decreased the mechanical strength to 147 kPa (Figure 4.25) due to the phase separation between the two polymers. The increase temperature of the blending solution before the phase separation clearly recovered the mechanical strength to around 350 kPa. Cell study also confirmed that PCL/PLCL blending showed a better cell response than neat PCL. This may relate with chemical structure of PCL, which contains longer alkyl chain

than PLCL, resulting more hydrophobic surface than PLCL. Hydrophilicity is often associated with cell attachment and proliferation [101]. The more hydrophilic of the surface, the better the cell attachment and proliferation. Therefore, PCL/PLCL blends and neat PLCL exhibited better cell proliferation than neat PCL.

The next approach involved the use of commercially available cotton candy to fabricate the microfibrous cylindrical scaffold. Since this machine is not particularly designed for research, the control parameters such as heat temperature and spinning head speed could not be modified. So far, this was only applicable for PLCL whose low glass transition temperature (Tg) of 16 °C and melting point (Tm) 164 °C. Using the same technique, other researcher was also able to produce microfibers from relatively low glass temperature polymers such as poly-lactide-co-glycolide (PLGA)[102]. A relatively high Tg polymer like polystyrene (PS) was also processable but with assisted solvent. It was also reported that the molecular weight of polymer also affected to the optimal fiber production [103]. We observed that a few times after the fibers extruded from the nozzle, the size became smaller and more uniform since the increasing temperature is likely causing the melted polymer became less viscous, thus the diameter decreased. For future plan, the effect of temperature and rotating speed will be further studied. Compared to the microporous scaffold fabricated by phase separation method, the microfibrous scaffold showed an improved mechanical strength, approximately 1.5 folds higher than microporous scaffold (single layer scaffold) (Figure 4.25). In the microfibrous scaffolds, fibers were randomly oriented and overlapped each other three-dimensionally which then mechanically interlocked to form a strong structure like a mesh. While in the microporous scaffold, the strength of material comes from struts and the pores act as voids that can reduce the material strength. However, the microfibrous cylindrical scaffold is still

approximately 4 folds lower than the tensile strength of native vein [104]. Figure 4.25 summarized the tensile strength of the fabricated cylindrical scaffold in this study, as compared to native vein [104].

One more parameter that is not less important is scaffold topography[105]. Sensitivity of cells to the surrounding physical feature was responded in the different cytosckeletal rearrangement. Studies of physical feature effects to cell response have been widely explored including roughness, micropattern, micropores, and fibers diameters[106]. Native blood vessel is contained abundant extracellular matrix (ECM) which majorly composed of fibrous collagen. Microfiber scaffold is therefore more beneficial to mimic the native feature of ECM over the microporous scaffold. Microfiber structure had relatively large surface area that provide more anchorage for cells binding. Our results confirmed that the microfibrous topography showed better cell morphology including cell area, perimeter and aspect ratio compared to the microporous scaffold. After 24 hours of culture, we found better cell proliferation on the microfiber scaffold than those on the microporous scaffold. This may relates to the different cell morphology during cell attachment. Eventually, better cell attachment in term of cytoskeletal arrangement would lead to the strong cell adhesion increase cell spreading, as similar results obtained by other researchers which reported that larger cell area and aspect ratio improved cell proliferation [101].

4.5 Conclusions

In this last chapter, approaches as mean to improve the mechanical strength of the PLCL scaffold have been discussed. The conclusions are obtained as follows:

1. In the first approach, developing the PLCL scaffold into double and triple layers improved the mechanical properties, approximately 400% and 600%, respectively, from the single layer scaffold.
2. In the second approach, polymer blends PCL/PLCL 25:75 decreased the mechanical strength to around 26%, however was able recovered and increased the strength to around 75% by increasing the temperature of the blending solution before phase separation process.
3. In the third approach, melt spinning method successfully developed the microfibrous PLCL scaffold by utilizing the cotton candy machine. This method significantly improved the mechanical strength, approximately 150% from the microporous scaffold (single layer). The initial cell study using hMSCs also suggested that the microfibrous scaffold provided more favorable environment for cells growth than the microporous cylindrical scaffold evidenced from better cell morphology and higher proliferation.

CHAPTER 5 : GENERAL CONCLUSIONS

In this dissertation, the hybrid cardiovascular constructs were successfully developed by combining PLCL scaffold and cell sheet and several attempts to improve the mechanical properties have also been investigated. The conclusions are summarized as follows:

1. In Chapter 2, the hybrid engineered-patch was developed by layering PLCL sheet with MSCs sheet. MSCs sheet was able to survive (even in high cell density) and actively proliferated on porous PLCL sheet, suggesting that a porous structure is important in transporting nutrient and oxygen supply while removing metabolic waste. MSC sheet was also able to infiltrate through porous structure and form new layer on the opposite side of PLCL sheet. The combined techniques between scaffold tissue engineering and cell sheet engineering is a promising strategy to develop a fully cellularized-cardiovascular graft in relatively short time.
2. In chapter 3, the hybrid tubular construct was developed by layering MSCs/ECs cell sheets on a porous cylindrical PLCL scaffold. The co-culture cell sheet within the scaffold demonstrated an enhanced proliferation and angiogenic differentiation compared to the monoculture sheet. Cells also infiltrates and spread to the luminal surface of the cylindrical scaffold. This

technique provides a simply technique to create the preformed-endothelial layer *in vitro*, mimicking the intima layer of native blood vessel.

3. In Chapter 4, several attempts to improve the mechanical properties of PLCL scaffold have been demonstrated. In term of mechanical properties, the triple layers scaffold is a potential candidate for vascular graft due to sufficient mechanical strength closed to the native blood vessels. But, the microfibrous scaffold fabricated by melt spinning method may provide more favorable environment for cell growing. Furthermore, the simplicity of melt spinning method provides an opportunity for scale-up in a simple and cost-effective way.

REFERENCES

[1] D.G. Seifu, A. Purnama, K. Mequanint, D. Mantovani, Small-diameter vascular tissue engineering, Nat Rev Cardiol. 10 (2013) 410–421. http://dx.doi.org/10.1038/nrcardio.2013.77.

[2] J.O. Menzoian, A.L. Koshar, N. Rodrigues, Alexis Carrel, Rene Leriche, Jean Kunlin, and the history of bypass surgery, J. Vasc. Surg. 54 (2012) 571–574. http://dx.doi.org/10.1016/j.jvs.2011.04.028.

[3] J.E. Connolly, The history of the in situ saphenous vein bypass, J. Vasc. Surg. 53 (2011) 241–244. doi:10.1016/j.jvs.2010.05.018.

[4] D.S. Baim, Percutaneous Treatment of Saphenous Vein Graft Disease: The Ongoing Challenge, J. Am. Coll. Cardiol. 42 (2003) 1370–1372. doi:10.1016/S0735-1097(03)01039-8.

[5] J.F. Sabik, Understanding saphenous vein graft patency, Circulation. 124 (2011) 273–275. doi:10.1161/CIRCULATIONAHA.111.039842.

[6] B.H. Bulkley, G.M. Hutchins, Accelerated “atherosclerosis”. A morphologic study of 97 saphenous vein coronary artery bypass grafts, Circulation. 55 (1977) 163–169. doi:10.1161/01.CIR.55.1.163.

[7] Z. Vlodaver, J.E. Edwards, Pathologic changes in aortic-coronary arterial saphenous vein grafts., Circulation. 44 (1971) 719–728. doi:10.1161/01.CIR.44.4.719.

[8] W.S. Weintraub, E.L. Jones, J.M. Craver, R.A. Guyton, Frequency of repeat coronary bypass or coronary angioplasty after coronary artery bypass surgery using saphenous venous grafts, Am. J. Cardiol. 73 (1994) 103–112.

http://dx.doi.org/10.1016/0002-9149(94)90198-8.

[9] R.Y. Kannan, H.J. Salacinski, P.E. Butler, G. Hamilton, A.M. Seifalian, Current status of prosthetic bypass grafts: a review, J. Biomed. Mater. Res. B Appl. Biomater. 74 (2005) 570–581.

[10] European Markets for Prosthetic Vacular Grafts, (2006).

[11] R.H. Schmedlen, W.M. Elbjeirami, A.S. Gobin, J.L. West, Tissue engineered small-diameter vascular grafts, Clin. Plast. Surg. 30 (2003) 507–517. doi:10.1016/S0094-1298(03)00069-5.

[12] O.E. Teebken, A.M. Pichlmaier, A. Haverich, Cell seeded decellularised allogeneic matrix grafts and biodegradable polydioxanone-prostheses compared with arterial autografts in a porcine model, Eur. J. Vasc. Endovasc. Surg. 22 (2001) 139–145. doi:10.1053/ejvs.2001.1403.

[13] W. Desmet, Isolated single coronary artery: a review of 50,000 consecutive coronary angiographies, Eur. Hear. J. 13 (1992) 1637–1640.

[14] M. Baguneid, A. De Mel, L. Yildirimer, B.J. Fuller, G. Hamilton, A.M. Seifalian, In vivo study of a model tissue-engineered small-diameter vascular bypass graft, Biotechnol. Appl. Biochem. 58 (2011) 14–24. doi:10.1002/bab.8.

[15] M. Desai, A.M. Seifalian, G. Hamilton, Role of prosthetic conduits in coronary artery bypass grafting, Eur. J. Cardiothorac. Surg. 40 (2011) 394–398.

[16] E.S. van Hattum, M.J.D. Tangelder, M. a Huis in ’t Veld, J. a Lawson, a Algra, F.L. Moll, Medical treatment after peripheral bypass surgery over the past decade., Eur. J. Vasc. Endovasc. Surg. 41 (2011) 805–13. doi:10.1016/j.ejvs.2010.12.016.

[17] R. Langer, J.P. Vacanti, Tissue engineering., Science. 260 (1993) 920–6. doi:10.1126/science.8493529.

[18] N. L'Heureux, Technology insight: the evolution of tissue-engineered vascular grafts[mdash]from research to clinical practice, Nat. Clin. Pr. Cardiovasc. Med. 4 (2007) 389–395. http://dx.doi.org/10.1038/ncpcardio0930.

[19] E. Rabkin, F.J. Schoen, Cardiovascular tissue engineering, Cardiovasc. Pathol. 11 (2002) 305–317. http://dx.doi.org/10.1016/S1054-8807(02)00130-8.

[20] C.B. Weinberg, E. Bell, A blood vessel model constructed from collagen and cultured vascular cells, Science (80). 231 (1986) 397–400. http://dx.doi.org/10.1126/science.2934816.

[21] G. Matsumura, N. Hibino, Y. Ikada, H. Kurosawa, T. Shin'oka, Successful application of tissue engineered vascular autografts: Clinical experience, Biomaterials. 24 (2003) 2303–2308. doi:10.1016/S0142-9612(03)00043-7.

[22] S.W. Cho, H.J. Park, J.H. Ryu, S.H. Kim, Y.H. Kim, C.Y. Choi, M.J. Lee, J.S. Kim, I.S. Jang, D.I. Kim, B.S. Kim, Vascular patches tissue-engineered with autologous bone marrow-derived cells and decellularized tissue matrices, Biomaterials. 26 (2005) 1915–1924. doi:10.1016/j.biomaterials.2004.06.018.

[23] S. Sundaram, L.E. Niklason, Smooth muscle and other cell sources for human blood vessel engineering, Cells Tissues Organs. 195 (2012) 15–25. doi:10.1159/000331409.

[24] V.K. Bajpai, S.T. Andreadis, Stem cell sources for vascular tissue engineering and regeneration, Tissue Eng Part B Rev. 18 (2012) 405–425. doi:10.1089/ten.TEB.2011.0264.

[25] W. Wagner, F. Wein, A. Seckinger, M. Frankhauser, U. Wirkner, U. Krause, J. Blake, C. Schwager, V. Eckstein, W. Ansorge, A.D. Ho, Comparative characteristics of mesenchymal stem cells from human bone marrow, adipose tissue, and umbilical cord blood, Exp. Hematol. 33 (2005) 1402–1416. doi:10.1016/j.exphem.2005.07.003.

[26] P.X. Ma, Scaffolds for tissue fabrication, Mater. Today. 7 (2004) 30–40. doi:10.1016/S1369-7021(04)00233-0.

[27] P.X. Ma, R. Langer, Fabrication of Biodegradable Polymer Foams for Cell Transplantation and Tissue Engineering, in: Tissue Eng., 1999: pp. 47–56. doi:10.1385/0-89603-516-6:47.

[28] Z. Ruiyun, M.P. X., Poly(α-hydroxyl acids)/hydroxyapatite porous composites for bone-tissue engineering. I. Preparation and morphology, J. Biomed. Mater. Res. 44 (1999) 446–455. doi:10.1002/(SICI)1097-4636(19990315)44:4<446::AID-JBM11>3.0.CO;2-F.

[29] L.E. Freed, R. Langer, I. Martin, N.R. Pellis, G. Vunjak-Novakovic, Tissue engineering of cartilage in space., Proc. Natl. Acad. Sci. U. S. A. 94 (1997) 13885–90. doi:10.1073/pnas.94.25.13885.

[30] L.E. Niklason, J. Gao, W.M. Abbott, K.K. Hirschi, S. Houser, R. Marini, R. Langer, Functional arteries grown in vitro, Science (80). 284 (1999) 489–493. doi:10.1126/science.284.5413.489.

[31] T. Shinoka, P.X. Ma, D. Shum-Tim, C.K. Breuer, R.A. Cusick, G. Zund, R. Langer, J.P. Vacanti, J.E. Mayer, Tissue-engineered heart valves. Autologous valve leaflet replacement study in a lamb model., Circulation. 94 (1996) II164-8. doi:10.1161/01.cir.0000092165.32213.61.

[32] M. Stevens, J. George, Exploring and engineering the cell surface interface, Science (80). (2005) 1135–1139. doi:10.1126/science.1106587.

[33] K. Sarkar, C. Gomez, S. Zambrano, M. Ramirez, E. De Hoyos, H. Vasquez, K. Lozano, Electrospinning to Forcespinning, Mater. Today. 13 (2010) 12–14. doi:10.1016/S1369-7021(10)70199-1.

[34] F. (S. T.V.X. D., S.C. X., C.W. Y., Synthesis and evaluation of biodegradable block copolymers of ε-caprolactone and DL-lactide, J. Polym. Sci. Polym. Lett. Ed. 21 (2018) 593–600. doi:10.1002/pol.1983.130210802.

[35] W.Y. Yeong, N. Sudarmadji, H.Y. Yu, C.K. Chua, K.F. Leong, S.S. Venkatraman, Y.C.F. Boey, L.P. Tan, Porous polycaprolactone scaffold for cardiac tissue engineering fabricated by selective laser sintering, Acta Biomater. 6 (2010) 2028–2034. doi:10.1016/j.actbio.2009.12.033.

[36] D.J. Mooney, G. Organ, J.P. Vacanti, R. Langer, Design and fabrication of biodegradable polymer devices to engineer tubular tissues., Cell Transplant. 3 (1994) 203–210.

[37] D.J. Mooney, C. Breuer, K. McNamara, J.P. Vacanti, R. Langer, Fabricating tubular devices from polymers of lactic and glycolic Acid for tissue engineering., Tissue Eng. 1 (1995) 107–118. doi:10.1089/ten.1995.1.107.

[38] I. Keun Kwon, S. Kidoaki, T. Matsuda, Electrospun nano- to microfiber fabrics made of biodegradable copolyesters: Structural characteristics, mechanical properties and cell adhesion potential, Biomaterials. 26 (2005) 3929–3939. doi:10.1016/j.biomaterials.2004.10.007.

[39] S.V. Khiste, V. Ranganath, A.S. Nichani, Evaluation of tensile strength of

surgical synthetic absorbable suture materials: An in vitro study, J. Periodontal Implant Sci. 43 (2013) 130–135. doi:10.5051/jpis.2013.43.3.130.

[40] L.E. Niklason, Functional arteries grown in vitro, Science (80). 284 (1999) 489–493. http://dx.doi.org/10.1126/science.284.5413.489.

[41] S. Ravi, E.L. Chaikof, Biomaterials for vascular tissue engineering., Regen. Med. 5 (2010) 107–20. doi:10.2217/rme.09.77.

[42] D. Shum-Tim, U. Stock, J. Hrkach, T. Shinoka, J. Lien, M.A. Moses, A. Stamp, G. Taylor, A.M. Moran, W. Landis, R. Langer, J.P. Vacanti, J.E. Mayer, Tissue engineering of autologous aorta using a new biodegradable polymer, Ann. Thorac. Surg. 68 (1999) 2298–2305. doi:10.1016/S0003-4975(99)01055-3.

[43] S.P. Higgins, A.K. Solan, L.E. Niklason, Effects of polyglycolic acid on porcine smooth muscle cell growth and differentiation, J. Biomed. Mater. Res. A. 67 (2003) 295–302. http://dx.doi.org/10.1002/jbm.a.10599.

[44] J.-E. Park, M. Todo, Compressive mechanical properties and deformation behavior of porous polymer blends of poly(ε-caprolactone) and poly(l-lactic acid), J. Mater. Sci. 46 (2011) 7850. doi:10.1007/s10853-011-5766-3.

[45] D.W. Hutmacher, J.C.H. Goh, S.H. Teoh, An introduction to biodegradable materials for tissue engineering applications, Ann. Acad. Med. Singapore. 30 (2001) 183–191.

[46] K. Garkhal, S. Verma, K. Tikoo, N. Kumar, Surface modified poly(L-lactide-co-epsilon-caprolactone) microspheres as scaffold for tissue engineering, J. Biomed. Mater. Res. A. 82 (2007) 747–756. doi:10.1002/jbm.a.31150.

[47] M.C. Serrano, R. Pagani, G.A. Ameer, M. Vallet-Regí, M.T. Portolés,

Endothelial cells derived from circulating progenitors as an effective source to functional endothelialization of NaOH-treated poly(caprolactone) films, J. Biomed. Mater. Res. - Part A. 87 (2008) 964–971. doi:10.1002/jbm.a.31728.

[48] N. L'Heureux, S. Paquet, R. Labbe, L. Germain, F.A. Auger, A completely biological tissue-engineered human blood vessel, FASEB J. 12 (1998) 47–56.

[49] M. Peck, N. Dusserre, T.N. McAllister, N. L'Heureux, Tissue engineering by self-assembly, Mater. Today. 14 (2011) 218–224. http://dx.doi.org/10.1016/S1369-7021(11)70117-1.

[50] T. Okano, N. Yamada, H. Sakai, Y. Sakurai, A novel recovery system for cultured cells using plasma-treated polystyrene dishes grafted with poly(N-isopropylacrylamide)., J. Biomed. Mater. Res. 27 (1993) 1243–1251. doi:10.1002/jbm.820271005.

[51] M. Yamato, M. Utsumi, A. Kushida, C. Konno, A. Kikuchi, T. Okano, Thermo-responsive culture dishes allow the intact harvest of multilayered keratinocyte sheets without dispase by reducing temperature., Tissue Engin. 7 (2001) 473–480. doi:10.1089/10763270152436517.

[52] A. Arauchi, T. Shimizu, M. Yamato, T. Obara, T. Okano, Tissue-engineered thyroid cell sheet rescued hypothyroidism in rat models after receiving total thyroidectomy comparing with nontransplantation models., Tissue Eng. Part A. 15 (2009) 3943–9. doi:10.1089/ten.TEA.2009.0119.

[53] H. Hata, G. Matsumiya, S. Miyagawa, H. Kondoh, N. Kawaguchi, N. Matsuura, T. Shimizu, T. Okano, H. Matsuda, Y. Sawa, Grafted skeletal myoblast sheets attenuate myocardial remodeling in pacing-induced canine heart failure model, J. Thorac. Cardiovasc. Surg. 132 (2006) 918–924.

doi:10.1016/j.jtcvs.2006.01.024.

[54] M. Kanzaki, M. Yamato, J. Yang, H. Sekine, R. Takagi, T. Isaka, T. Okano, T. Onuki, Functional closure of visceral pleural defects by autologous tissue engineered cell sheets, Eur. J. Cardio-Thoracic Surg. 34 (2008) 864–869. doi:10.1016/j.ejcts.2008.05.048.

[55] T. Iwata, M. Yamato, H. Tsuchioka, R. Takagi, S. Mukobata, K. Washio, T. Okano, I. Ishikawa, Periodontal regeneration with multi-layered periodontal ligament-derived cell sheets in a canine model, Biomaterials. 30 (2009) 2716–2723. doi:10.1016/j.biomaterials.2009.01.032.

[56] Y. Miyahara, N. Nagaya, M. Kataoka, B. Yanagawa, K. Tanaka, H. Hao, K. Ishino, H. Ishida, T. Shimizu, K. Kangawa, S. Sano, T. Okano, S. Kitamura, H. Mori, Monolayered mesenchymal stem cells repair scarred myocardium after myocardial infarction, Nat. Med. 12 (2006) 459–465. doi:10.1038/nm1391.

[57] H. Sekine, T. Shimizu, J. Yang, E. Kobayashi, T. Okano, Pulsatile myocardial tubes fabricated with cell sheet engineering, Circulation. 114 (2006). doi:10.1161/CIRCULATIONAHA.105.000273.

[58] K. Nishida, M. Yamato, Y. Hayashida, K. Watanabe, K. Yamamoto, E. Adachi, S. Nagai, A. Kikuchi, N. Maeda, H. Watanabe, T. Okano, Y. Tano, Corneal Reconstruction with Tissue-Engineered Cell Sheets Composed of Autologous Oral Mucosal Epithelium, N. Engl. J. Med. 351 (2004) 1187–1196. doi:10.1056/NEJMoa040455.

[59] C. Burillon, L. Huot, V. Justin, S. Nataf, F. Chapuis, E. Decullier, O. Damour, Cultured autologous oral mucosal epithelial cell sheet (CAOMECS) transplantation for the treatment of corneal limbal epithelial stem cell

deficiency., Invest. Ophthalmol. Vis. Sci. 53 (2012) 1325–31. doi:10.1167/iovs.11-7744.

[60] N. Matsuda, T. Shimizu, M. Yamato, T. Okano, Tissue engineering based on cell sheet technology, Adv. Mater. 19 (2007) 3089–3099. doi:10.1002/adma.200701978.

[61] H. Masumoto, T. Ikuno, M. Takeda, H. Fukushima, A. Marui, S. Katayama, T. Shimizu, T. Ikeda, T. Okano, R. Sakata, J.K. Yamashita, Human iPS cell-engineered cardiac tissue sheets with cardiomyocytes and vascular cells for cardiac regeneration, Sci. Rep. 4 (2014). doi:10.1038/srep06716.

[62] K. Matsuura, M. Wada, T. Shimizu, Y. Haraguchi, F. Sato, K. Sugiyama, K. Konishi, Y. Shiba, H. Ichikawa, A. Tachibana, U. Ikeda, M. Yamato, N. Hagiwara, T. Okano, Creation of human cardiac cell sheets using pluripotent stem cells, Biochem. Biophys. Res. Commun. 425 (2012) 321–327. doi:10.1016/j.bbrc.2012.07.089.

[63] T. Ohki, M. Yamato, D. Murakami, R. Takagi, J. Yang, H. Namiki, T. Okano, K. Takasaki, Treatment of oesophageal ulcerations using endoscopic transplantation of tissue-engineered autologous oral mucosal epithelial cell sheets in a canine model, Gut. 55 (2006) 1704–1710. doi:10.1136/gut.2005.088518.

[64] T. Shin'oka, Y. Imai, Y. Ikada, Transplantation of a tissue-engineered pulmonary artery, N. Engl. J. Med. 344 (2001) 532–533. doi:10.1056/NEJM200009283431303.

[65] G. Matsumura, N. Hibino, Y. Ikada, H. Kurosawa, T. Shin'oka, Successful application of tissue engineered vascular autografts: clinical experience,

Biomaterials. 24 (2003) 2303–2308. doi:S0142961203000437 [pii].

[66] T. Shin'oka, G. Matsumura, N. Hibino, Y. Naito, M. Watanabe, T. Konuma, T. Sakamoto, M. Nagatsu, H. Kurosawa, Midterm clinical result of tissue-engineered vascular autografts seeded with autologous bone marrow cells, J. Thorac. Cardiovasc. Surg. 129 (2005). doi:10.1016/j.jtcvs.2004.12.047.

[67] N. Hibino, E. McGillicuddy, G. Matsumura, Y. Ichihara, Y. Naito, C. Breuer, T. Shinoka, Late-term results of tissue-engineered vascular grafts in humans, J. Thorac. Cardiovasc. Surg. 139 (2010). doi:10.1016/j.jtcvs.2009.09.057.

[68] A. Patel, B. Fine, M. Sandig, K. Mequanint, Elastin biosynthesis: the missing link in tissue-engineered blood vessels, Cardiovasc. Res. 71 (2006) 40–49. http://dx.doi.org/10.1016/j.cardiores.2006.02.021.

[69] P.A. Schneider, S.R. Hanson, T.M. Price, L.A. Harker, Preformed confluent endothelial cell monolayers prevent early platelet deposition on vascular prostheses in baboons, J. Vasc. Surg. 8 (1988) 229–235. doi:10.1016/0741-5214(88)90272-8.

[70] M. Deutsch, J. Meinhart, P. Zilla, N. Howanietz, M. Gorlitzer, A. Froeschl, A. Stuempflen, D. Bezuidenhout, M. Grabenwoeger, Long-term experience in autologous in vitro endothelialization of infrainguinal ePTFE grafts, J. Vasc. Surg. 49 (2009) 352–362. doi:10.1016/j.jvs.2008.08.101.

[71] H. Sekine, T. Shimizu, I. Dobashi, K. Matsuura, N. Hagiwara, M. Takahashi, E. Kobayashi, M. Yamato, T. Okano, Cardiac Cell Sheet Transplantation Improves Damaged Heart Function via Superior Cell Survival in Comparison with Dissociated Cell Injection, Tissue Eng. Part A. 17 (2011) 2973–2980. doi:10.1089/ten.tea.2010.0659.

[72] I.A. Memon, Y. Sawa, N. Fukushima, G. Matsumiya, S. Miyagawa, S. Taketani, S.K. Sakakida, H. Kondoh, A.N. Aleshin, T. Shimizu, T. Okano, H. Matsuda, Repair of impaired myocardium by means of implantation of engineered autologous myoblast sheets, J. Thorac. Cardiovasc. Surg. 130 (2005) 1333–1341. doi:10.1016/j.jtcvs.2005.07.023.

[73] T. Shimizu, Polysurgery of cell sheet grafts overcomes diffusion limits to produce thick, vascularized myocardial tissues, FASEB J. (2006). doi:10.1096/fj.05-4715fje.

[74] W. Sekine, Y. Haraguchi, Thickness limitation and cell viability of multi-layered cell sheets and overcoming the diffusion limit by a porous-membrane culture insert, J. Biochips Tissue Chips. 1 (2011) 1–9. doi:10.4172/2153-0777.S1-007.

[75] Q. Li, Z. Wang, Influence of Mesenchymal stem cells with endothelial progenitor cells in co-culture on osteogenesis and angiogenesis: An in vitro study, Arch. Med. Res. 44 (2013) 504–513. doi:10.1016/j.arcmed.2013.09.009.

[76] J. Oswald, S. Boxberger, B. Jørgensen, S. Feldmann, G. Ehninger, M. Bornhäuser, C. Werner, Mesenchymal Stem Cells Can Be Differentiated Into Endothelial Cells In Vitro, Stem Cells. 22 (2004) 377–384. doi:10.1634/stemcells.22-3-377.

[77] A. Ratcliffe, Tissue engineering of vascular grafts, Matrix Biol. 19 (2000) 353–357. doi:Doi 10.1016/S0094-1298(03)00069-5.

[78] M.A. Cleary, Vascular tissue engineering: the next generation, Trends Mol. Med. 18 (2012) 394–404. http://dx.doi.org/10.1016/j.molmed.2012.04.013.

[79] H. Ahn, Y.M. Ju, H. Takahashi, D.F. Williams, J.J. Yoo, S.J. Lee, T. Okano, A. Atala, Engineered small diameter vascular grafts by combining cell sheet engineering and electrospinning technology, Acta Biomater. 16 (n.d.) 14–22. doi:http://dx.doi.org/10.1016/j.actbio.2015.01.030.

[80] M.Y. Tondreau, V. Laterreur, R. Gauvin, K. Vallières, J.M. Bourget, D. Lacroix, C. Tremblay, L. Germain, J. Ruel, F.A. Auger, Mechanical properties of endothelialized fibroblast-derived vascular scaffolds stimulated in a bioreactor, Acta Biomater. 18 (2015) 176–185. doi:10.1016/j.actbio.2015.02.026.

[81] W. Sekine, Y. Haraguchi, T. Shimizu, M. Yamato, A. Umezawa, T. Okano, Chondrocyte differentiation of human endometrial gland-derived MSCs in layered cell sheets, Sci. World J. 2013 (2013). doi:10.1155/2013/359109.

[82] C.H. Mun, Y. Jung, S.H. Kim, H.C. Kim, S.H. Kim, Effects of Pulsatile Bioreactor Culture on Vascular Smooth Muscle Cells Seeded on Electrospun Poly (lactide-co-ε-caprolactone) Scaffold, Artif. Organs. 37 (2013). doi:10.1111/aor.12108.

[83] B.S. Jang, Y. Jung, I.K. Kwon, C.H. Mun, S.H. Kim, Fibroblast culture on poly(L-lactide-co-ε-caprolactone) an electrospun nanofiber sheet, Macromol. Res. 20 (2012) 1234–1242. doi:10.1007/s13233-012-0180-5.

[84] I.A. Pangesty, T. Arahira, M. Todo, Characterization of Tensile Mechanical Behavior of MSCs/PLCL Hybrid Layered Sheet, J. Funct. Biomater. 7 (2016). doi:10.3390/jfb7020014.

[85] S.J. Bidarra, C.C. Barrias, M.A. Barbosa, R. Soares, J. Amédée, P.L. Granja, Phenotypic and proliferative modulation of human mesenchymal stem cells via crosstalk with endothelial cells, Stem Cell Res. 7 (2011) 186–197.

doi:10.1016/j.scr.2011.05.006.

[86] B. Zhang, S. Yang, Y. Zhang, Z. Sun, W. Xu, S. Ye, Co-culture of mesenchymal stem cells with umbilical vein endothelial cells under hypoxic condition., J. Huazhong Univ. Sci. Technolog. Med. Sci. 32 (2012) 173–80. doi:10.1007/s11596-012-0031-9.

[87] S.G. Ball, A.C. Shuttleworth, C.M. Kielty, Direct cell contact influences bone marrow mesenchymal stem cell fate, Int. J. Biochem. Cell Biol. 36 (2004) 714–727. doi:10.1016/j.biocel.2003.10.015.

[88] V. Laterreur, J. Ruel, F.A. Auger, K. Vallières, C. Tremblay, D. Lacroix, M. Tondreau, J.M. Bourget, L. Germain, Comparison of the direct burst pressure and the ring tensile test methods for mechanical characterization of tissue-engineered vascular substitutes, J. Mech. Behav. Biomed. Mater. 34 (2014) 253–263. doi:10.1016/j.jmbbm.2014.02.017.

[89] F.J. O'Brien, Biomaterials & scaffolds for tissue engineering, Mater. Today. 14 (2011) 88–95. doi:10.1016/S1369-7021(11)70058-X.

[90] J. a Hubbell, Biomaterials in tissue engineering., Biotechnology. (N. Y). 13 (1995) 565–576. doi:10.1038/nbt0695-565.

[91] L. Soletti, Y. Hong, J. Guan, J.J. Stankus, M.S. El-Kurdi, W.R. Wagner, D.A. Vorp, A bilayered elastomeric scaffold for tissue engineering of small diameter vascular grafts, Acta Biomater. 6 (2010) 110–122. doi:http://dx.doi.org/10.1016/j.actbio.2009.06.026.

[92] W. Wang, J. Hu, C. He, W. Nie, W. Feng, K. Qiu, X. Zhou, Y. Gao, G. Wang, Heparinized PLLA / PLCL nanofibrous scaffold for potential engineering of

small-diameter blood vessel : Tunable elasticity and anticoagulation property, J. Biomed. Mater. Res. - Part A. 103A (2015) 1784–1797. doi:10.1002/jbm.a.35315.

[93] Y. Zhang, H. Ouyang, T.L. Chwee, S. Ramakrishna, Z.M. Huang, Electrospinning of gelatin fibers and gelatin/PCL composite fibrous scaffolds, J. Biomed. Mater. Res. - Part B Appl. Biomater. 72 (2005) 156–165. doi:10.1002/jbm.b.30128.

[94] D. Steiner, F. Lampert, G.B. Stark, G. Finkenzeller, Effects of endothelial cells on proliferation and survival of human mesenchymal stem cells and primary osteoblasts, J. Orthop. Res. 30 (2012) 1682–1689. doi:10.1002/jor.22130.

[95] M. Grellier, L. Bordenave, J. Amédée, Cell-to-cell communication between osteogenic and endothelial lineages: implications for tissue engineering, Trends Biotechnol. 27 (2009) 562–571. doi:10.1016/j.tibtech.2009.07.001.

[96] D. Kaigler, P.H. Krebsbach, E.R. West, K. Horger, Y.-C. Huang, D.J. Mooney, Endothelial cell modulation of bone marrow stromal cell osteogenic potential., FASEB J. 19 (2005) 665–7. doi:10.1096/fj.04-2529fje.

[97] Yamada Hiroshi, Strength of Biological Materials, Williams & Wilkins Company, Baltimore, 1970.

[98] J.B. Lee, X. Wang, S. Faley, B. Baer, D.A. Balikov, H. Sung, L.M. Bellan, Development of 3D Microvascular Networks Within Gelatin Hydrogels Using Thermoresponsive Sacrificial Microfibers, Adv. Healthc. Mater. 5 (2016) 781–785. doi:10.1002/adhm.201500792.

[99] C.A. Schneider, W.S. Rasband, K.W. Eliceiri, NIH Image to ImageJ: 25 years

of image analysis, Nat. Methods. 9 (2012) 671–675. doi:10.1038/nmeth.2089.

[100] L. Palacio, P. Prádanos, J.I. Calvo, A. Hernández, Porosity measurements by a gas penetration method and other techniques applied to membrane characterization, Thin Solid Films. 348 (1999) 22–29. doi:10.1016/S0040-6090(99)00197-2.

[101] Sunarso, R. Toita, K. Tsuru, K. Ishikawa, Immobilization of calcium and phosphate ions improves the osteoconductivity of titanium implants, Mater. Sci. Eng. C. 68 (2016) 291–298. doi:http://dx.doi.org/10.1016/j.msec.2016.05.090.

[102] L. Wang, J. Shi, L. Liu, E. Secret, Y. Chen, Fabrication of polymer fiber scaffolds by centrifugal spinning for cell culture studies, Microelectron. Eng. 88 (2011) 1718–1721. doi:http://dx.doi.org/10.1016/j.mee.2010.12.054.

[103] M. Huttunen, M. Kellomäki, A simple and high production rate manufacturing method for submicron polymer fibres, J. Tissue Eng. Regen. Med. 5 (2011) e239--e243. doi:10.1002/term.421.

[104] G. Konig, T.N. McAllister, N. Dusserre, S.A. Garrido, C. Iyican, A. Marini, A. Fiorillo, H. Avila, W. Wystrychowski, K. Zagalski, M. Maruszewski, A.L. Jones, L. Cierpka, L.M. de la Fuente, N. L'Heureux, Mechanical properties of completely autologous human tissue engineered blood vessels compared to human saphenous vein and mammary artery, Biomaterials. 30 (2009) 1542–1550. doi:10.1016/j.biomaterials.2008.11.011.

[105] A. Curtis, C. Wilkinson, Topographical control of cells, Biomaterials. 18 (1997) 1573–1583. doi:http://dx.doi.org/10.1016/S0142-9612(97)00144-0.

[106] C.A. Bashur, L.A. Dahlgren, A.S. Goldstein, Effect of fiber diameter and

orientation on fibroblast morphology and proliferation on electrospun poly(d,l-lactic-co-glycolic acid) meshes, Biomaterials. 27 (2006) 5681–5688. doi:http://dx.doi.org/10.1016/j.biomaterials.2006.07.005.

APPENDIXES

1. A.I. Pangesty, T. Arahira, M. Todo, Characterization of Tensile Mechanical Behavior of MSCs/PLCL Hybrid Layered Sheet, J. Funct. Biomater. 7 (2016).
2. A.I. Pangesty, T. Arahira, M. Todo, Development and characterization of hybrid tubular structure of PLCL porous scaffold with hMSCs/ECs cell sheet, J. Mater. Sci. Mater. Med. 28 (2017) 165.
3. A.I. Pangesty, M. Todo, Preparation and Characterization of porous tubular scaffold made of PCL/PLCL blends for vascular tissue engineering, J. Mech. Eng. 4 (2017) 34-46.
4. A.I. Pangesty, M. Todo, Development of Cylindrical Microfibrous Scaffold Using Melt-Spinning Method for Vascular Tissue Engineering. Mater. Lett. 228 (2018) 334-338.

GLOSSARY

Artery	:	Blood vessels carrying oxygenated blood away from heart to the tissues, except for pulmonary arteries.
Dilatation	:	An abnormal enlargement of blood vessels
Hyperplasia	:	Enlargement of an organ or tissue caused by an increase in the reproduction rate of its cells, often as an initial stage in the development of cancer
Ischemic	:	A restriction in blood supply to tissues, causing a shortage of oxygen that is needed for cellular metabolism
Stenosis	:	An abnormal narrowing of blood vessel
Thrombosis (thrombus formation)	:	Formation of a blood clot inside a blood vessel
Vein	:	Blood vessels carrying deoxygenated blood toward the heart.